

Functional Characterization of *Bartonella* Effector Protein - BepE during *in vivo* and *in vitro* infection

Inauguraldissertation

zur

Erlangung der Würde eines Doktors der Philosophie

vorgelegt der

Philosophisch-Naturwissenschaftlichen Fakultät

der Universität Basel

von

Rusudan Okujava

aus Georgien

Basel, 2011

Original document stored on the publication server of the University of Basel

edoc.unibas.ch



This work is licenced under the agreement „Attribution Non-Commercial No Derivatives – 2.5 Switzerland“. The complete text may be viewed here:
creativecommons.org/licenses/by-nc-nd/2.5/ch/deed.en

Genehmigt von der Philosophisch-Naturwissenschaftlichen
Fakultät auf Antrag von:

Prof. Christoph Dehio

Prof. Dirk Bumann

Basel, den 24.05.2011

Prof. Dr. Martin Spiess

(Dekan)



Attribution-Noncommercial-No Derivative Works 2.5 Switzerland

You are free:



to Share — to copy, distribute and transmit the work

Under the following conditions:



Attribution. You must attribute the work in the manner specified by the author or licensor (but not in any way that suggests that they endorse you or your use of the work).



Noncommercial. You may not use this work for commercial purposes.



No Derivative Works. You may not alter, transform, or build upon this work.

- For any reuse or distribution, you must make clear to others the license terms of this work. The best way to do this is with a link to this web page.
- Any of the above conditions can be waived if you get permission from the copyright holder.
- Nothing in this license impairs or restricts the author's moral rights.

Your fair dealing and other rights are in no way affected by the above.

This is a human-readable summary of the Legal Code (the full license) available in German:
<http://creativecommons.org/licenses/by-nc-nd/2.5/ch/legalcode.de>

Disclaimer:

The Commons Deed is not a license. It is simply a handy reference for understanding the Legal Code (the full license) — it is a human-readable expression of some of its key terms. Think of it as the user-friendly interface to the Legal Code beneath. This Deed itself has no legal value, and its contents do not appear in the actual license. Creative Commons is not a law firm and does not provide legal services. Distributing of, displaying of, or linking to this Commons Deed does not create an attorney-client relationship.

for my little son

Statement of my Thesis

This work has been performed in the group of prof. Christoph Dehio in the focal area of infection Biology at the Biozentrum of University of Basel, Switzerland. My PhD committee consists of:

Prof. Christoph Dehio

Prof. Dirk Bumann

Prof. Antonius Rolink

My thesis is written in a cumulative format. It consists of a synopsis covering the major aspects related to my work. It is followed by results and discussion chapter presenting my research that contains the manuscript in preparation and the additional data related to my project. Finally, I resume the major findings of my thesis, discuss the open questions of this work and provide suggestions for the future progression of the project.

TABLE OF CONTENTS

1. Introduction	pp.1-32
1.1. Cell migration	pp.2-7
1.1.1. The definition and discovery	
1.1.2. Main steps in cell migration	
1.1.2.1. Protrusion of lamellipodia and filopodia	
1.1.2.2. Formation of focal adhesions	
1.1.2.3. Cell-body contraction	
1.1.2.4. Tail retraction	
1.2. The effective clearance of pathogen by immune System	pp.8-13
1.2.1. Dendritic cell – a linker between innate and adaptive immune systems	
1.2.2. DC types and subsets	
1.2.3. DCs – professional Ag-presenting cells	
1.2.4. Trafficking of DCs	
1.3. Pathogens modulating host cell adhesion and migration	pp.14-22
1.3.1. Bacterial pathogens modulating host cell migration	
1.3.1.1. <i>Helicobacter pylori</i>	
1.3.1.2. <i>Listeria monocytogenes</i>	
1.3.1.3. <i>Yersinia pestis</i>	

1.3.1.4.	<i>Borrelia garinii</i>	
1.3.1.5.	<i>Shigella flexneri</i>	
1.3.1.6.	<i>Salmonella typhimurium</i>	
1.3.1.7.	<i>Chlamidia trachomatis</i>	
1.3.2.	Parasites subverting the migration of infected cell	
1.3.2.1.	<i>Toxoplasma gondii</i>	
1.3.2.2.	<i>Leishmania</i>	
1.3.3.	Viral proteins interfering with the cell migration	
1.4.	<i>Bartonella</i> spp.	pp.23-25
1.5.	References	pp.26-32
2.	Aim of the Thesis	pp.33-34
3.	Results and Discussion	pp.35-142
3.1.	Functional Characterization of <i>Bartonella</i> Effector Protein - BepE during <i>in vivo</i> and <i>in vitro</i> Infection	pp.35-121
3.2.	Additional work	pp.123-142
4.	Conclusions	pp.143-145
5.	Outlook	pp.146-150
6.	Acknowledgments	pp.151-153
7.	Curriculum vitae	pp.154-156

1 - Introduction

1. Introduction

The introduction highlights molecular mechanisms of the migration of eukaryotic cell and its importance for an effective immune response on the example of dendritic cells; includes a brief description of biology of dendritic cells and their migratory property. Followed with discussion how some pathogens (bacteria, viruses and parasites) favor by modulating the host cell migration properties. All in all, the introduction provides the reader of this thesis a sound basis for understanding the subsequent aspects of the results and discussion parts of the thesis.

1.1. Cell migration

1.1.1. The definition and discovery

Cell migration is an essential feature of eukaryotic life, a central process in the development and maintenance of multicellular organism. Tissue formation during embryonic development, wound healing, angiogenesis, nerve growth and immune responses - all require the orchestrated movement of cells in particular directions to specific locations. Errors during this process have serious consequences, including mental retardation, vascular disease, tumor formation and metastasis [1,2].

Cell movement was observed as early as 1675 when Anton van Leeuwenhoek discovered the tiny creatures crawling in rainwater across his microscope slide. In a letter published by the *Philosophical Transactions of the Royal Society of London*, he described living atoms that put forth little horns, extended and contracted, and had pleasing and nimble motions [3]. Despite the early discovery, the molecular mechanisms behind cell movement have become a scientific focus only in the past few decades. Advances in fluorescence microscopy, molecular biology and biochemistry have enabled the understanding of the processes underlying motility and the identification of the major proteins behind these processes [4].

1.1.2. Main steps in cell migration

Cell migration requires series of repetitive, integrated processes to produce coordinated cellular movements [2]. The migration process of cultured cells is described as a four step cycle consisting of: (i) the protrusion of a lamellipodia and filopodia, the actin rich filaments, at the leading edge. (ii) Following the protrusions, new, small, punctate sites of cell attachment to the extracellular matrix (ECM), focal complexes are formed close to the leading edge, the precursors of larger, more elongated contacts known as focal adhesion. (iii) The next event in the migratory process is acto-myosin based cell-body translocation (iv) and the final phase is the release of cell contacts at the rear of the cell (Figure 1) [5,6,7].

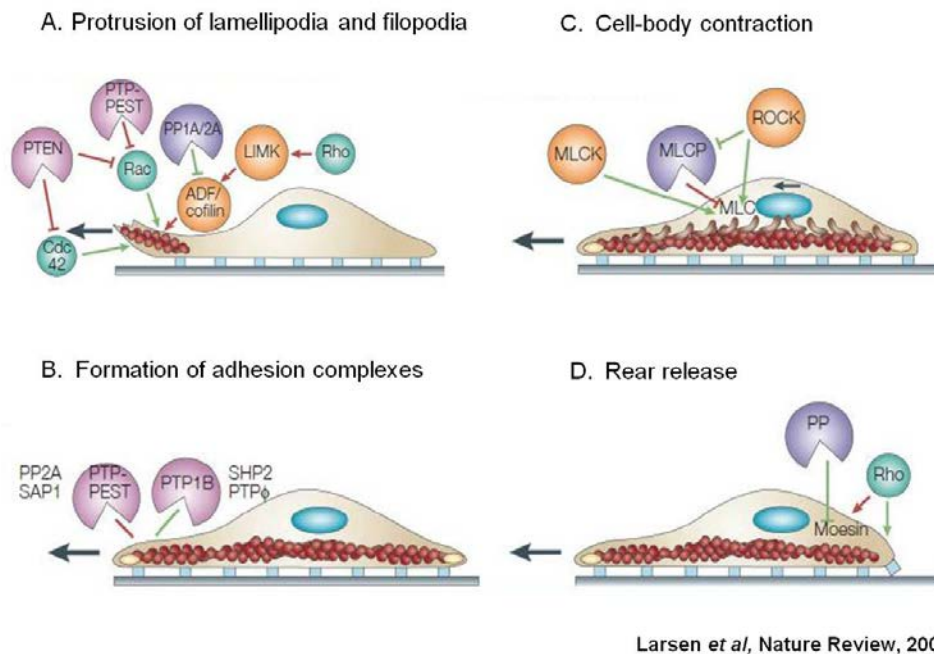


Figure 1: Major steps of endothelial cell migration.

Endothelial cell migration can be divided in 4 sequential events: A. Cdc42 dependent sensing of the motile stimuli by filopodia; cellular extension involving the Rac1-dependent formation of protruding lamellipodia; B. Attachment of the protrusions to the extracellular matrix at focal adhesions; C. Stress fiber-mediated contraction of the cell-body allowing forward progression; D. Rear release by stress fiber-mediated traction forces.

Optimal cell migration requires a quick and precise regulation by spatio-temporally integrated components in each of these 4 steps that will be discussed in followed manner.

1.1.2.1. Protrusion of lamellipodia and filopodia

Migration is initiated by protrusion of the leading edge and formation of new actin filaments. The process is dependent on an extensive remodeling of the actin cytoskeleton [2]. For protrusion, mainly two types of organelles are described, branched filaments leading to the sheet like lamellipodium and the spike like filopodium [7]. Lamellipodia as characteristic feature at the leading edge of motile cells are believed to have two major functions for cell migration. Firstly, actin polymerization closely behind the lamellipodial leading edge creates the necessary forces to pull the front of the cell in the direction of movement [8,9]. Furthermore, the formation of new adhesion structures to the substrate is described to occur closely behind the leading edge by forming focal complexes that can develop to mature focal adhesions within the lamellipodium [10]. In contrast, filopodia are thin, dynamic membrane extensions comprising tight bundles of parallel oriented, cross-linked actin filaments [11]. Their proximal parts are usually embedded in the lamellipodial actin network whereas their distal ends can either protrude beyond the leading edge or remain as microspikes within the lamellipodium [12]. Functionally, filopodia are described as structures mainly probing the substrate for proper matrix composition and therefore adhesion properties [7]. The generation of either branched or linear filament arrays is triggered by the receptors in the plasma membrane and signalling through the small GTPases such as Rho, Rac, and Cdc42. They can trigger nucleation of new actin filaments via specific downstream pathways. Rac induces lamellipodia and Cdc42 stimulates filopodia (Figure 1)[13].

The primary complex involved in branching of actin filaments is the actin-nucleating Arp (actin-related protein) 2/3 complex, which is composed of multiple F-actin-binding proteins [2]. The main activators of Arp2/3 complex are the WASP family proteins, of which the best known are Wiskott-Aldrich Syndrome Protein (WASP) and Suppressor of cyclic AMP receptor mutation/WASP and Verprolin homologous protein (SCAR/WAVE), which have multiple isoforms in mammals. WASP family proteins act as scaffolds that couple signal intermediates to the initiation of actin branches by the Arp2/3 complex, and thus allow signalling to catalyze rapid filament growth [1]. Arp2/3 complex nucleates new actin filaments in the form of branches on the sides of preexisting filaments leading to lamellipodia. Spiky filopodia can be formed in two ways: from branched networks by the

actions of actin bundling proteins such as fascin, or directly nucleated as unbranched actin filaments by the formin family of proteins [1].

Another important regulator in formation of actin containing structures is the actin depolymerizing factor (ADF)/cofilin family of proteins. ADF and cofilin are actin-binding proteins that have filament disassembly/severing activity and are required for breaking down older parts of the actin network so that the resulting globular G-actin subunits can be recycled and re-used. Furthermore, cofilin is required at the initiation of protrusion for barbed-end-mediated actin assembly at the leading edge and thereby increases levels of Arp2/3-mediated polymerization [1,14].

Various guanine nucleotide exchange factors (GEFs, which activate GTPases) and GTPase activating proteins (GAPs, which cause inactivation) provide specificity and thus allow signalling networks to drive multiple cell processes via a relatively small (around 25 in humans) set of Rho family members. Additionally, lipids and proteins in the plasma membrane provide spatial information and an additional level of control for actin-based protrusions [1].

Lamellipodia/filopodia formation is dynamically regulated by phosphatases. Rac and Cdc42 are opposed by phosphatase and tensin homologue (PTEN). Rac activation is also opposed indirectly by protein tyrosine phosphatase (PTP)-PEST [2,14,15]. The ADF/cofilin can be dephosphorylated by protein phosphatases (PP) 1A and PP2A to stimulate migration (Figure 1.A) [2].

Lamellipodia and filopodia are seen as the main types of protrusions that cells produce when moving on 2D surfaces. When cells are moving in 3D matrices, they need to squeeze through the matrix, rather than just walk across it. They frequently appear to use fat, bubble-like protrusions called blebs, which are initially driven by hydrostatic pressure rather than by actin polymerization. Cells in 3D matrices also move using pseudopods that are bulkier and rounder than the sheet-like lamellipodia seen in cells moving on flat surfaces [16-19].

1.1.2.2. Formation of focal adhesions

Adhesion site formation starts with integrin molecules binding to the extracellular matrix (ECM). These dot-like so called focal complexes (FCs) can mature and grow in size to form focal adhesions (FAs) that built up more than 100 proteins [20,21]. FA are highly dynamic

structures and are the master control machinery of cell migration [22]. They link the ECM with the actin cytoskeleton and serve as bidirectional mechanical biosensors that allow cells to integrate intracellular and extracellular cues. Additionally, closely regulated turnover of FA proteins within FA sites allows cells to respond appropriately to their environment, thereby impacting on cell shape and function [22].

Three basic categories of proteins are recruited to FAs: (i) integrin-binding proteins, (ii) adaptors and/or scaffolding proteins that lack intrinsic enzymatic activity, and (iii) enzymes. Talin is an example of a protein that directly binds to integrin cytoplasmic domains and is important for regulating integrin activation and signalling [23]. Adaptors and/or scaffolding factors, such as vinculin, paxillin, and α -actinin, link integrin-associated proteins with actin or other proteins. The enzymes that modify integrin downstream effectors include the non-receptor tyrosine kinases FAK and Src [20-24].

The transformation from FCs to FAs highly depends on regulatory tyrosine phosphorylation and dephosphorylation events (Figure 1.B) as well as on forces applied to adhesion sites by the acto-myosin contractile apparatus. Myosin inhibitors diminish adhesion formation and induce accumulation of FCs [7].

1.1.2.3. Cell-body contraction

The cell is pulled forward, mainly by contractile forces that are produced by myosin motors sliding on actin filaments, presented in the cell body and at the rear [4,25]. The contractile F-actin module extends from nascent FAs at the lamellipodium base to near the nucleus and is comprised of F-actin-myosin II networks and bundles in the lamella, convergence zone, and central cell area [26]. The slow myosin II-powered F-actin retrograde flow from the lamella and anterograde flow from the central cell region merge in the convergence zone, where F-actin remains stationary and depolymerizes [27]. This myosin II-driven actin convergence is thought to pull on strong FAs at the front to generate traction in the third step of cell migration [4,28].

1.1.2.4. Tail retraction

Trailing adhesions restrain the cell body and maintain cell spreading but they need to be released for successful cell body relocation. The regulation of adhesion turnover modulates the relative rates of association versus dissociation of molecules at adhesion

sites. Src and/or FAK kinase activity regulate the recruitment of protein complexes to adhesions. The phosphorylation of paxillin kinase linker (PKL) promotes the binding of PKL to the adaptor protein, paxillin. Paxillin likely induces adhesion turnover depending on its phosphorylation state [29].

Besides phosphorylation-associated regulation, it is likely that proteolysis of adhesion components can also contribute to the turnover process. Talin proteolysis by calpain has been shown to stimulate the dissociation of several major adhesion components, including paxillin, vinculin, and zyxin [30,31].

Coordinated asymmetry of adhesion disassembly as well as the assembly in the leading edge of the migrating cell is regulated by microtubules, which in general play a key role in the polarized distribution of signals within a cell. There are several ideas how the regulation may work. First, microtubules could facilitate adhesion disassembly by local release of tension. Indeed, the tyrosine kinase Arg, which requires microtubules for proper localization and activity, can inhibit Rho and p190RhoGAP [32], RhoA activates p160ROCK (ROCK1) that is known to be required for tail retraction [33]. Additionally, microtubules could release tensile forces by the uncoupling of adhesion proteins through calpain-driven proteolysis. Finally, the ripping off of adhesions by cell edge retraction at the rear may also be microtubule dependent since it requires myosin contractility. Contractility is strongly regulated by the microtubule-associated Rho GEFs, H1 and Lfc [34]. These GEFs reside on the microtubule lattice in an inactive form where they can be released and cause local Rho activity upon microtubule depolymerization [35].

Cell migration and the tight regulation of it have a great importance for a proper function of immune system, discussed on the example of dendritic cell migration in the following chapter.

1.2. The effective clearance of pathogen by immune system

The immune system can be broadly divided into innate and adaptive components, with extensive crosstalk between the two [36]. The innate immune response functions as the first line of defense against infections. It consists of soluble factors, such as complement proteins, and diverse cellular components including granulocytes (basophils, eosinophils and neutrophils), mast cells, macrophages (MΦs), dendritic cells (DCs) and natural killer (NK) cells. The adaptive immune response is slower to develop, but manifests as increased antigenic specificity and memory. It is mediated by CD4⁺ and CD8⁺ T lymphocytes, B cells, and antibodies [37].

The cross talk between innate and adaptive systems is made by antigen presenting cells (APC) and the cytokines secreted from different cell types of the immune system.

1.2.1. Dendritic cell – a linker between adaptive and innate immune systems

DCs are the most powerful and versatile APCs in the immune system. They acquire and process antigens (Ags). At the same time, DCs express high levels of co-stimulatory molecules in order to present Ags and drive T-cell activation effectively. In addition to initiation of the adaptive immunity, DCs fine-tune immune responses by instructing T-cell differentiation and polarization. DCs transmit a distinct set of commands to T cells that is based on their state of differentiation or maturation. The outcome of these instructions ranges from humoral to cytolytic to regulatory T-cell responses [38]. Thus, DCs are specialized in linking innate and adaptive immune systems. These unique functions of DCs are mediated by combination of different properties: localization, high phagocytic activity and mobility.

1.2.2. DC types and subsets

DCs represent a heterogenous cell population. They reside in most peripheral tissues, particularly at the sites of interface with environment (skin and mucosa), where they represent 1–2% of the total cell numbers. Additionally, in the absence of ongoing inflammatory and immune responses, DCs (migratory DCs) constitutively patrol through the blood, peripheral tissues, lymph and secondary lymphoid organs [38].

The DC system contains conventional dendritic cells (cDCs), which already have dendritic form and exhibit DC functions in steady state, and pre-DCs, that require microbial or inflammatory stimulus to further develop to DCs. Examples of pre-DCs are plasmacytoid dendritic cells (type I interferon producers DCs) (pDCs) and monocytes, (precursors of macrophages that can also serve as pre-DCs) [39].

DCs in the skin are diverse: some are resident in the dermis, named dermal DCs; some are resident in the epidermis, Langerhans cells (LCs); and others are recruited from the blood and remain only transiently in the skin before entering lymphatic vessels. LCs have been investigated in the most detail with regard to migration to lymph nodes (discussed briefly in next sub chapter 2.4.)[40].

Although the common functions of DCs are antigen-processing and T-lymphocyte activation, they differ in surface markers, migratory patterns, and cytokine output. These differences make heterogeneity of DCs, which in turn can determine the fate of the T cells they activate. The recent studies demonstrated that DCs can be derived from both myeloid and lymphoid-restricted precursors. Moreover, it has been shown recently that both cDCs and pDCs can be generated by the Flt3 expressing hemopoietic progenitors regardless of their myeloid- or lymphoid-origin [39].

1.2.3. DCs - professional Ag-presenting cells

DCs are positioned as sentinels in all peripheral tissues and accumulate at the sites of pathogen entry, where they encounter foreign antigens [40]. DCs have high phagocytic activity, both in peripheral tissues and in secondary lymphoid organs. However, DCs joined the group of phagocytes more recently [38,39,41-46].

Phagocytes represent a heterogeneous family of cells that include neutrophils, MΦs and DCs. The first two cell types are critical effectors of innate immunity, as they both are involved in the immediate clearance of pathogens through local inflammatory responses. Unlikely, DCs are not directly involved in immediate pathogen clearance. In contrary to macrophages and neutrophils, the phagocytic–endocytic proteolysis in DCs is aimed at degrading proteins “partially” (processing) rather than “totally” [46]. To achieve partial or controlled proteolysis in their endocytic pathway, DCs have developed various specializations of their endosomal and phagosomal pathways, including a tight control of the pH. The pH in phagosomes is controlled by recruitment of two multisubunit

complexes, the NADPH oxidase (NOX2) and the V-ATPase. Neutrophils massively recruit NOX2 to early phagosomes during the oxidative burst, what leads to a transient alkalization (up to pH 8) of the phagosomal lumen. The subsequent recruitment of the V-ATPase results in a rapid acidification and the pH drops to 5–4.5. In MΦs the respiratory burst is triggered during engulfment; the majority of ROS production takes place at the plasma membrane, thus the NOX2 activity is much less important than in neutrophils. A massive recruitment of the V-ATPase to phagosomes is observed very early during phagocytosis, resulting in a very strong acidification of the lumen. These processes are even different in DCs, a discrete but sustained recruitment of NOX2 to phagosomes together with low levels of V-ATPase activity provokes a stabilization of the phagosomal pH above neutrality for several hours [46]. As a result, DCs process and degrade the cargo relatively partially.

Phagocytic DCs are referred to as immature. Immature DCs express a large array of phagocytic receptors, including lectins, scavenger receptors, Toll-like receptors (TLRs) and other pattern recognition receptors (PRRs). Selective expression of different phagocytic receptors on these DC subpopulations results in the selective uptake of different particles. A signal from pathogens, often referred to as a “danger signal”, induces DCs to enter a developmental program, maturation. The maturation transforms DCs into efficient APCs and T cell activators. During this process DCs process internalized antigens into proteolytic peptides. These peptides are loaded onto MHC class I and II molecules and subsequently exposed on the surface of DCs [38]. At the same time, DCs acquire a migratory phenotype associated with the up-regulation of CCR7 (a homing chemokine receptor) and express receptors linked with DC maturation, including co-stimulatory molecules: CD40, CD80, and CD86. On the way of maturation DCs lose the phagocytic capacity and acquire immunogenic phenotype [47].

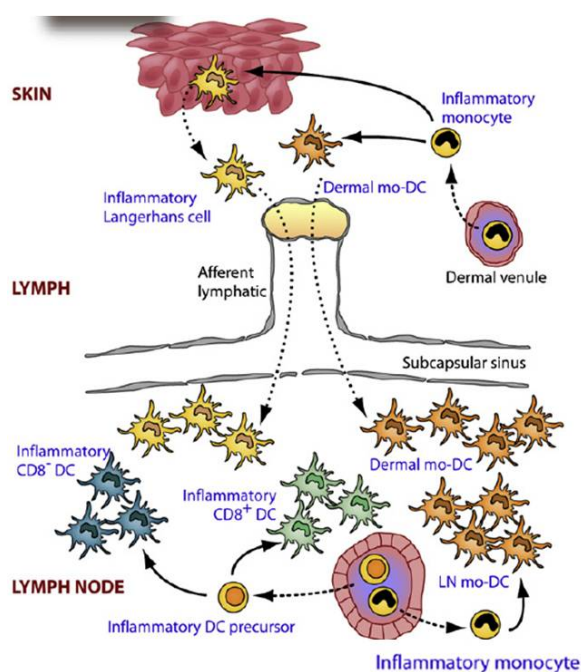
One additional feature that make DCs professional APCs is formation of DALIS (Dendritic cell Aggresome-Like Induced Structures) [44,45], an accumulation of polyubiquitinated protein aggregates in the cytosol. DALIS formation is a transient event starting 6–8 h after activation of DCs with TLR-ligands or viruses and reaching a maximum at 15 hs. After around 20–24 hs no DALIS can be found anymore. At this time, DCs are thought to have reached the draining lymph nodes and have expressed co-stimulatory molecules. Thus, DALIS can function as antigen depots which delay the antigen presentation in DCs until a proper maturation status has been achieved [44,48-50].

1.2.4. Trafficking of DCs

DCs are highly mobile cells. They are present in the right place at the right time for the regulation of immunity. Upon stimulation with foreign antigens, they readily relocate from peripheral tissues to secondary lymphoid organs to position themselves optimally with naive or central memory T cells. The trafficking of DCs to lymph nodes through afferent lymphatic vessels is crucial for the execution of their functions (Figure 2) [40,51].

Concomitant with the modifications of their antigen presentation abilities, DC maturation also induces massive migration of DCs out of peripheral tissues. The migratory phenotype of DCs includes modifications in the expression of chemokine receptors and adhesion molecules, as well as profound changes of the cytoskeleton organization.

The chemokines that arise under inflammatory conditions act on CCR1, CCR2, CCR5 and CCR6 to attract immature DCs to the affected sites. After antigen uptake, during maturation, chemokine receptor expression changes: CCR1, CCR2 and CCR5 are down-regulated and replaced by CCR7 and CXCR4, thus enabling DCs to migrate in the draining lymph nodes in response to corresponding chemokines [51].



Lopes-Bravo& Ardavin, Immunity review,2008

Figure 2: LC and dermal DC migration towards the lymph nodes (LNs) upon infection

During inflammatory reactions caused by infection, pre-existing LCs and dermal DCs rapidly migrate to the peripheral LNs and are replaced by newly formed LCs and dermal mo-DCs derived from inflammatory Ly-6C⁺ monocytes recruited to the dermis. Dermal mo-DCs are phenotypically similar to dermal DCs and also migrate to the peripheral LNs

as mature DCs. Inflammatory monocytes are also recruited to the LNs and differentiate into mo-DCs. Finally, resident inflammatory CD8⁺ and CD8⁻ DCs are also formed during infection, but their precursors have yet to be defined.

DC migration to lymphatic vessels and positioning to lymph nodes is controlled prominently by CCR7, the “gate-keeper” chemokine receptor. Study of CCR7-deficient mice revealed a marked defect in DC migration to lymph nodes. However, the expression of CCR7 alone is not sufficient for DC migration, as it can be expressed in a biologically “insensitive” state. Signals that are expected to be found at sites of inflammation, including the lipid mediators cysteinyl leukotrienes and prostaglandin E₂ and the ADP-ribosyl cyclase CD38 [52,53] are required to sensitize CCR7 to its ligands CC-chemokine ligand 19 (CCL19) and CCL21. The mechanisms by which these mediators alter CCR7 functionality is not known, but they probably trigger signalling events that, in turn, alter the signalling cascades that are engaged when CCR7 binds its ligands. The prevailing model to explain how CCR7⁺ DCs arrive at peripheral lymphatic vessels is that they respond to a chemotactic gradient of CCL19 and/or CCL21 that originates from the lymphatic vessel. But how the DCs enter the vessels, whether DC passage across the lymphatic endothelium is passive, or whether molecular interactions occur between the endothelium and the DCs, is not clear yet [51].

Some migratory DCs or their precursors from the blood can enter lymph nodes through the hematogenous route, the route that naive lymphocytes use to access lymph nodes: passage across the specialized high endothelial venules (HEVs) within lymph nodes [52].

DCs derived from a peripheral organ or lymph node can generally mobilize back into blood and ultimately home to another organ. Mechanisms to reenter the bloodstream is hypothesized and could include either direct migration across vascular endothelium in the abluminal-to-luminal direction, or failure of DCs to be trapped in lymph nodes such that they emerge into efferent lymph that accesses the bloodstream [53].

These properties of DCs can be used by different pathogens as a strategy to spread the infection throughout the host - disseminate to blood stream or even to colonize certain organs.

1.3. Pathogens modulating host cell adhesion and migration

Numbers of bacterial and parasite pathogens, various viruses are known to modulate host cell adhesion and migration properties. Some of them induce the arrest of the cell migration, such as inhibition of DC migration, thus delaying the Ag presentation properties to T cells and effective adaptive immune responses. Others induce the hyper activity of infected cell and by this promoting to the spread of the bacteria or viruses through the organism.

1.3.1. Bacterial pathogens modulating host cell migration

1.3.1.1. *Helicobacter pylori*

Infection with *Helicobacter pylori* strains bearing *cagA* (cytotoxin-associated gene A)-positive strains is the strongest risk factor for the development of gastric carcinoma, the second leading cause of cancer-related death worldwide [54]. CagA is a bacterial effector protein of *H. pylori* that is translocated via a type IV secretion system (T4SS) into gastric epithelial cells [58-60].

CagA delivery results in a dramatic cellular elongation of epithelial cells referred to as "hummingbird" phenotype, which is characterized by the development of one or two long and thin protrusions resembling the beak of the hummingbird. It has been thought that the hummingbird phenotype is related to the oncogenic action of CagA [58-62]. Pathophysiological relevance for the hummingbird phenotype in gastric carcinogenesis is that infection with *H. pylori* carrying CagA with greater ability to induce the hummingbird phenotype is more closely associated with gastric carcinoma. Bacteria disrupt the organization and assembly of apical junctions in polarized epithelial cells [55]. Elevated motility of hummingbird cells may also contribute to invasion and metastasis of gastric carcinoma [55-57,63].

In host cells, CagA interacts with the SHP-2 phosphatase, C-terminal Src kinase, and Crk adaptor in a tyrosine phosphorylation-dependent manner and also associates with Grb2 adaptor and c-Met in a phosphorylation-independent manner. Among these CagA targets, much attention has been focused on SHP-2 because the phosphatase has been recognized as a *bona fide* oncoprotein, gain-of-function mutations of which are found in various human malignancies. Stable interaction of CagA with SHP-2 requires CagA

dimerization, which is mediated by a 16-amino acid CagA-multimerization (CM)² sequence present in the C-terminal region of CagA. Upon complex formation, CagA aberrantly activates SHP-2 and thereby elicits sustained ERK/MAPkinase activation that promotes mitogenesis. Also, CagA-activated SHP-2 dephosphorylates and inhibits focal adhesion kinase (FAK), causing impaired focal adhesions. Both aberrant ERK activation and FAK inhibition by CagA-deregulated SHP-2 are involved in induction of the hummingbird phenotype [55-57].

Consistent with a model in which CagA causes cell elongation by inhibiting the disassembly of adhesive cell contacts at migrating cells lagging ends, immunohistochemical analysis revealed that focal adhesion complexes persist at the distal tips of elongated cell projections. The elongation phenomenon revealed that this phenotype is due to a cell retraction defect rather than from filopodial protrusions [63].

1.3.1.2. *Listeria monocytogenes*

Listeria monocytogenes is a facultative intracellular, gram-positive bacterium that invades humans via the gastrointestinal tract and causes bacteremia as well as a variety of materno-fetal and CNS infections [64,65,66]. It invades and grows in most of the types of host cells, including macrophages and bone marrow myeloid precursors differentiated to monocytes *in vitro* [65,66]. Interactions between *Listeria* and mononuclear phagocytes are an interesting *in vivo* paradigm of the balance between inflammation and regulation because these cells can function as bactericidal effector cells but also can be permissive for intracellular bacterial growth. In particular, Ly-6C^{high} monocytes serve as Trojan horses in the pathogenesis by transporting intracellular *L. monocytogenes* into the CNS [67].

L. monocytogenes infection increases the percentage of Ly-6C^{high} monocytes in the blood. This is in accordance with their role as the main monocyte subset that exits the bone marrow in response to peripheral demand. Ly-6C^{high} monocytes harbor the majority of cell-associated *L. monocytogenes* in the bloodstream. The mechanisms by which Ly-6C^{high} monocytes are first enriched (migrated) in to the blood and then attracted to CNS during infection is not known yet. The phenotypic similarities from functional studies indicate that Ly-6C^{high} monocytes are recent emigrants from the bone marrow. Similarly, recent studies show that the phenotype of infected monocytes in the peripheral blood is similar in many respects to that of monocytes in the bone marrow suggesting that *L. monocytogenes*-parasitized monocytes originate in the bone marrow [68].

It has been reported that CSF-1 knockout mice, which are depleted in monocytes and macrophages, show a reduced susceptibility to CNS infection by *L. monocytogenes* [69].

1.3.1.3. *Yersinia pestis*

Yersinia pestis, a gram-negative facultative intracellular bacterium, a causative agent of plague [70] and responsible for the Black Death in the Middle Ages, is primarily a rodent pathogen. It can be transmitted intradermally to humans through the bite of an infected flea. *Y. pestis* was responsible for the Black Death in the Middle Ages [71-73].

Y. pestis modulates its gene expression in a temperature-dependent manner, which is proposed to correspond to the adaptation to the two different environment, within fleas and mammals [74]. As a result, *Y. pestis* grown on 26°C (temperature of flea) and at 37°C (temperature of mammals) targets DCs differently during *in vitro* infection [71,75,76]. The activation of DCs is mediated by the nature of *Y. pestis* lipid A, the immunostimulatory moiety of LPS. Upon transition from 26°C to 37°C, *Y. pestis* modifies the structure of its cell surface lipidA [77-79]. At lower temperatures the acyl transferase LpxP enables the biosynthesis of hexa-acylated lipid A. At 37°C, *Y. pestis* LpxP is presumably not produced and/or is inactivated and lipid A becomes mostly tetra-acylated. Hexa-acylated lipid A is recognized by TLR4 on DCs of rodents. In response, TLR4 induces IL-12p40 secretion and DC migration towards the lymph nodes [71]. DCs deficient in IL-12p40 fail to migrate toward CCR7 ligands upon exposure to bacterial stimuli [80]. Because the flea-borne bacteria (on rather low temperature, close to 26°C) need to reach and initiate infection of the lymph nodes, the ability of the hexa-acylated lipid A to induce DC activation and migration would allow efficient colonization of the lymph node. On the other hand, the temperature-sensitive induction of the tetra-acylated lipid A (already in lymph nodes) could allow the bacteria to remain and grow within the lymph node without stimulating immunity as it is not recognized by TLR4, thereby enabling development of very high bacteremia [71].

1.3.1.4. *Borrelia garinii*

Spirochete Borrelia garinii is the causative agent of chronic Lyme disease. In many cases, the infection is limited to the skin and subsides even without treatment. However, in some patients, the bacterium evades the immune response and disseminates into various organs [55,81].

B. garinii-stimulated DCs *in vitro* do not migrate effectively toward CCL19 and CCL21. The mouse model of *B. garinii* infection shows that the number of DCs migrating from the infection site to draining lymph nodes is only half that induced by the control, *Escherichia coli*, infection [81]. This inhibition is due to the significant down-regulation of CD38 and CCR7 expression in DCs [52], the two important factors, needed in DC chemotaxis and migration to lymph nodes. By impairing the migratory capacity of DC, *B. garinii* could lead to poor antigen presentation in the lymphoid organs and weaken the humoral immune response directed against it. This could account for some of the immune abnormalities seen in Lyme borreliosis. LC, DC of the epidermis, are present in Erythema migrans (EM) and Acrodermatitis atrophicans (ACA), the early and late skin manifestations of Lyme borreliosis, but the MHC II expression of these cells is decreased [81].

1.3.1.5. *Shigella flexneri*

The intestinal epithelium forms a barrier against microbial invaders. However, many food borne pathogens manage to overcome all four functional elements of the barrier: commensal bacterial flora, rapid turnover of the epithelium, innate immune responses and epithelial barrier integrity [82]. *Shigella*, while colonization of intestinal barrier hijacks the exfoliation of epithelial cells, one of the mechanisms of innate immune system against bacterial invaders. *Shigella flexneri* effector protein OspE, which is highly conserved among enteropathogenic *E. coli*, enterohaemorrhagic *E. coli*, *Citrobacter rodentium* and *Salmonella* strains, is delivered into the infected cell by means of Type 3 secretion system (T3SS). It localizes to the focal adhesions and binds to integrin linked kinase (ILK). The ILK–OspE complex stabilizes integrin-containing adhesion sites by suppression of FAK phosphorylation and increase of $\beta 1$ integrin cell surface levels, thus reduces adhesion turnover and suppresses the detachment of infected cells from the basement membrane. OspE enables the pathogen to maintain an infectious foothold and bacteria evade being removed [83].

Recently, it was shown that *Shigella* invasion and presumably injection of effectors in a bystander manner (absence of invasion into the cell cytoplasm) results in the inhibition of chemokine-induced migration of T lymphocytes. The interference with T cell trafficking mediated by the effector IpgD and was dependent on its phosphoinositol 4-phosphatase activity, which leads to hydrolysis of PIP₂ with a resulting decrease of its pool at the

plasma membrane. In epithelial cells, IpgD-mediated PIP₂ cleavage is responsible for dramatic morphological changes that lead to a decrease in membrane tether force associated with membrane blebbing and actin filament remodeling [84].

1.3.1.6. *Salmonella typhimurium*

Another gastrointestinal pathogen using T3SS as a tool for manipulation of the host is *Salmonella*. The bacteria has a strategy preferentially to enter microfold (M) cells, a specialized epithelial cell types for sampling the intestinal antigens and transporting them to lymphoid cells in the underlying Peyer's Patches (PP) [85,86]. The ability of *Salmonella* to survive inside of host cells is dependent on the SPI2-encoded T3SS that injects virulence/effector proteins into host cells. Some of the SPI2 T3SS translocated effector proteins have evolved to allow intracellular bacteria to subvert the bactericidal properties of macrophages and to create a specialized *Salmonella*-containing vacuole in which it can replicate. In addition, certain SPI2 secreted effectors can specifically interfere with DC-mediated antigen presentation to CD4⁺ T cells [87,88], which are required to control bacterial replication within the host during a long-term systemic *Salmonella* infection [89]. The microarray analysis has revealed Ssel, SPI2 T3SS effector of *S. typhimurium*, as a factor for long-term systemic infection in mice. Specifically, Ssel blocks migration of macrophages and DC *in vitro*, by a mechanism that involves the interaction of Ssel with the host factor IQGAP1, an important regulator of the cytoskeleton and cell migration. *Salmonella* reduces also DC migration *in vivo* in Ssel-dependent manner. Thus, *Salmonella* uses Ssel as a novel mechanism to manipulate host cell migration to dampen the ability of the host to clear systemic bacteria [90,91].

1.3.1.7. *Chlamydia trachomatis*

Chlamydia trachomatis is an obligate intracellular bacterium responsible for the most cases of bacterial sexually transmitted infections. Three million new cases occur in the USA each year and the majority of cases (70%) are asymptomatic and not treated. Untreated, persistent infection or reinfection results in pelvic inflammatory disease, ectopic pregnancy and tubal infertility. In addition, chlamydial sexually transmitted infections enhance the transmission of human immunodeficiency virus and contribute to human papillomavirus-induced cervical neoplasia.

Prostaglandin E₂ (PGE₂) is induced by a chlamydial genital infection within epithelial cells. PGE₂ is a well-known immune regulator that has both, stimulatory and inhibitory effects on the activation of DC subsets depending on the order of exposure to PGE₂ and DC-activating stimulants [92]. The PGE₂-induced IL-10 secretion may promote but also inhibit the host response. Potentially, the enigma of the presence of increased DC migration, antigen uptake and the increase in IL-10 could be a means of promoting protective immunity while not generating destructive inflammatory responses [92].

1.3.2. Parasites subverting the migration of infected host cell

1.3.2.1. *Toxoplasma gondii*

Toxoplasma gondii is an obligate intracellular parasite of the phylum apicomplexa that causes chronic infections in up to one-third of the human population and in animals. When hosts, including humans, ingest *T. gondii*-containing cysts or oocysts, free *T. gondii* zoites are released in the gut lumen. They subsequently enter enterocytes, where they multiply and initiate the parasitic process. Enterocytes loaded with zoites secrete chemokines such as monocyte chemotactic protein 1 (MCP-1/CCL-2), macrophage inflammatory protein 1 α , and β (MIP-1 α and β /CCL3 and CCL4), as well as MIP-2/CXCL2, which recruit leukocytes in the lamina propria (LP) extravascular space. Parasites then disseminate to several distant tissues, including the brain, a major site supporting *T. gondii* progeny latency [93].

T. gondii infects a great variety of cell types including epithelial cells and blood leucocytes [94]. However, a preference for *T. gondii* to infect dendritic cells (DC) *in vitro* over other blood cells has been reported [95]. *In vitro* studies on human and murine DC revealed that active invasion of DC by *Toxoplasma* induces a state of hypermotility of infected cells, enabling transmigration of infected DC across endothelial cell monolayers in the absence of chemotactic stimuli. Infected DC exhibited up-regulation of maturation markers and co-stimulatory molecules. When migration of *Toxoplasma*-infected DC was compared with migration of LPS-stimulated DC *in vivo*, similar or higher numbers of *Toxoplasma*-infected DC reached the mesenteric lymph nodes and spleen respectively. Adoptive transfer of *Toxoplasma*-infected DC resulted in more rapid dissemination of parasites to distant organs and in exacerbation of infection compared with inoculation with free

parasites. *Toxoplasma* is able to subvert the regulation of host cell motility and likely exploits the host's natural pathways of cellular migration for parasite dissemination, during early, the acute phase of infection prior to the onset of protective host responses [6,96,97].

1.3.2.2. *Leishmania*

Leishmaniasis is one of the most diverse and complex of all vector borne diseases. At present, more than 20 species of *Leishmania* are known, which are primarily characterized by their tissue tropism (cutaneous, mucocutaneous and visceral infection). Humans, as well as small animals (e.g. rodents) and dogs, are natural reservoirs for the parasite. The parasite residing in the sand fly's salivary glands is transmitted into the upper dermis of the skin. The promastigote (infectious life stage of the parasite) are rapidly phagocytosed by MΦs and transform into the obligate intracellular life form, the amastigote. During early silent phase of 4-5 weeks, the parasites replicate (up to 1,000-fold) until finally more infectious amastigotes are released into the tissue from lysed MΦ. In the second phase, development of clinically evident lesions occurs coincident with the influx of inflammatory cells, including neutrophils, eosinophils and MΦ [98].

Although the MΦ comprise a major parasite reservoir *in vivo* and represent the primary host cell, *Leishmania* was shown to modify the motility and chemotaxis of various cells, including monocytes, polymorphonuclear neutrophils and phagocytes [99]. Agonist and antagonist effects of *Leishmania* upon cell migration and chemotaxis have been reported; this could be accounted for by the use of different strains of parasite and life cycle stages and dissimilar preparations of the parasite [100]. Products secreted by *L. major* promastigotes inhibit the motility of murine splenic DCs *in vitro* [99], and *L. major* lipophosphoglycan (LPG) inhibits migration of murine LCs [101]. Interestingly, after chronic infection with *L. donovani* in mice, there was IL-10-mediated inhibition of CCR7 expression and inhibition of DC migration from the marginal zone to the T-cell areas of the spleen, which may contribute to the development of visceral leishmaniasis [102].

1.3.3. Viral proteins interfering with the cell migration

The HIV-1 (Human Immunodeficiency Virus-1) pathogenicity factor Nef, a 25-35 kDa myristoylated protein, interferes with cell motility by blocking chemoattractant-triggered actin remodeling. The effect of Nef on cell motility occurs independently of the cellular context *ex vivo* in Nef-expressing fibroblasts and HIV-1-infected primary T lymphocytes, as well as in zebrafish PGCs *in vivo*, and represents a conserved activity of Nef proteins from various HIV-1, HIV-2, and SIV (Simian Immunodeficiency Virus) strains. Mechanistic analyses demonstrate that inhibition of actin remodeling is mediated by Nef via its ability to associate with the cellular kinase Pak2, resulting in hyperphosphorylation and thereby inactivation of the evolutionary conserved actin depolymerization factor, cofilin [104].

The cell migration may even be modified differently by pathogen at different stages of the infection. As for SIV, DC mobilization facilitates virus spread to susceptible lymph node T cell populations, whereas depressed DC function during advanced infection promotes generalized immunosuppression [105].

Vaccinia, a close relative of variola virus, the causative agent of smallpox, was used to eradicate the disease during the past century [106]. Once cells are infected, vaccinia induces a number of major cytoskeletal changes, including the reorganization of microtubules, the loss of centrosome integrity and function, the loss of actin stress fibers, and the formation of actin tails [107]. In some cell types, vaccinia infection stimulates cell migration, loss of adhesion, and the formation of long cellular extensions, which make the cells appear as if they have a neuronal-like morphology [108]. The vaccinia virus-induced phenotype is dependent on the viral protein F11L [107,109]. The expression of F11L in uninfected cells results in a loss of actin stress fibers even in the presence of activated RhoA, which suggests that it inhibits signalling by this GTPase. This inhibition is the consequence of a direct interaction between F11L and RhoA, which prevents RhoA from interacting with its downstream effectors ROCK and mDia (formin homology protein). The region of F11L, involved in Rho binding, shares essential sequence homology with that of the Rho-binding motif of ROCK. Although in contrast to ROCK, F11L interacts with both GDP- and GTP-bound RhoA [107]. One can envisage that migration of an infected cell will increase the efficiency of virus spread because extracellular virus particles associated with

the plasma membrane, which are responsible for direct cell to cell spread, will come into contact with more neighboring uninfected cells than they would if the infected cell were static [109].

1.4. *Bartonella* spp.

Bartonella species (spp.) are fastidious, gram-negative, facultative intracellular bacteria that are highly adapted to a mammalian reservoir host [110-112]. The list of *Bartonella* spp. is continuously increasing as new spp. are discovered. There are more than 22 named and numerous unnamed or candidate species known for today [113].

Commonly, *Bartonella* infection in mammalian hosts is a prolonged period of intra-erythrocytic bacteremia. Disease in the reservoir host, depending on the adaptation level to the host, varies from an asymptomatic or sub-clinical to clinical manifestations with low morbidity and limited mortality, as in case of human-specific *B. quintana* (*Bqu*) infection, or even to life-threatening severe hemolytic anemia associated with the human-specific infection by *B. bacilliformis* (*Bba*). [112].

Besides erythrocytes, endothelial cells represent another major target cell type for *Bartonellae*. The phenomenon of host-restriction is determined by the specific capacity of *Bartonellae* to preferentially infect the erythrocytes of a given mammalian host, while endothelial cells may also become infected during incidental infection of non-reservoir hosts e.g., human infection by cat-specific *B. henselae* (*Bhe*), which may lead to bacillary angiomatosis lesions where bacteria are found in close association with proliferating endothelial cells [112].

Bartonellae are mainly transmitted by arthropod vectors. Three species are known to infect and replicate in the digestive tract of their respective vectors: *Bqu* in body lice, *Bhe* in cat fleas and *Bsch* in the deer ked. The transmission strategy involves replication in the gut of the arthropod vector and excretion in the feces. There *Bartonellae* are thought to survive for several days [114]. The arthropods defecate while feeding with the blood meal. Thereby, the skin of the person (or animal) at the bitten area becomes contaminated with *Bartonella*-containing feces, where from then bacteria is inoculated in the derma of the reservoir host as the host scratches the skin and delivers the feces in underlying layers of the skin [115]. The primary infected cells in the derma or how the bacteria reach the blood system is not known yet. The blood stage life-cycle of *Bartonella* within the reservoir host was studied on the example *Btr* infection of rats by Schulein *et al.*, 2001 [116]. In this model intravenously injected wild-type *Btr* are rapidly cleared from the bloodstream. The blood stays sterile for at least three days. The *Bartonella*-infected cell type within which the bacteria reside during these three days, where they survive and

replicate is yet unknown. On day four, *Btr* re-appears in the bloodstream, adhere to and invade erythrocytes. Within erythrocytes bacteria replicate for a few rounds without shortening the lifespan of the infected cells. Approximately every five days, a new wave of bacteria enters the bloodstream and invades the erythrocytes, sustaining the bacteremia for about ten weeks. The affinity of *Bartonella* for endothelial cells *in vitro* and the fact that these cells coat the blood vessels proposes the endothelial cells being another type of cells, other than erythrocytes, to be infected *in vivo*, where the bacteria hide the first three to four days, and from where they seed into the bloodstream.

Bartonellae encode Type 4 Secretion Systems (T4SSs) as an adaptation tool for the establishment of host colonization. The Trw T4SS is essential for intra erythrocytic infection of *Btr* as it was shown in an animal model [117-119], it mediates the host specific adhesion of *Bartonella* to erythrocytes in wide range of animals [120]. Another VirB/VirD4 T4SS represents a translocation system of *Bartonella* effector proteins – Beps into the endothelial and epithelial cells *in vitro* [121]. *In vivo* functional study of one of the effectors of *Bartonella* is presented in the next chapter of the thesis.

Bhe translocates 7 Beps (BepA-BepG) into human endothelial cells. The Beps display a highly modular structure. At the C-terminus, each effector contains an approximately 140 amino acid Bep intracellular delivery (BID) domain and a short positively charged tail sequence, both together compose signal for protein translocation via T4SS [121]. Additional BID domains are present in a subset of the Beps (BepE–BepG), which apparently are not required for protein translocation via VirB, but rather have adopted effector functions within the host cell [122]. BepG exclusively consists of four BID domains. Other evident domains are present in the N-termini of BepA–BepF. BepA, BepB and BepC contain a filamentation induced by cAMP (FIC) domain. BepD, BepE and BepF, each contain tandem-repeated peptide motifs in their N-terminal regions that resemble eukaryotic tyrosine-phosphorylation motifs (Figure 3) [123].

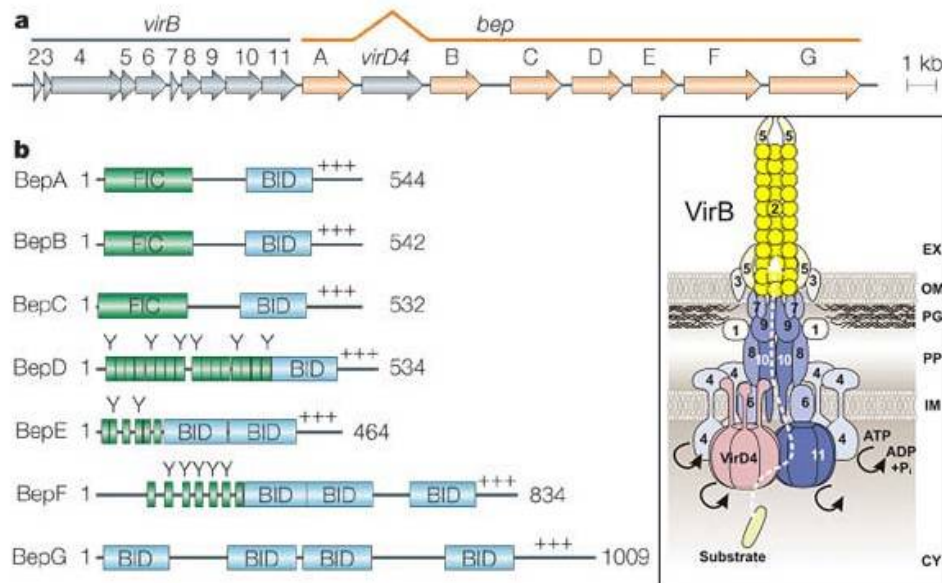


Figure 3: a) The genetic structure of the *virB/virD4/bep* pathogenicity island. b) Model of the VirB/VirD4 T4SS machinery and modular domain structure of BepA-G. Green boxes represent tyrosine-containing sequence repeats resembling tyrosine-phosphorylation motifs (indicated by Y) or FIC (filamentation induced by cAMP) domain and blue the BID (Bep intracellular delivery) domain [124].

Several functional phenotypes are known to be induced by Beps. BepA has been shown to be targeted to the host cell plasma membrane and to inhibit apoptosis in HUVECs via elevating the cytosolic concentration of the second messenger cAMP [125]. BepA FIC domain was shown to adenylylate Hela cell extracts, however exact target proteins are unknown [126]. BepD and BepE are tyrosine-phosphorylated upon translocation in ECs (Guye, 2006) [122]. The c-Src tyrosine kinase (Csk) binds to a tyrosine-phosphorylation motif, which is very similar to the Csk-binding site in VE-cadherin, in the N-terminus of BepE. Also the protein tyrosine phosphatase SHP1/2 and adaptor proteins Grb2/7 bind to BepE and BepD in a tyrosine-phosphorylation-dependent manner [123]. Thus, BepE and BepD are hypothesized to provide docking sites for cell signalling proteins once translocated into the host cell [122-123]. BepG alone (in endothelial cells, ECs) or the combinations BepC/BepF and BepC/BepG (in ECs and Hela cells) are able to promote actin rearrangements required for invasome-mediated invasion. This process seems independent of the small GTPase RhoA but relying on Rac1 and Cdc42 involving the recruitment of the Arp2/3 complex (Figure 4) [127-129].

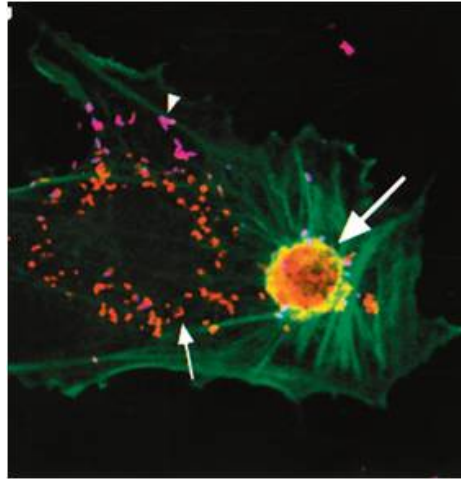


Figure 4: Invasome formation triggered by *Bhe* in HUVECs.

Extracellular bacteria (arrowheads), intracellular bacteria residing within perinuclear endosomes (small arrows) and the bacterial aggregate within the invasome structure (large arrows) [126].

Despite those striking VirB/Bep-dependent changes in ECs (current *in vitro* model), the causal role and importance of the VirB/VirD4/Bep system in host invasion is unknown mainly due to the lack of appropriate animal models for *Bartonella* strains used for effector translocation studies. The animal model with a consideration of natural host specificity and the route of transmission is needed for the studies about *in vivo* relevance of *Bartonella* effectors. These aspects are emphasized and addressed in next chapters of the thesis.

References:

1. Insall, R. H. and L. M. Machesky (2009). "Actin dynamics at the leading edge: from simple machinery to complex networks." *Dev Cell* **17**(3): 310-322.
2. Larsen, M., M. L. Tremblay, et al. (2003). "Phosphatases in cell-matrix adhesion and migration." *Nat Rev Mol Cell Biol* **4**(9): 700-711.
3. Chicurel, M. (2002). "Cell biology. Cell migration research is on the move." *Science* **295**(5555): 606-609.
4. Ananthakrishnan, R. and A. Ehrlicher (2007). "The forces behind cell movement." *Int J Biol Sci* **3**(5): 303-317.
5. Lamalice, L., F. Le Boeuf, et al. (2007). "Endothelial cell migration during angiogenesis." *Circ Res* **100**(6): 782-794.
6. Lambert, H., N. Hitziger, et al. (2006). "Induction of dendritic cell migration upon *Toxoplasma gondii* infection potentiates parasite dissemination." *Cell Microbiol* **8**(10): 1611-1623.
7. Schafer, C., B. Borm, et al. (2009). "One step ahead: role of filopodia in adhesion formation during cell migration of keratinocytes." *Exp Cell Res* **315**(7): 1212-1224.
8. Pollard, T. D. and G. G. Borisy (2003). "Cellular motility driven by assembly and disassembly of actin filaments." *Cell* **112**(4): 453-465.
9. Ponti, A., M. Machacek, et al. (2004). "Two distinct actin networks drive the protrusion of migrating cells." *Science* **305**(5691): 1782-1786.
10. Zaidel-Bar, R., C. Ballestrem, et al. (2003). "Early molecular events in the assembly of matrix adhesions at the leading edge of migrating cells." *J Cell Sci* **116**(Pt 22): 4605-4613.
11. Wood, W. and P. Martin (2002). "Structures in focus--filopodia." *Int J Biochem Cell Biol* **34**(7): 726-730.
12. Svitkina, T. M., E. A. Bulanova, et al. (2003). "Mechanism of filopodia initiation by reorganization of a dendritic network." *J Cell Biol* **160**(3): 409-421.
13. Heasman, S. J. and A. J. Ridley (2008). "Mammalian Rho GTPases: new insights into their functions from in vivo studies." *Nat Rev Mol Cell Biol* **9**(9): 690-701.
14. Bamburg, J. R. and B. W. Bernstein (2010). "Roles of ADF/cofilin in actin polymerization and beyond." *F1000 Biol Rep* **2**: 62.
15. Ichetovkin, I., W. Grant, et al. (2002). "Cofilin produces newly polymerized actin filaments that are preferred for dendritic nucleation by the Arp2/3 complex." *Curr Biol* **12**(1): 79-84.
16. Charras, G. and E. Paluch (2008). "Blebs lead the way: how to migrate without lamellipodia." *Nat Rev Mol Cell Biol* **9**(9): 730-736.
17. Charras, G. T., J. C. Yarrow, et al. (2005). "Non-equilibration of hydrostatic pressure in blebbing cells." *Nature* **435**(7040): 365-369.
18. Fackler, O. T. and R. Grosse (2008). "Cell motility through plasma membrane blebbing." *J Cell Biol* **181**(6): 879-884.
19. Mitchison, T. J., G. T. Charras, et al. (2008). "Implications of a poroelastic cytoplasm for the dynamics of animal cell shape." *Semin Cell Dev Biol* **19**(3): 215-223.
20. Berrier, A. L. and K. M. Yamada (2007). "Cell-matrix adhesion." *J Cell Physiol* **213**(3): 565-573.
21. Hu, K., L. Ji, et al. (2007). "Differential transmission of actin motion within focal adhesions." *Science* **315**(5808): 111-115.

22. Goetz, J. G. (2009). "Bidirectional control of the inner dynamics of focal adhesions promotes cell migration." Cell Adh Migr **3**(2): 185-190.
23. Calderwood, D. A. (2004). "Integrin activation." J Cell Sci **117**(Pt 5): 657-666.
24. Mitra, S. K., D. A. Hanson, et al. (2005). "Focal adhesion kinase: in command and control of cell motility." Nat Rev Mol Cell Biol **6**(1): 56-68.
25. Miao, L., O. Vanderlinde, et al. (2003). "Retraction in amoeboid cell motility powered by cytoskeletal dynamics." Science **302**(5649): 1405-1407.
26. Salmon, W. C., M. C. Adams, et al. (2002). "Dual-wavelength fluorescent speckle microscopy reveals coupling of microtubule and actin movements in migrating cells." J Cell Biol **158**(1): 31-37.
27. Vallotton, P., S. L. Gupton, et al. (2004). "Simultaneous mapping of filamentous actin flow and turnover in migrating cells by quantitative fluorescent speckle microscopy." Proc Natl Acad Sci U S A **101**(26): 9660-9665.
28. Gupton, S. L. and C. M. Waterman-Storer (2006). "Spatiotemporal feedback between actomyosin and focal-adhesion systems optimizes rapid cell migration." Cell **125**(7): 1361-1374.
29. Brown, M. C., L. A. Cary, et al. (2005). "Src and FAK kinases cooperate to phosphorylate paxillin kinase linker, stimulate its focal adhesion localization, and regulate cell spreading and protrusiveness." Mol Biol Cell **16**(9): 4316-4328.
30. Franco, S. J., M. A. Rodgers, et al. (2004). "Calpain-mediated proteolysis of talin regulates adhesion dynamics." Nat Cell Biol **6**(10): 977-983.
31. Chan, K. T., D. A. Bennin, et al. (2010). "Regulation of adhesion dynamics by calpain-mediated proteolysis of focal adhesion kinase (FAK)." J Biol Chem **285**(15): 11418-11426.
32. Peacock, J. G., A. L. Miller, et al. (2007). "The Abl-related gene tyrosine kinase acts through p190RhoGAP to inhibit actomyosin contractility and regulate focal adhesion dynamics upon adhesion to fibronectin." Mol Biol Cell **18**(10): 3860-3872.
33. Somlyo, A.V., D. Bradshaw, et al. (2000). "Rho-kinase inhibitor retards migration and in vivo dissemination of human prostate cancer cells." FEBS Lett. **269**:652-659.
34. Krendel, M., F. T. Zenke, et al. (2002). "Nucleotide exchange factor GEF-H1 mediates cross-talk between microtubules and the actin cytoskeleton." Nat Cell Biol **4**(4): 294-301.
35. Broussard, J. A., D. J. Webb, et al. (2008). "Asymmetric focal adhesion disassembly in motile cells." Curr Opin Cell Biol **20**(1): 85-90.
36. Dranoff, G. (2004). "Cytokines in cancer pathogenesis and cancer therapy." Nat Rev Cancer **4**(1): 11-22.
37. Medzhitov R, Janeway Jr C J. Innate immunity. N Engl J Med 2000; **43**: 338-344
38. Guermonprez, P., J. Valladeau, et al. (2002). "Antigen presentation and T cell stimulation by dendritic cells." Annu Rev Immunol **20**: 621-667.
39. Wu, L. and A. Dakic (2004). "Development of dendritic cell system." Cell Mol Immunol **1**(2): 112-118.
40. Randolph, G. J., V. Angeli, et al. (2005). "Dendritic-cell trafficking to lymph nodes through lymphatic vessels." Nat Rev Immunol **5**(8): 617-628.
41. Randolph, G. J., J. Ochando, et al. (2008). "Migration of dendritic cell subsets and their precursors." Annu Rev Immunol **26**: 293-316.
42. Kissenpfennig, A., S. Henri, et al. (2005). "Dynamics and function of Langerhans cells in vivo: dermal dendritic cells colonize lymph node areas distinct from slower migrating Langerhans cells." Immunity **22**(5): 643-654.

43. Rennert, P. D., P. S. Hochman, et al. (2001). "Essential role of lymph nodes in contact hypersensitivity revealed in lymphotoxin-alpha-deficient mice." J Exp Med **193**(11): 1227-1238.
44. Fassbender, M., S. Herter, et al. (2008). "Correlation of dendritic cell maturation and the formation of aggregates of poly-ubiquitinated proteins in the cytosol." Med Microbiol Immunol **197**(2): 185-189.
45. Lelouard, H., E. Gatti, et al. (2002). "Transient aggregation of ubiquitinated proteins during dendritic cell maturation." Nature **417**(6885): 177-182
46. Savina, A. and S. Amigorena (2007). "Phagocytosis and antigen presentation in dendritic cells." Immunol Rev **219**: 143-156.
47. Reis e Sousa, C. (2006). "Dendritic cells in a mature age." Nat Rev Immunol **6**(6): 476-483.
48. Herter, S., P. Osterloh, et al. (2005). "Dendritic cell aggresome-like-induced structure formation and delayed antigen presentation coincide in influenza virus-infected dendritic cells." J Immunol **175**(2): 891-898.
49. Lelouard, H., V. Ferrand, et al. (2004). "Dendritic cell aggresome-like induced structures are dedicated areas for ubiquitination and storage of newly synthesized defective proteins." J Cell Biol **164**(5): 667-675.
50. Lelouard, H., E. Gatti, et al. (2002). "Transient aggregation of ubiquitinated proteins during dendritic cell maturation." Nature **417**(6885): 177-182.
51. Lopez-Bravo, M. and C. Ardavin (2008). "In vivo induction of immune responses to pathogens by conventional dendritic cells." Immunity **29**(3): 343-35
52. Hartiala, P., J. Hytonen, et al. (2007). "Transcriptional response of human dendritic cells to *Borrelia garinii*--defective CD38 and CCR7 expression detected." J Leukoc Biol **82**(1): 33-43.
53. Martin-Fontecha, A., S. Sebastiani, et al. (2003). "Regulation of dendritic cell migration to the draining lymph node: impact on T lymphocyte traffic and priming." J Exp Med **198**(4): 615-621.
54. Lu, H., N. Murata-Kamiya, et al. (2009). "Role of partitioning-defective 1/microtubule affinity-regulating kinases in the morphogenetic activity of *Helicobacter pylori* CagA." J Biol Chem **284**(34): 23024-23036.
55. Bagnoli, F., L. Buti, et al. (2005). "*Helicobacter pylori* CagA induces a transition from polarized to invasive phenotypes in MDCK cells." Proc Natl Acad Sci U S A **102**(45): 16339-16344.
56. Hatakeyama, M. (2009). "*Helicobacter pylori* and gastric carcinogenesis." J Gastroenterol **44**(4): 239-248.
57. Al-Ghoul, L., S. Wessler, et al. (2004). "Analysis of the type IV secretion system-dependent cell motility of *Helicobacter pylori*-infected epithelial cells." Biochem Biophys Res Commun **322**(3): 860-866.
58. Segal, E. D., J. Cha, et al. (1999). "Altered states: involvement of phosphorylated CagA in the induction of host cellular growth changes by *Helicobacter pylori*." Proc Natl Acad Sci U S A **96**(25): 14559-14564.
59. Higashi, H., R. Tsutsumi, et al. (2002). "SHP-2 tyrosine phosphatase as an intracellular target of *Helicobacter pylori* CagA protein." Science **295**(5555): 683-686.
60. Hatakeyama, M. (2004). "Oncogenic mechanisms of the *Helicobacter pylori* CagA protein." Nat Rev Cancer **4**(9): 688-694.
61. Hatakeyama, M. (2006). "*Helicobacter pylori* CagA -- a bacterial intruder conspiring gastric carcinogenesis." Int J Cancer **119**(6): 1217-1223.

62. Saadat, I., H. Higashi, et al. (2007). "Helicobacter pylori CagA targets PAR1/MARK kinase to disrupt epithelial cell polarity." Nature **447**(7142): 330-333.
63. Bourzac, K. M., C. M. Botham, et al. (2007). "Helicobacter pylori CagA induces AGS cell elongation through a cell retraction defect that is independent of Cdc42, Rac1, and Arp2/3." Infect Immun **75**(3): 1203-1213.
64. Drevets, D. A., M. J. Dillon, et al. (2004). "The Ly-6Chigh monocyte subpopulation transports Listeria monocytogenes into the brain during systemic infection of mice." J Immunol **172**(7): 4418-4424.
65. Join-Lambert, O. F., S. Ezine, et al. (2005). "Listeria monocytogenes-infected bone marrow myeloid cells promote bacterial invasion of the central nervous system." Cell Microbiol **7**(2): 167-180.
66. Kolb-Maurer, A., M. Wilhelm, et al. (2002). "Interaction of human hematopoietic stem cells with bacterial pathogens." Blood **100**(10): 3703-3709.
67. Drevets, D. A., J. E. Schawang, et al. (2010). "Severe Listeria monocytogenes infection induces development of monocytes with distinct phenotypic and functional features." J Immunol **185**(4): 2432-2441.
68. Drevets, D. A. and M. S. Bronze (2008). "Listeria monocytogenes: epidemiology, human disease, and mechanisms of brain invasion." FEMS Immunol Med Microbiol **53**(2): 151-165.
69. Jin, Y., L. Dons, et al. (2002). "Colony-stimulating factor 1-dependent cells protect against systemic infection with Listeria monocytogenes but facilitate neuroinvasion." Infect Immun **70**(8): 4682-4686.
70. Perry, R. D. and J. D. Fetherston (1997). "Yersinia pestis--etiologic agent of plague." Clin Microbiol Rev **10**(1): 35-66
71. Robinson, R. T., S. A. Khader, et al. (2008). "Yersinia pestis evades TLR4-dependent induction of IL-12(p40)₂ by dendritic cells and subsequent cell migration." J Immunol **181**(8): 5560-5567.
72. Gage, K. L. and M. Y. Kosoy (2005). "Natural history of plague: perspectives from more than a century of research." Annu Rev Entomol **50**: 505-528.
73. Raoult, D., G. Aboudharam, et al. (2000). "Molecular identification by "suicide PCR" of Yersinia pestis as the agent of medieval black death." Proc Natl Acad Sci U S A **97**(23): 12800-12803.
74. Motin, V. L., A. M. Georgescu, et al. (2004). "Temporal global changes in gene expression during temperature transition in Yersinia pestis." J Bacteriol **186**(18): 6298-6305.
75. Zhang, P., M. Skurnik, et al. (2008). "Human dendritic cell-specific intercellular adhesion molecule-grabbing nonintegrin (CD209) is a receptor for Yersinia pestis that promotes phagocytosis by dendritic cells." Infect Immun **76**(5): 2070-2079.
76. Marketon, M. M., R. W. DePaolo, et al. (2005). "Plague bacteria target immune cells during infection." Science **309**(5741): 1739-1741.
77. Montminy, S. W., N. Khan, et al. (2006). "Virulence factors of Yersinia pestis are overcome by a strong lipopolysaccharide response." Nat Immunol **7**(10): 1066-1073.
78. Rebeil, R., R. K. Ernst, et al. (2006). "Characterization of late acyltransferase genes of Yersinia pestis and their role in temperature-dependent lipid A variation." J Bacteriol **188**(4): 1381-1388.
79. Kawahara, K., H. Tsukano, et al. (2002). "Modification of the structure and activity of lipid A in Yersinia pestis lipopolysaccharide by growth temperature." Infect Immun **70**(8): 4092-4098.

80. Khader, S. A., S. Partida-Sanchez, et al. (2006). "Interleukin 12p40 is required for dendritic cell migration and T cell priming after Mycobacterium tuberculosis infection." J Exp Med **203**(7): 1805-1815.
81. Hartiala, P., J. Hytonen, et al. (2010). "TLR2 utilization of Borrelia does not induce p38- and IFN-beta autocrine loop-dependent expression of CD38, resulting in poor migration and weak IL-12 secretion of dendritic cells." J Immunol **184**(10): 5732-5742.
82. Parsot, C. (2005). "Shigella spp. and enteroinvasive Escherichia coli pathogenicity factors." FEMS Microbiol Lett **252**(1): 11-18.
83. Kim, M., M. Ogawa, et al. (2009). "Bacteria hijack integrin-linked kinase to stabilize focal adhesions and block cell detachment." Nature **459**(7246): 578-582.
84. Konradt, C., E. Frigimelica, et al. (2011). "The Shigella flexneri Type Three Secretion System Effector IpgD Inhibits T Cell Migration by Manipulating Host Phosphoinositide Metabolism." Cell Host Microbe **9**(4): 263-272.
85. Kohbata, S., H. Yokoyama, et al. (1986). "Cytopathogenic effect of Salmonella typhi GIFU 10007 on M cells of murine ileal Peyer's patches in ligated ileal loops: an ultrastructural study." Microbiol Immunol **30**(12): 1225-1237.
86. Jones, B. D., N. Ghori, et al. (1994). "Salmonella typhimurium initiates murine infection by penetrating and destroying the specialized epithelial M cells of the Peyer's patches." J Exp Med **180**(1): 15-23.
87. Cheminay, C., A. Mohlenbrink, et al. (2005). "Intracellular Salmonella inhibit antigen presentation by dendritic cells." J Immunol **174**(5): 2892-2899
88. Halici, S., S. F. Zenk, et al. (2008). "Functional analysis of the Salmonella pathogenicity island 2-mediated inhibition of antigen presentation in dendritic cells." Infect Immun **76**(11): 4924-4933.
89. Tobar, J. A., L. J. Carreno, et al. (2006). "Virulent Salmonella enterica serovar typhimurium evades adaptive immunity by preventing dendritic cells from activating T cells." Infect Immun **74**(11): 6438-6448.
90. Brodsky, I. E., N. Ghori, et al. (2005). "Mig-14 is an inner membrane-associated protein that promotes Salmonella typhimurium resistance to CRAMP, survival within activated macrophages and persistent infection." Mol Microbiol **55**(3): 954-972.
91. McLaughlin, L. M., G. R. Govoni, et al. (2009). "The Salmonella SPI2 effector Ssel mediates long-term systemic infection by modulating host cell migration." PLoS Pathog **5**(11): e1000671.
92. Courret, N., S. Darche, et al. (2006). "CD11c- and CD11b-expressing mouse leukocytes transport single Toxoplasma gondii tachyzoites to the brain." Blood **107**(1): 309-316.
93. Joiner, K. A. and J. F. Dubremetz (1993). "Toxoplasma gondii: a protozoan for the nineties." Infect Immun **61**(4): 1169-1172.
94. Channon, J. Y., R. M. Seguin, et al. (2000). "Differential infectivity and division of Toxoplasma gondii in human peripheral blood leukocytes." Infect Immun **68**(8): 4822-4826.
95. Reis e Sousa, C., S. Hieny, et al. (1997). "In vivo microbial stimulation induces rapid CD40 ligand-independent production of interleukin 12 by dendritic cells and their redistribution to T cell areas." J Exp Med **186**(11): 1819-1829.
96. Scanga, C. A., J. Aliberti, et al. (2002). "Cutting edge: MyD88 is required for resistance to Toxoplasma gondii infection and regulates parasite-induced IL-12 production by dendritic cells." J Immunol **168**(12): 5997-6001.
97. Liu, W. and K. A. Kelly (2008). "Prostaglandin E2 modulates dendritic cell function during chlamydial genital infection." Immunology **123**(2): 290-303.

98. Von Stebut, E. (2007). "Immunology of cutaneous leishmaniasis: the role of mast cells, phagocytes and dendritic cells for protective immunity." Eur J Dermatol **17**(2): 115-122.
99. Jebbari, H., A. J. Stagg, et al. (2002). "Leishmania major promastigotes inhibit dendritic cell motility in vitro." Infect Immun **70**(2): 1023-1026.
100. Panaro, M. A., V. Puccini, et al. (1996). "Leishmania donovani lipophosphoglycan (LPG) inhibits respiratory burst and chemotaxis of dog phagocytes." New Microbiol **19**(2): 107-112.
101. Ponte-Sucre, A., D. Heise, et al. (2001). "Leishmania major lipophosphoglycan modulates the phenotype and inhibits migration of murine Langerhans cells." Immunology **104**(4): 462-467.
102. Brandonisio, O., R. Spinelli, et al. (2004). "Dendritic cells in Leishmania infection." Microbes Infect **6**(15): 1402-1409.
103. Nordal, H. J., S. S. Froland, et al. (1976). "Measles virus-induced migration inhibition of human leukocytes in vitro: an expression of cell-mediated immunity?" Scand J Immunol **5**(8): 969-977
104. Stolp, B., M. Reichman-Fried, et al. (2009). "HIV-1 Nef interferes with host cell motility by deregulation of Cofilin." Cell Host Microbe **6**(2): 174-186.
105. Barratt-Boyes, S. M., M. I. Zimmer, et al. (2002). "Changes in dendritic cell migration and activation during SIV infection suggest a role in initial viral spread and eventual immunosuppression." J Med Primatol **31**(4-5): 186-193.
106. Harrison, S. C., B. Alberts, et al. (2004). "Discovery of antivirals against smallpox." Proc Natl Acad Sci U S A **101**(31): 11178-11192
107. Munter, S., M. Way, et al. (2006). "Signalling during pathogen infection." Sci STKE **2006**(335): re5.
108. Sanderson, C. M. and G. L. Smith (1998). "Vaccinia virus induces Ca²⁺-independent cell-matrix adhesion during the motile phase of infection." J Virol **72**(12): 9924-9933.
109. Valderrama, F., J. V. Cordeiro, et al. (2006). "Vaccinia virus-induced cell motility requires F11L-mediated inhibition of RhoA signalling." Science **311**(5759): 377-381.
110. Chomel BB, Boulouis HJ, Maruyama S, et al. Bartonella spp. in pets and effect on human health. Emerg Infect Dis 2006; **12**: 389–394.
111. Boulouis HJ, Chang CC, Henn JB, et al. Factors associated with the rapid emergence of zoonotic Bartonella infections. Vet Res 2006; **36**:383–410.
112. Chomel BB, Boulouis HJ, Breitschwerdt EB, et al. Ecological fitness and strategies of adaptation of Bartonella species to their hosts and vectors. Vet Res 2009; **40**:29
113. Breitschwerdt, E. B., R. G. Maggi, et al. (2010). "Bartonellosis: an emerging infectious disease of zoonotic importance to animals and human beings." J Vet Emerg Crit Care (San Antonio) **20**(1): 8-30
114. Foil L., Andress E., Freeland R.L., Roy A.F., Rutledge R., Triche P.C., O'Reilly K.L., Experimental infection of domestic cats with Bartonella henselae by inoculation of Ctenocephalides felis (Siphonaptera: Pulicidae) feces, J. Med. Entomol. (1998) **35**: 625–628
115. Raoult D., Roux V., The body louse as a vector of reemerging human diseases, Clin. Infect. Dis. (1999) **29**:888–911.
116. Schulein, R., A. Seubert, C. Gille, C. Lanz, Y. Hansmann, Y. Piemont, and C. Dehio. 2001. Invasion and persistent intracellular colonization of erythrocytes. A unique parasitic strategy of the emerging pathogen Bartonella. J Exp Med **193**:1077-1086.

117. Koesling, J., T. Aebischer, C. Falch, R. Schulein, and C. Dehio. 2001. Cutting edge: antibody-mediated cessation of hemotropic infection by the intraerythrocytic mouse pathogen *Bartonella grahamii*. *J Immunol* 167:11-14.
118. Seubert, A., R. Hiestand, F. de la Cruz, and C. Dehio. 2003. A bacterial conjugation machinery recruited for pathogenesis. *Mol Microbiol* 49:1253-1266.
119. Vayssier-Taussat, M., D. Le Rhun, et al. (2010). "The Trw type IV secretion system of *Bartonella* mediates host-specific adhesion to erythrocytes." *PLoS Pathog* 6(6)
120. Saenz, H. L., P. Engel, et al. (2007). "Genomic analysis of *Bartonella* identifies type IV secretion systems as host adaptability factors." *Nat Genet* 39(12): 1469-1476.
121. Schulein, R., P. Guye, et al. (2005). "A bipartite signal mediates the transfer of type IV secretion substrates of *Bartonella henselae* into human cells." *Proc Natl Acad Sci U S A* 102(3): 856-861.
122. Pulliainen, A. T. and C. Dehio (2009). "*Bartonella henselae*: subversion of vascular endothelial cell functions by translocated bacterial effector proteins." *Int J Biochem Cell Biol* 41(3): 507-510.
123. Selbach, M., F. E. Paul, et al. (2009). "Host cell interactome of tyrosine-phosphorylated bacterial proteins." *Cell Host Microbe* 5(4): 397-403.
124. Dehio, C. (2005). "*Bartonella*-host-cell interactions and vascular tumour formation." *Nat Rev Microbiol* 3(8): 621-631.
125. Schmid, M. C., F. Scheidegger, et al. (2006). "A translocated bacterial protein protects vascular endothelial cells from apoptosis." *PLoS Pathog* 2(11): e115.
126. Palanivelu, D. V., A. Goepfert, et al. (2011). "Fic domain-catalyzed adenylylation: insight provided by the structural analysis of the type IV secretion system effector BepA." *Protein Sci* 20(3): 492-499.
127. Dehio, C., M. Meyer, et al. (1997). "Interaction of *Bartonella henselae* with endothelial cells results in bacterial aggregation on the cell surface and the subsequent engulfment and internalisation of the bacterial aggregate by a unique structure, the invasome." *J Cell Sci* 110 (Pt 18): 2141-2154.
128. Rhomberg, T. A., M. C. Truttmann, et al. (2009). "A translocated protein of *Bartonella henselae* interferes with endocytic uptake of individual bacteria and triggers uptake of large bacterial aggregates via the invasome." *Cell Microbiol* 11(6): 927-945.
129. Truttmann, M. C., T. A. Rhomberg, et al. (2011). "Combined action of the type IV secretion effector proteins BepC and BepF promotes invasome formation of *Bartonella henselae* on endothelial and epithelial cells." *Cell Microbiol* 13(2): 284-299.

2 - Aim of the Thesis

2. Aim of the Thesis

Started in December 2006, the primary aim of my thesis was to investigate *Bartonella* effector protein BepE in pathogen - natural host interaction interface. Following the establishment of the rat model of reservoir host with an intra-dermal delivery of bacteria, I identified an essential role of BepE in bacteremic colonization of the natural host. I then focused to elucidate the cellular basis how *Bartonella* fine-tunes the host manipulation by introducing BepE into the infected cells. For that, I have applied live cell imaging technics on *in vitro* infected endothelial cells with an emphasis on studding the interference of BepE with an impaired cell migration, potentially caused by other effectors proteins of *Bartonella*. Additionally, I aimed to reveal the primary infected cells in murine model of reservoir host infection to be able to translate the effect of BepE on the cells targeted by *Bartonella in vivo*.

3 – Results and Discussion

Functional Characterization of *Bartonella* Effector Protein - BepE during *in vivo* and *in vitro* Infection

Rusudan Okujava, Patrick Guye, Claudia Mistl, Florine Scheidegger, Philipp Engel, Marco Faustmann, Jing Wang, Muriel Vayssier-Taussat, Antonius Rolink and Christoph Dehio

Manuscript in preparation

Statement of own contribution

I established the animal, rat *intra-dermal (i.d.)*, infection model. All *in vitro* and *in vivo* experiments included in this manuscript were performed by me with the supervision of prof. Christoph Dehio. The time course animal experiments were carried out by me with the help of Claudia Mistl, Dr. Philipp Engel and Marco Faustmann. The fragmentation phenotype was primarily described by Patrick Guy. He contributed also with most of the mutant strains of *B. henselae* used for the experiments and did immunohistochemical staining of translocated BepE included in supplementary materials. Dr. Florine Scheidegger performed initial *in vivo intra-venous* infections with *B. tribocorum* and generated the in frame deletions of the strain as part of her master thesis. Prof. Jing Wang provided us with the sequence of *Bartonella bitlesii virB* locus annotated by me in the supplementary materials. Dr. Muriel Vayssier-Taussat helped to establish the *i.d.* animal infection model. Prof. Antonius Rolink provided us with the knowledge and material to establish *in vitro* differentiation of BMDCs. The manuscript was written by me and prof. Christoph Dehio.

Functional Characterization of *Bartonella* Effector Protein - BepE during *in vivo* and *in vitro* Infection

Rusudan Okujava¹, Patrick Guye², Claudia Mistl¹, Florine Scheidegger¹, Philipp Engel¹, Marco Faustmann¹, Jing Wang³, Muriel Vayssier-Taussat⁴, Antonius Rolink⁵ and Christoph Dehio^{1*}

¹Focal Area Infection Biology, Biozentrum, University of Basel
Klingelbergstrasse 50/70, 4056 Basel, Switzerland

²Division of Biological Engineering&Computer Science and Artificial Intelligence
Massachusetts Institute of Technology (MIT), USA

³Behavioral Genetics Center, Institute of Psychology, Chinese Academy of Sciences

⁴Unité Sous Contrat Bartonella, INRA, Maisons-Alfort, France

⁵Department of Biomedicine (DBM), University of Basel
Mattenstrasse 28, 4058 Basel, Switzerland

Corresponding author: Prof. Christoph Dehio
Focal Area Infection Biology
Biozentrum, University of Basel
Klingelbergstrasse 50/70
CH-4056 Basel, Switzerland
Tel. +41-61-267-2140
Fax: +41-61-267-2118
E-mail:christoph.dehio@unibas.ch

Condensed title: *Bartonella* effector protein – BepE

Abstract

The *bartonellae* is a family of gram negative, facultative intracellular, zoonotic bacteria that cause long lasting bacteremic infections of their various mammalian reservoir hosts. *Bartonella* uses a VirB type IV secretion system (T4SS) to translocate *Bartonella* effector proteins (Beps) into infected cells and thereby subverts host cellular functions. Here we functionally describe one of the effector proteins – BepE. An *in vivo* intra dermal (*i.d.*) model of rat infection with *B. tribocorum* (*Btr*) demonstrates a key role for BepE in the early stages of the infection in reservoir host. A *Btr* strain with two effector genes deleted ($\Delta bepDE$) did not result in bacteremia, a hallmark of reservoir host infection. Single complementation with BepE from *Btr* (BepE_{*Btr*}) or heterologous complementation with the two C-terminal BID (*Bartonella* intracellular delivery) domains of *B. henselae* (*Bhe*) BepE (BID1/2E_{*Bhe*}) was sufficient to enable *Bartonella* to reach the blood. The same dependency on the BID domains was observed *in vitro*. Primary endothelial cells (HUVECs) infected with a *Bhe* mutant lacking BepE (*Bhe* $\Delta bepE$) underwent strong morphological changes. These changes developed as a result of disturbed rear edge detachment during cell migration, a phenotype we named cell fragmentation. Cell fragmentation was not observed when infecting HUVECs with the effector-free or T4SS-mutated ($\Delta virB4$) *Bhe*, and was restored by over expression of BID1/2E_{*Bhe*} in *Bhe* $\Delta bepE$. Thus, BID1/2E_{*Bhe*} specifically interferes with the function of certain Beps secreted into the host cell during infection, thereby fine-tuning the manipulation of the host. Moreover, we were able to show the *in vitro* infectivity of primary mouse dendritic cells (DCs) with the host specific *B. birtlesii* (*Bbi*). This finding builds strong bases for future investigations to understand the nature and molecular mechanisms targeted by Beps as DCs may be the cell type primarily infected in derma and responsible to disseminate *Bartonella* into the blood.

Introduction

A number of pathogenic bacteria have evolved a variety of virulence factors as tools to manipulate the host defence system to reach a replicative niche - a safe compartment to proliferate, that ensures easy transmissibility as well. All that enables bacteria to establish a long lasting persistent infection of the reservoir host [1]. Translocation of bacterial effector proteins into the host cell is one of the mechanisms to manipulate the host by interfering with its signalling pathways. The most prominent example of that is *Helicobacter pylori* (*Hpy*). More than half of the world population is infected with *Hpy* for their lifetime in the gastric mucosa but only <20% of them actually develop peptic ulcer disease. Together with other mechanisms and by secretion of a virulence factor VacA and type IV secretion (T4SS) apparatus dependent translocation of an effector protein CagA, *Hpy* succeeds to modulate the innate and adaptive immune responses of the host [1]. Another example is *Brucella*, an intracellular pathogen able to persist for long periods of time within the host and to develop a chronic disease. A functional VirB T4SS is required for *Brucella* to establish and maintain a persistent infection in an animal model [2]. Furthermore, this locus is required for intracellular survival in macrophages and HeLa cells by controlling the maturation of *Brucella* containing vacuole (BCV) into an organelle permissive for replication [3]. There are more examples; such as *Legionella* Dot/Icm T4SS which translocates a large number of bacterial effectors into the host cell in order to establish an intracellular replication in specialized vacuoles [4]; *Salmonella* SPI1 and SPI2 type III secretion systems (T3SS) [1] and *Shigella* T3SS effectors play a critical role in invasion of non-phagocytic intestinal cells, for further dissemination and modulation of the host inflammatory responses [5,6].

Bartonella species are fastidious, gram-negative, facultative intracellular bacteria that are highly adapted to a mammalian reservoir host, within which the bacteria colonize erythrocytes as privileged host niche and develop long-lasting persistent infections [7-10]. The infections in the reservoir host range from an asymptomatic or sub-clinical (most animal-specific species) to clinical manifestations with low morbidity and limited mortality, such as human-specific *B. quintana* (*Bqu*) infections, or even to life-threatening disease, such as severe hemolytic anemia associated with the human-specific infection by *B. bacilliformis* (*Bba*) [9,11].

Besides erythrocytes, endothelial cells represent another major target cell type for *Bartonellae*. The host-restriction is predominately determined by the specific capacity of a *Bartonella* species to preferentially infect the erythrocytes of a given mammalian host, while endothelial cells are known to become infected during incidental infection of non-reservoir hosts e.g., human infection by cat-specific *Bhe*, which may lead to bacillary angiomatosis, lesions where bacteria are found in close association with proliferating endothelial cells [9,11,12].

Bartonellae transmission is mediated by blood sucking arthropod vectors. The strategy involves replication of bacteria in the gut of the arthropod vector and excretion in the feces, with subsequent survival in the environment for several days [13]. The arthropods usually defecate when feeding and provide a source of local irritation that result in itching, followed by scratching and inoculation of *Bartonella*-containing feces into the derma [14]. Later, *Bartonella* is known to appear in the blood of reservoir host, invades erythrocytes and stays hidden from immune clearance for more than a year for some species. Nevertheless, which cells are infected before the onset of blood infection is not clearly understood yet [11,15].

Bartonellae evolved two T4SSs (Trw and VirB) while adapting to the wide range of mammalian host colonization. Both of them are essential for host interaction but at different stages of the infection cycle [15-18]. In more details, the Trw system seems to mediate the host specific adhesion of *Bartonella* to erythrocytes by binding to the cell surface with its manifold variants of pilus subunits [19,20], while the VirB system translocates a cocktail of evolutionarily related effector proteins, Beps, into the host cell. The Beps are encoded within the *virB* locus of *Bartonellae* (named BepA-G in *Bhe*). They have been evolved by duplication of an ancestral *bep* gene followed by their functional diversification and conservation of certain domains and motives [16]. All Beps have at least one BID domain (*Bartonella* intracellular delivery domain) and a positively charged tail in the C-terminus as a signal for translocation through the T4SS [21]. Beps have been intensively studied *in vitro* in the human endothelial cell infection model where they are able to subvert multiple physiological functions, such as actin dynamics, innate immune responses and apoptosis [21-25].

BepE is one of the effector proteins, conserved within many species of *bartonellae*. *Bhe* BepE (BepE_{Bhe}) consists of 464 aa. The N terminus of BepE_{Bhe}, similarly to BepD_{Bhe} and BepF_{Bhe}, contains short repeated peptide sequences (EPLYA) with conserved putative tyrosine phosphorylation sites, similar to the EPIYA motive of *Hpy* effector CagA. BepE_{Bhe} has two BID domains in the C-terminal part [21]. The use of a model mimicking the incidental host invasion revealed some SH2 domain-containing eukaryotic interaction partners for BepE_{Bhe}. The kinase Crk, cellular phosphatases SHP1/2 and adaptor proteins Grb2/7 were identified to interact with the N-terminal phosphotyrosines of BepE_{Bhe} within a Csk like binding domain and an ITIM/ITSM (immunotyrosine inhibitory motif/immunotyrosine switch motif) tandem of the effector protein [26]. These specific motives of BepE_{Bhe} and the described interaction partners suggest a molecular mimicry of ITIM-containing receptors by bacterial protein. The fact that reservoir host infection is long lasting and displays almost no clinical manifestations indicates an efficient adaptation of *Bartonella* to the host niche and increases the interest to BepE to be investigated *in vivo* in the reservoir host infection model as a potential immune modulatory molecule.

Bartonella-reservoir host interaction has been studied in a rat model developed by Schulein *et al* [15]. In this model, intravenously (*i.v.*) injected wild-type *Btr* are rapidly cleared from the bloodstream, which remains sterile for at least three days. On day four, the bacteria re-appear in the blood, adhere to and invade erythrocytes, where they replicate for few rounds without shortening the lifespan of red blood cells. Approximately every five days, a new wave of bacteria enters the bloodstream and invades the erythrocytes, sustaining the bacteremia for about ten weeks. This is in accordance with other animal models, such as *B. grahamii* (*Bgr*) *i.v.* infection of mice [27]. The affinity of *Bartonella* to endothelial cells *in vitro* and the fact that these cells coat the blood vessels, proposes the endothelial cells as another type of cells, other than erythrocytes, to be infected *in vivo*, where the bacteria hide the first three to four days, and from where they seed into the bloodstream. Rat *i.v.* infection model is a good model to study the long lasting colonization of blood by *Bartonella*. However, this model does not account for the first stages, the first interface of bacterial interaction with the immune system, as *Bartonella* is delivered directly into the blood stream. Recently, an intra-dermal (*i.d.*) infection model of *Bbi* has been introduced by Marignac *et al* [28], where the bacteria are inoculated in the derma of the ear. This model more likely reflects the natural route of

infection, mimicking the animal scratching a bitten area. Although not experimentally supported yet, the primary niche may comprise primary immune cells in the derma e.g. migratory cells such as dendritic cells which might assist the passage of bacteria from the site of inoculation to the lymphatic-blood system.

In this study, we identify BepE as a critical bacterial factor for the early stages of *Bartonella* reservoir host invasion, prior the establishment of bacteremia. We found that BepE enabled the otherwise abacteremic - *Btr* Δ *bepDE* strain to reach the blood. This specific function was assigned to the C-terminal part of BepE_{Bhe} including the two BID domains. The same BID domains are interfering with the fragmentation phenotype of an infected endothelial cell; an *in vitro* observation induced by the other Beps as a secondary effect. Heterologous complementation of BepE loss-of-function phenotypes from different species either *in vivo* or *in vitro* strongly supports the idea that BepE has been evolved as a fine-tune mechanism to regulate host cell manipulation by *Bartonella* while colonizing its own reservoir mammalian host. Further, we show that *Bartonella* translocates the effector fusion protein into dendritic cells. Indicating that these cells could represent one of the cell-types infected in the animal before *Bartonella* reaches the blood system.

Results

The *intra-dermal* rat infection model mimics the natural way of *Btr* infection

Previous work gives some evidence that *Bartonella* effector protein BepE_{Bhe} could be a molecular mimicry of the immune inhibitory receptors. The work, based on *in vitro* studies in endothelial cell infection model, shows that BepE_{Bhe} is indeed translocated into the infected cell via T4SS and localizes to the plasma membrane (suppl. Figure 1). There it is tyrosine phosphorylated by cellular kinases at specific tyrosines within the motives that show similarity to Csk-like motive and ITIM/ITSM tandem of eukaryotic cells receptors [26]. Thus, BepE could potentially interfere with the host immune response during the establishment of *Bartonella* infection by modulating the signaling pathways in immune cells. To assess the immunomodulatory capacity of BepE we decided to investigate it *in vivo* during the infection of the reservoir host. First we aimed to establish a suitable animal model, to closely mimic the natural way of transmission of *Bartonella*, taking into account the site of the infection and the specificity of *Bartonella* species to its reservoir host with its characteristic erythrocytic and asymptomatic long lasting infection. Thus, we decided to adapt the existing rat persistent intra venous (*i.v.*) infection model (established by Schulein *et al*, 2001) [15] to the mouse intra dermal (*i.d.*) model (Marignac *et al*, 2010) [28]. We introduced the intra dermal way of bacterial inoculation in the ear dermis of a rat using *Btr* for the infection. The rat is a susceptible host for *Btr* and at the same time a convenient animal model to monitor the development of blood infection in time course. The derma, the underling layers of the skin, is the first site where *Bartonella* is inoculated during the infection of the mammalian reservoir host via the feces of the arthropod vector and the place where *Bartonella* has to interact and infect other cell types than erythrocytes, the so far known cells to be infected in reservoir host. In contrast to this new model of infection, the previously established *i.v.* model, inoculation of *Bartonella* directly into the tail vein, is lacking an important stage – the cell-bacteria interactions that need to take place before bacteria enter the blood system.

First we decided to compare the two routes of infection; *i.d.* versus *i.v.* and monitor the bacteremia of infected animals. As a first observation after infection, during the first few

days, the infected animals did not develop the redness or any other sign of inflammation at the site of inoculation on the ear or on the tail. To follow the time course of infection and the bacterial titer in the blood of the rats, the blood from tail vein of infected animals was sampled. Sodium-citrate supplemented blood samples were lysed by freezing at -70°C and serial dilutions of lysed blood in phosphate buffered saline (PBS) were plated on columbia agar plates with defibrinated sheep blood (CBA) to count the colony forming units (CFUs) per mL of blood. In the group of *i.d.* infected rats, *Btr* was first detected in the blood starting at day 7-8 post infection (dpi) and it reached around 10^6 bacteria /mL blood the next days (10 dpi). After 30 dpi bacterial titer started to decrease and in 10 weeks of followed bacteremia *Bartonella* was almost cleared away from the blood system. This was in accordance with the consequences described previously in *i.v.* infection (by Schulein *et al*, 2001). Compared to *i.v.* infection a delay of about 4-5 days in time was observed until bacteria appeared in the blood of the ear inoculated animals. But once *Btr*, in *i.d.* infected animals, was already in the blood, it immediately reached almost as high titers as in case of *i.v.* infection (around 10^6 - 10^7 *Bartonella*/mL of blood).

The delay in blood colonization in the *i.d.* infection route clearly corresponds to the way that *Bartonella* has to make before seeding into the blood system to be taken up by innate immune cells and probably transported to the lymphatic-blood system.

***Btr* Δ bepDE loses the ability to colonize rat blood in *i.d.* infection**

Having an ideal persistent infection model for *Bartonella in vivo* studies, we decided to examine the role of BepE in the development of the infection. We therefore used a *Btr* strain that has an in frame deletion of *bepD* and *bepE*. BepD_{*Btr*} and BepE_{*Btr*}, both are homologs of BepE_{*Bhe*} and show high similarity in regards of having putative tyrosine-containing motives and the BID domains (suppl Figure 2).

Three groups of rats were injected intradermally either with PBS (mock) or with PBS solution containing *Btr* wild type (wild-type) or *Btr* Δ bepDE. Blood samples were collected from the tail vein with an immediate sodium-citrate supplementation at different time points up to 10 weeks (Figure 2). The blood was frozen to lyse red blood cells. Undiluted and serial dilutions of thawed blood in PBS were plated on CBA to enumerate colony

forming units (CFU) per mL of blood. Plotted graphs represent a time course for single infected animals from which bacteria were recovered at a given time point post-infection. Almost all *Btr ΔbepDE*-infected animals stayed abacteremic. In one case (one in 13 *Btr ΔbepDE* infected animals, combined results from 3 independent experiments) bacteria appeared in the blood with few days delay compared to rats infected with wild-type, but when the knockout strain actually reached the blood system it was as successful as wild-type in colonization of blood showing high titers of bacteremia.

In contrast to this observation, *Btr ΔbepDE* when directly delivered into the blood stream of rats by *i.v.* infection, behaved as wild-type (Figure 3.A).

The clones retrieved from the rat tail vein blood were confirmed by PCR for the absence of the knocked out effectors to verify that the strain from the one animal that showed delayed colonization of blood was really *Btr ΔbepDE* and not the wild-type by miss handling (suppl. Figure.3).

These data suggest that either one of the missing effectors in *Btr ΔbepDE*, BepD_{Btr} or BepE_{Btr}, or both of them, are of pivotal importance for *Bartonella* to colonize the reservoir host. Even more, there appears to be a cell type(s) in the dermis, other than erythrocytes, that is targeted by *Bartonella*. *Btr ΔbepDE* does not succeed within these cells, as the strain is not able to reach the blood.

Expression of BepE alone in *Btr ΔbepDE* restores the bacteremia

To further investigate the *Btr ΔbepDE* mutant strain in *i.d.* rat infection, complementation experiments were designed by expressing either both BepD_{Btr} and BepE_{Btr}, or single effector BepE_{Btr} *in trans* on the plasmid under the control of their native promoter. The blood was sampled at two time points, at 10 (suppl. Figure 4) and day 16 dpi (Figure 3). Previous experiments showed that at day 10 wild-type *Btr* was able to reach high titer in the blood (Figure 1 and 2). The second time point was chosen to avoid missing any late seeding in rat blood as it was observed in a single case in *Btr ΔbepDE* infected animal.

As shown on Figure 3, *pbepDE_{Btr}* complementation was able to restore the Δ *bepDE*-phenotype to wild-type infection level and even the expression of *BepE_{Btr}* alone was sufficient to complement the *Btr* Δ *bepDE* mutant.

Moreover, heterologous complementation was performed with *Bhe* *BepE*. At protein level *BepE_{Bhe}* was well expressed in *Btr* (Figure 4.B). In rat infections *BepE_{Bhe}* was able to functionally replace *BepE_{Btr}* and bring back the capability of *Btr* Δ *bepDE* mutant to colonize the blood stream (Figure 3). The *Beps* from *Bhe* and *Btr* are homologs of each other, *BepE* and *BepD* from both species share conserved tyrosine containing motives on their N-terminus and a C-terminal BID domain. The amino acid sequence similarity to *BepE_{Bhe}* for *BepD_{Btr}* is 22,7%, while for *BepE_{Btr}* it is slightly higher - 35,6% (suppl. Figure2).

Plasmid complemented *Btr* strains from infected rats were checked for the stability of the plasmid. For this, the blood from infected animals was plated on CBA plates with/without plasmid resistance marker (suppl. Figure 5). From CFU numbers counted on both plates we could observe that during the colonization of red blood cells *Bartonella* tends to lose the plasmid encoded *BepE* and *BepD*, suggesting that there is no selection pressure any more in the blood to keep the plasmids.

The BID domains of *BepE_{Bhe}* are sufficient to enable *Btr* to reach the blood

To elucidate which part of the *BepE* molecule is responsible for the complementation of abacteremic phenotype of the *Btr* Δ *bepDE*, different mutant forms of *BepE_{Bhe}* were over expressed in the *Btr* Δ *bepDE* background and then the infectivity of those *Btr* strains was examined in the rat *i.d.* model. Two mutants of *BepE_{Bhe}* were chosen, one with all five tyrosines exchanged to phenylalanine (Y_{37,64,91,106,129}->F) and the second, a truncated version of *BepE_{Bhe}*, with only the two BID domains and positively charged C-tail. Plasmids encoding the mutated *BepE_{Bhe}* were conjugated into *Btr* Δ *bepDE* and the expression of the *BepE_{Bhe}* protein was confirmed by western blotting (Figure 4.B). Heterologous complemented *Btr* Δ *bepDE* were administered in the ear of the rats. The Figure 4.A shows the CFUs per mL of rat tail vein blood of the animals infected with *Btr* Δ *bepDE* strains complemented with *BepE_{Bhe}* and *BepE_{Bhe}* mutants at 16 dpi. Similar results were obtained at 10 dpi (suppl. Figure 6).

The *Btr* strain with the tyrosine to phenylalanine exchanged mutant of BepE_{Bhe} could colonize the blood almost with the same titers as wild-type *Btr* and *Btr* Δ bepDE-pBepE_{Bhe}. The bacteremia was also observed for the strain that contained only the two BID domains and positively charged C-tail of BepE_{Bhe}. Thus, the tyrosine containing motives of BepE_{Bhe} and the N-terminal part seem not to be essential for *Bartonella* to reach the replicative niche in the reservoir host and the functional part of BepE in this system can be assigned to the BID domains.

Infection of endothelial cells with *Bhe* Δ bepE (or Δ bepDEF) leads to the fragmentation of endothelial cells

Another well-established model to study *Bartonella* is *in vitro* infection of human umbilical vein endothelial cells (HUVECs) with *Bhe*. The model was established in Prof. C. Dehio's group to study the molecular mechanisms of *Bartonella*-incidental host cell interaction and the modulation of host cell signaling by *Bhe* effector proteins, including tumorigenic vasoproliferations [23-26,31]. Despite being a model for bacteria-incidental host interaction, HUVECs can serve as a model to study the cellular basis of the BepE effect observed *in vivo*. By this we change the host specificity and further findings that we may observe from HUVEC *in vitro* infection model, have to be validated on reservoir host cells that are infected by *Bartonella* in nature. However BepE could possibly have a dual function in both, incidental and reservoir host infection.

To explore the BepE function in the infection of HUVECs, a *Bhe* mutant with an in-frame deletion of BepE (Δ bepE) was used. Compared to wild-type *Bhe* infection, late time points post infection showed striking changes in the morphology of the infected cells if infected with the Δ bepE mutant. Δ bepE-infected cells looked more elongated and often two parts of a cell remained connected only by a thin fiber-like structure, (as if two or more spots of the cells strongly adhered to the surface with focal adhesion complexes). Fragments of the cells without the nucleus were observed. We described this phenomenon as a fragmentation of the cell (Figure 5 and 6). A similar phenotype, even with a stronger effect, was observed when using a Δ bepDEF mutant of *Bhe* (Figure 5).

The fragmentation of HUVECs was followed and assessed in time with time lapse movies. For that we first generated HUVEC cells expressing mCherry LifeAct using Lenti viral vectors to visualize the actin cytoskeleton of the cells. Actin fluorescent cells were infected either with GFP-expressing *Bartonella* or *Bartonella* without fluorescence. Infected cells were monitored for 72 hours starting acquisition at 8 hours post infection (hpi). Infection with the *Bhe* mutants mentioned above showed a prominent phenotype, with the effect starting about 20-24 hpi. The *Bhe* (either wild-type or the mutant) infected cells formed filopodia and lamellipodia in the leading edge of the cell. The leading edge firmly adhered to the surface and the cell elongated. Next, the cell contracted and the rear edge detachment had to take place. *Bhe* Δ *bepE* (or Δ *bepDEF*) infected cells showed difficulties to detach from the surface while the cell was still actively moving forward, thus the cell became more and more elongated and at some point the thin connection between the cell body and rear broke, left a fragment behind. The cell body got smaller by continuous fragmentation. The fragments roamed on the substrate for a few hours and then came to a halt (for the movies of uninfected, wild-type *Bhe*, *Bhe* Δ *bepE*, and *pBepE_{Bhe}* complemented strain infected HUVECs see suppl. movie 1 on the CD attached and Figure 6).

The fragmentation of infected cells was observed in wild-type *Bhe* infection as well but rather on late time points, starting after 48 hpi.

BepE_{Bhe}* alone is sufficient to complement the fragmentation phenotype of *Bhe* Δ *bepDEF

BepD_{Bhe}, *BepE_{Bhe}* and *BepF_{Bhe}* are the three Beps from *Bhe* harboring tyrosine containing motives and they show similarity to eukaryotic SH2-binding domains. Having these features all three of them could function as a mimicry of immune inhibitory receptors [62,63] and be involved in modulation of host signaling pathways. To test the hypothesis single complementation *in trans* was used for infections to see which Beps individually or in combination would be able to restore the fragmentation phenotype of the *Bhe* Δ *DEF* strain.

The phenomenon described above was not present in the case of *Bhe* Δ *bepE* or Δ *bepDEF* strains complemented with plasmid encoded BepE_{Bhe}. Neither BepD_{Bhe} nor BepF_{Bhe} without BepE_{Bhe} could functionally complement Δ *bepDEF* (Figure 7).

The two BID domains of BepE_{Bhe} can interfere with the fragmentation of ECs

As the inhibition of cell fragmentation could be linked specifically to BepE_{Bhe}, the next question to answer was whether it is associated to the N-terminal tyrosine containing motives or to the BID domains of BepE_{Bhe}. As described earlier, BepE_{Bhe} has two *Bartonella* Intracellular Delivery (BID) domains on its C-terminus and positively charged C-tail. The BID domain together with the C-tail is a translocation signal recognized by the T4SS of *Bartonella* [21].

To understand which part of BepE_{Bhe} was responsible for the effect observed during the infection of HUVECs, BID1/2E_{Bhe} and BID2E_{Bhe} were expressed in *Bhe* Δ *bepE* (Δ *bepDEF*) (Figure 8 D) and then used to infect HUVECs.

The BID domains (BID1E_{Bhe} and BID2E_{Bhe}) of BepE_{Bhe} show high similarity (pair wise identity is 53.3%) (Figure 8 B) and seem to be originated from a duplication event [15].

The results of the HUVECS infected with BID domain complemented strains indicate that the effect observed by BepE_{Bhe} was indeed mediated specifically by the two BID domains of BepE_{Bhe}. Compared to the two domains expressed together the last single BID alone was not efficient to overcome the fragmentation (Figure 8 A and C).

Fragmentation of ECs can be rescued by heterologous complementation of BepE_{Bhe} by BepE_{Btr}, BepE_{Bqu} and BepH_{Bgr}

Since both phenotypes connected to the BepE are related to the BID domains and we have seen that BepE_{Bhe} is functionally replacing the BepE_{Btr} in the rat *i.d.* model, we were interested to see if *Btr* homologs of BepE_{Bhe}, BepD_{Btr} and BepE_{Btr} could also complement

the *in vitro* phenotype of the *Bhe* Δ *bepE* (Δ *bepDEF*). Next to *Btr* homologs we used heterologous complementation from *Bqu* (BepE_{Bqu}) and *Bgr* (BepH_{Bgr}). For the amino acid sequence similarity of BID domains of BepE homologs see suppl. Figure 2. Compared to other homologs the BID domain of BepD_{Btr}, has less amino acid sequence similarity to the BID domains of BepE_{Bhe}.

BepE from *Btr* (BepE_{tr}), *Bqu* (BepE_{qu}), and *Bgr* (BepH_{gr}) were also able to complement the lack of BepE and infected HUVECs looked like wild-type *Bhe* infection. Amongst all the homologs of BepE_{Bhe} the BepD_{Btr} was less potent to prevent cell fragmentation (Figure 9.A and B).

Ectopic expression of BepE_{Bhe} in ECs abrogates the cell fragmentation

As all *in vitro* complementation experiments to rescue the fragmentation phenotype were based on expression of BepE_{Bhe} by plasmid in *Bartonella*, one could think induction of over expression as such may interfere with the secretion of the other Beps via T4SS actually responsible for the fragmentation of infected cells. Previous experiments showed that fragmentation is effector dependent (infection with a VirB/T4SS defective mutant of *Bhe* does not lead to fragmentation, suppl. movie 4, see CD attached), is not linked to BepA_{Bhe} (*Bhe* Δ *bepB-G* strain is not leading to the disorganization of EC migration, data not shown), BepD_{Bhe} and BepF_{Bhe} but connected to the lack of BepE_{Bhe} (Δ *bepDEF* and single in trans complementation infections described above on Figure 7). Thus, three candidates are left BepB_{Bhe}, BepC_{Bhe} and BepG_{Bhe} that may affect the cells alone or in combination even with BepA_{Bhe}.

To prove that BepE_{Bhe} effect was specific to its function and not due to the passive outcome of being expressed in large amounts and consequently competing with other effectors for the translocation, we decided to transfect HUVECs by nucleofection method and express CMV promoter driven *gfp-bepE_{Bhe}* and then infect HUVECs with *Bhe* Δ *bepE* (Δ *bepDEF*). Using this approach we introduced BepE_{Bhe} into HUVECs in a T4SS-independent way. Thus the other Beps from *Bartonella* would not be affected in the translocation.

GFP-BepE_{Bhe} ectopic expression was evaluated by FACS measurements and confocal microscopy (Figure 10.A). After 24h post transfection more than 50% of the cells were expressing GFP-BepE_{Bhe}.

Confocal microscopy of GFP-BepE_{Bhe} expressing HUVECs showed the localization of BepE_{Bhe} to plasma membrane with a clear exclusion of signal in the nucleus. In addition we observed a new phenotype for BepE_{Bhe}-expressing cells. They were rather flat and dispersed compared to untransfected or plain GFP-expressing cells (Figure 10.B). This phenotype was a specific effect of BepE_{Bhe} on primary endothelial cells but was not further investigated in this study.

24 hours post transfection (hpt) HUVECs expressing GFP or GFP-BepE_{Bhe} were infected either with *Bhe* wild-type, or $\Delta bpeE$ ($\Delta bpeDEF$). The infection was fixed at different time points and analysed by confocal microscopy (Figure 11).

In control samples, where the plain GFP encoding plasmid was transfected, we still observed the fragmentation of green cells induced by *Bhe* $\Delta bpeE$ (or $\Delta bpeDEF$, suppl Figure 8) infection (Figure 11). In contrast to that, the cells ectopically expressing GFP-BepE_{Bhe} did not undergo fragmentation. Interestingly, within the same samples untransfected cells, the cells that did not express GFP-BepE_{Bhe}, underwent the fragmentation upon infection with knockout strains of *Bhe*. Similar results were observed when GFP-BepE_{Bhe} transfected cells were infected with *Bhe* $\Delta bpeDEF$, T4SS independent expression of BepE_{Bhe} also rescued *Bhe* $\Delta bpeDEF$ -infected HUVECs from fragmentation (suppl. Figure 8).

***Bbi* infects *in vitro* differentiated mouse BMDCs**

In vivo experimental data from rat *i.d.* model suggested a role for BepE in the establishment of infection at the early stages, prior to the invasion of blood. In addition, *in vitro* experiments showed that BepE was essential to inhibit the fragmentation of infected primary endothelial cells by interfering with the effect of other Beps.

For a better understanding of BepE function in the infected cells and to further investigate the fragmentation phenomenon it is critical to reveal which cells are targeted

by *Bartonella in vivo* prior entering the blood. Assuming, that the bacteria are transmitted by arthropods from one reservoir host to another and the first site of infection is the derma, we can speculate that primary infected cells are innate immune cells in the skin. Neutrophils, dendritic cells and macrophages are the cells that should encounter the bacteria at the infected site. In the *i.d.* infection model *Bartonella* is detected in the blood at day 7. *Bartonella* has to migrate from derma to the blood system in order to establish a complete scenario of the reservoir host colonization. The candidate cell type for primary infected cell by *Bartonella* needs the capability to migrate from the site of infection towards the lymph nodes. Such a candidate is a dendritic cell. Dendritic cells (DCs) have high phagocytic activity in peripheral tissues and secondary lymphoid organs. The pH change in lysosomal granules is also rather moderate (7,2-7,4) compared to neutrophils (from pH8 sudden drop to pH5-4,5) and macrophages that have a very strong acidification of lysosomal lumens. DCs are professional Ag presenting cells to mount an effective immune response. They mediate the link between innate and adaptive immune responses and are “the decision makers” for the type of immune reactions [32,33]. These features make them attractive targets for some bacterial pathogens to hijack their functions and use them as Trojan horses during the invasion of their mammalian host [34].

To tackle the DCs as possible candidates for the primary infected cells we decided to assess the infectivity of bone marrow derived DCs *in vitro*. The rat intra dermal model is a very convenient persistent infection model of natural host to study pathogen-reservoir host interaction. It allows a good handling of the tail vein blood sampling in time course experiments of bacteremia. Thus, it is a perfect tool for the investigation of *Btr* and some *in vitro* characterized BepE_{Bhe} mutants. But on the other hand, in order to characterize and find primary infected cells *in vivo* we opted for the mouse model of *i.d.* infection [28]. Available reporter, *Rosa 26-loxP-egfp* Balb/c mouse line (from Matthias Mueller, Novartis pharma) adds the value of tools for such investigations. These mice have a floxed stop signal between β -actin promoter and *egfp*. At the same time, we already know that NLS-Cre-BID fusion protein has the ability to be translocated by the T4SS of *Bartonella* into the infected cells [21]. Thus, we assumed that the infection with a *Bbi* strain (*Bbi-Tn-cre*) that encodes a *NLS-Cre-BID* fusion in the chromosome after transposon mutagenesis should recombine the floxed sites and allow GFP to be expressed. By this method any type of nucleated cells targeted by *Bbi* could be visualized by microscopy or flow cytometry.

In order to show *in vitro* infectivity of bone marrow differentiated dendritic cells (BMDCs) by *Bbi* bone marrow cells from, *Rosa 26-loxP-egfp* Balb/c mouse were cultured for 10 days in the presence of Flt3 ligand. After differentiation, BMDCs were infected either with wild-type *Bbi* or *Bbi-Tn-cre*. Two days after infection GFP expression was detected by flow cytometry and inverted fluorescence microscopy in about 15% of BMDCs. The percentage of GFP-expressing cells increased up to 20% on day 3 (Figure 12).

As most of the cells expressing GFP in the *Bbi-Tn-cre* infected BMDC culture were morphologically round and rather small in size, we wondered whether the GFP-signal was really specific and coming from live cells. Thus, we decided to check the viability of infected cells. In order to differentiate live and dead cells in infected DC co-culture the samples were stained with propidium iodide (PI). With that we confirmed that GFP-expressing cells were PI negative, indicating that the plasma membrane integrity was not disturbed and thus the cells alive (Figure 12.B).

Bbi* infects both: plasmacytoid and conventional DCs *in vitro

Flt3L-dependent *in vitro* differentiation of dendritic cells allows the generation of large numbers of plasmacytoid (pDCs) and conventional (cDCs) dendritic cells from bone marrow precursors [30]. However, BMDC culture is still a mixture of some “nondendritic” (CD11C⁻) cells and cells differentiated into DCs (~ 80-90% of cells are CD11c⁺) (Figure 13 and 14).

To further characterize the phenotype of *Bbi* infected cells, and to distinguish the subpopulations affected by *Bartonella*, the BMDC culture infected either with wild-type *Bbi* or *Bbi-Tn-cre* was stained with anti-CD11c antibodies either in combination with anti-MHCIIb or anti-B220 antibodies. Anti-CD11c staining could confirm that GFP-expressing cells are differentiated dendritic cells (Figure 13.A and B). The most of the GFP positive DCs are expressing major histocompatibility complex IIb molecules (MHCIIb), meaning that infected dendritic cells have undergone maturation and have upregulated the antigen presentation system on the cell surface (Figure 14.A and B). With anti-B220 staining two populations of GFP positive DCs can be distinguished. More than half of *Bbi*

infected cells were negative for the marker of pDCs, thus they represent conventional DCs (B220⁻) (Figure 14.A). In summary, *Bbi* is able to infect both: plasmacytoid and conventional DCs *in vitro* (Figure 14.C).

The *in vitro* infectivity of BMDCs gave a strong basis to start the *in vivo* infections of *Rosa 26-loxP-egfp* Balb/c mouse with *Bbi-Tn-cre*. With that we should be able to understand whether the DCs are infected in the primary infection site and serve as transporters of *Bartonella* from derma to lymphatic-blood system. In order to define an exact time of *Bbi* entry into the blood we characterized the time course of *i.d.* infection of *Bbi* in wild-type Balb/c mice. Although the number of bacteria per mL of blood did not exceeded more than 10⁴, all infected animals developed blood stage infection and *Bbi* started to colonize blood at 5-6 dpi. (Suppl. Figure 9). Preliminary results from *Rosa 26-loxP-egfp* Balb/c mouse infected with *Bbi-Tn-cre* showed that in at 3 dpi CD11c⁺ GFP-expressing cells can be detected in the draining lymph nodes. Whether these DC migrated from the derma or whether they were infected by *Bartonella* in the lymph nodes cannot be answered at this time. To understand it better and to prove that impaired cell migration and fragmentation (*in vitro* observations) of infected cells have a relevance to *in vivo* infection of primary cells we need to perform *i.d.* infection of *Rosa 26-loxP-egfp* Balb/c mice with *Bbi-Tn-cre* Δ *bepE* next to *Bbi-Tn-cre*. By flow cytometry or histological analysis we should be able to observe the lack or decrease of GFP-expressing cells in draining lymph nodes of the mice. (For the homology of BepE_{Bbi} to BepE_{Bhe} and BepE_{Btr} and the *virB* locus of *Bbi* see suppl. Figure 11).

Discussion

The T4SSs of *Bartonellae* and their effector proteins have been evolved as a toolbox for the adaptation to and colonization of different mammalian reservoir hosts [16,35]. In most of the cases of *Bartonella* infection, the reservoir host develops a long lasting infection with only mild or no clinical manifestations [7-10]. This is a prominent example of a high degree adaptation, where bacteria are able to persist, multiply and transmit to another host, without compromising the host niche. In this study we report that *Bartonella* effector protein BepE is crucial for the establishment of reservoir host infection. Using the rat *i.d.* model of *Btr* infection we were able to mimic the natural way of *Bartonella* infection by an arthropod. This allowed us to focus on an early stage of the host colonization where BepE revealed its important role in restoring bacteremia of *Btr* Δ bepDE-infected animals. This *in vivo* functionality of BepE was linked to its C-terminal part harboring the two BID domains. For the same BID domains we found *in vitro* that they interfered with the effect of other Bep proteins. These Beps have distinct functions within the host cell; however they may result in an impaired cell migration and subsequent fragmentation of the infected endothelial cells (ECs). Furthermore, based on our results, we suggest DCs, professional antigen presenting cells, as a candidate cell-type to be infected *in vivo* on the early stages of pathogen-host interaction. Summarizing, BepE could interfere with an impaired migration of the DCs once infected and help *Bartonella* to be transported as a cargo to the lymph nodes in order to disseminate further into the blood stream.

Several of the known phenotypes of *Bartonella* infection are linked to the function of the VirB T4SS and its translocated effectors, such as activation of the transcription factor NF- κ B and stimulation of a pro-inflammatory response, protection from apoptosis and cell invasion by a unique cellular structure termed the invasome [22-25,31]. These morpho-physiological changes upon infection with *Bhe* were observed in *in vitro* incidental host infection models, such as infection of human ECs. However, the incidental cases of human infection with *Bartonella* are rather too few to be a driving force for the evolution of bacteria to acquire special adaptation tools. Accordingly, we rather consider that T4SSs and Beps have been evolved within the process of reservoir host colonization.

This study describes for the first a role for *Bartonella* effector protein *in vivo* during reservoir host colonization. Previous animal model of rat *i.v.* infection with *Btr* (established by Schulein *et al*, 2001) did not reveal any function of *Btr* effectors *in vivo*. Compared to the proposed natural route of infection [13,14], the *i.v.* infection model lacks the early components of the reservoir host infection, the primary site of *Bartonella* inoculation – namely the derma and the first interaction with the innate immune cells. For that reason, we adapted the rat *i.v.* model to an intra-dermal infection route (Marignac *et al*, 2010). Our new rat *i.d.* infection model kept the host specificity for *Btr* and developed long-term infection with high bacterial burden in the blood (Figure 1). Most importantly, it mimicked the natural way of transmission, the scratching by animal after arthropod bite and the consequent inoculation of bacteria from the feces of the vector into derma. Thus differently from the *i.v.* route, the *i.d.* model enabled us to focus on an early phase of the infection prior bacterial entry into the blood stream and followed bacteremia. We observed 4-5 days delay of bacteremia in *i.d.* infected rats with wild-type *Btr* (Figure 1). This time delay could correspond to the way that *Bartonella* has to take, passing from derma (the site of inoculation) to the blood (the only place in the reservoir host *in vivo* where *Bartonella* has been detected) and to the possible interaction with the innate immune cells. Interestingly, at the site of infection, on the ear, the rats did not develop inflammation or any obvious signs of innate immune response. It is noteworthy to mention that *Bartonella* LPS is not recognized by TLR4 receptors. Moreover, there is evidence that the lipid A of *Bhe* and *Bqu* LPS is modified, has a cylindrical conformation and may act as a potent antagonist of TLR4, thus the production of proinflammatory cytokines in human monocytes is not induced [38,39]. In addition, human (a natural host) infection with *Bqu* is characterized with an over-production of the anti-inflammatory cytokine, interleukin-10 (IL-10) and an attenuated inflammatory cytokine profile [40]. All in all, this could explain the absence of inflammation at the inoculation site of *Btr*, indicating once more on how well *bartonellae* are adapted to their reservoir host.

The *Btr* Δ *bepDE* in our rat *i.d.* infection model did not lead to the bacteremia of animals, while complementation with the two effectors, BepE_{*Btr*} and BepD_{*Btr*} or BepE_{*Btr*} alone restored the blood colonization of *i.d.* infected animals (Figure 2 and 3). This observation shows that BepE_{*Btr*} is sufficient to complement and is an essential factor for the establishment of the infection, enabling *Bartonella* to reach the blood. This statement is

also supported with a single case of *Btr* Δ *bepDE* *i.d.* infection, where the BepD/BepE effector-less bacteria appeared in blood on day 16 post infection. However, when the bacteria actually reached the blood, bacteremia developed with the same titers as observed for the wild-type *Btr* infection (Figure 2), indicating that the effectors are rather needed in the early stage but not to maintain the infection in blood stream any more. At the same time, we saw that *Btr* Δ *bepDE* was bacteremic when directly delivered into the blood stream by the *i.v.* route (in contrast to *i.d.*) and the plasmid complementation restored the bacteremia in *i.d.* infection. These observations prove that the abacteremic phenotype of the *Btr* Δ *bepDE* in *i.d.* infected animals is not because a consequence of any attenuation of the strain after genetic manipulations for in-frame deletion of the effector proteins. Further supporting the role of BepE_{*Btr*} prior to seeding of the bacteria into the blood, plasmid-complemented *Btr* Δ *bepDE* strains tended to lose the effector encoding plasmid in the blood. Less than half of the *Bartonella* pool contained the plasmid at day 10. The percentage of plasmid-containing bacteria in blood decreased gradually in time (suppl. Figure 5), suggesting that there is no more selection pressure to maintain the effector-encoding plasmids during erythrocyte invasion. Following the same tendency, the *virB4* and *virD4*-encoding plasmids of *Btr* are lost in the rat *i.v.* infection [18]. These plasmid segregations indicate that VirB T4SS is no longer essential for the erythrocyte invasion. All these data suggest that *Bartonella* is targeting a cell type *in vivo*, apart from erythrocytes, where it survives in the presence of BepE_{*Btr*} and is able to further develop the infection with bacteremia, while the *Btr* Δ *bepDE* strain does not succeed to reach the blood.

Bartonella effectors are known to have functional redundancy, the ability of structurally different elements to perform the same function or yield the same output [41]. *Bhe* is capable of triggering invasome formation on epithelial and ECs in two different ways, by BepC_{*Bhe*}/BepF_{*Bhe*} or BepG_{*Bhe*}-triggered actin cytoskeleton rearrangements [24]. The other three effectors, BepD_{*Bhe*}, BepE_{*Bhe*} and BepF_{*Bhe*} bare N-terminal putative tyrosine-containing motives (ITIM/ITSM). Within these motives they interact with SH2 domain-containing cellular partners in tyrosine phosphorylation dependent manner. These interaction partners are identical for BepD_{*Bhe*} and BepE_{*Bhe*}: Csk, Shp1/2, and Grb2/7 [26]. Moreover, in addition to the BID domains, these phospho-tyrosine motives are present in both, BepE_{*Btr*} and BepD_{*Btr*} but whether these two effectors have a redundant effect on

the restoration of bacteremia *in vivo* or whether BepD_{Btr} is not involved in this process has not been addressed in this study.

Heterologous complementation of *Btr* Δ bepDE with pBepE_{Bhe} and the subsequent bacteremia observed in rats speak for a conserved function of BepE between different species of *bartonellae* (Figure 3). Surprisingly, the BID domains of BepE_{Bhe} were sufficient to restore the bacteremia but the ITIM/ITSM tandem containing N-terminal part did not reveal an essential role (Figure 4). Thus, we were not able to support the hypothesis of a molecular mimicry of immune inhibitory receptors by BepE_{Bhe} [26]. However, we suggest that this may still be valid and has to be addressed again in “primary niche” cells. There was a slight decrease in the bacterial burden in blood when complementing with the two BID domains of BepE_{Bhe} compared to BepE_{Bhe} wild-type. This could be explained with some conformational role of N-terminal part of BepE for the full length protein. The N-term might play a role even together with other effectors not showing phenotype strong enough to be visible in our *in vivo* model by looking only at blood colonization. It is also noteworthy to mention that the number of bacteria (10^7 bacteria) that we take for the *i.d.* inoculation is by far a lot compared to what in nature could be delivered via the feces of the arthropod. Thus, by providing such an amount of inoculum we may lose the phenotype of BepE N-term. It is important to mention that most of the phenotypes associated with the Beps of *Bhe* are related to the BID domains. This conserved domain is present in at least one copy in all Beps as it constitutes the secretion signal for the transport via the VirB T4SS. Interestingly, the BIDs seem to be capable of adopting various functions in the host cell [16]. The anti-apoptotic effect of BepA_{Bhe} is delineated to the BID domain of this protein [25]. BepF_{Bhe} acts as a GEF (guanine nucleotide exchange factor) protein for Cdc42 and this activity is also contained in the two BID domains, BID1F_{Bhe} and BID2F_{Bhe} (M. Truttmann, Thesis work, 2010).

Using the rat *i.d.* model we were able to clearly demonstrate that BepE, more specifically the BID domains of BepE_{Bhe}, are essential for the development of a complete picture of *Bartonella* infection of the reservoir host. These domains enable bacteria to reach the replicative niche – invading erythrocytes and persisting for long times without obvious clinical manifestations of disease and without harming their natural host. The same *in vivo* model revealed that BepE is essential before *Bartonella* seeds into the blood;

proposing that there are other cell type(s) than erythrocytes infected in the animal. Within these cells *Btr ΔbepDE* strain is not able to succeed in the absence of BID domains of BepE. To address the cellular basis and what happens with the infected cells in the absence of BepE, we decided to move to a well-established *in vitro* infection model, infection of primary endothelial cells, HUVECs, with *Bhe*.

HUVECs infected with *Bhe ΔbepE* strain showed a sticking phenotype. The infection with this strain affected cell migration process. As described elsewhere, cell migration is a coordinated cellular movement that requires a series of repetitive, integrated processes. The first step is the forward protrusion of lamellipodia and filopodia, which is dependent on extensive remodeling of the actin cytoskeleton. Next, attachment at the leading edge occurs with focal adhesion complexes. After the formation of new adhesions, the cell undergoes actomyosin-dependent contraction to pull the cell body forward. Once the cell body contracts, attachments at the rear of the cell are released so that the cell can move forward [42,64-70]. HUVECs are characterized with a random migration in cell culture (suppl. movie 1, see on CD attached). The wild-type *Bhe* infected HUVECs (similarly to uninfected ones) develop through all the four steps of cell migration described above. However, the cell migration looked different when HUVECs were infected with *Bhe ΔbepE*, cells could not detach at the rear and underwent fragmentation (Figure 5 and 6, suppl. movie 2, see CD attached). The similar but even stronger phenotype was observed when infecting HUVECs with *Bhe* strain lacking the three effectors: BepD_{Bhe}, BepE_{Bhe} and BepF_{Bhe} (Figure 5), the three Beps with putative tyrosine-containing motives on the N-terminal part and the BID domains with positive C-term as a bipartite signal for translocation via T4SS [21]. We assume that the fragmentation of infected HUVECs is clearly T4SS dependent, as the infection with *ΔvirB4* (defective VirB T4SS) did not lead to the fragmentation of ECs (suppl movie 5, see CD attached). Even more, the induction of the phenotype is connected to the translocation of Beps, BepA_{Bhe} can be ruled out as the fragmentation was not observable when infecting cells with a *Bhe ΔbepB-G* strain (data not shown). Thus, only three candidates left to be responsible for the impaired cell migration: BepB_{Bhe}, BepC_{Bhe} and BepG_{Bhe}, or different combinations of them even with BepA_{Bhe} or with any unknown factor of *Bartonella*. BepD_{Bhe}, BepE_{Bhe} and BepF_{Bhe} need to be deleted to see the fragmentation; hence they do not induce but may rather interfere with the process.

Further, we showed that over-expression of BepE_{Bhe} in either *Bhe ΔbepE* or *ΔbepDEF* background can rescue infected ECs from fragmentation. This was explicitly characteristic for BepE_{Bhe} as BepD_{Bhe} and BepF_{Bhe} could not interfere with *Bhe ΔbepDEF*-induced cell fragmentation (Figure 7). In addition, T4SS-independent expression of BepE_{Bhe} into infected HUVECs indicated that BepE_{Bhe} is actively interfering with the cell fragmentation process due to the specific function and not by stressing *Bhe* to produce BepE in large amounts and block the translocation of the rest of the Beps into the target cell, the Beps that may even be responsible for the fragmentation (Figure 11, and suppl. Figure 8).

Similarly to the *in vivo* phenotype, the function of BepE_{Bhe} *in vitro* was assigned to the BID domains and not to the N-terminal part of the protein. The two BID domains of BepE_{Bhe} are similar with 53,3% of pair wise aa identity of (Figure 8.B). A single last BID domain was not enough to protect cells from fragmentation, but two together do interfere with the process (Figure 8.A and C). It may be that the last BID domain, BID2E_{Bhe}, together with the C-tail maintained a bipartite translocation signal via T4SS, while the BID1E_{Bhe} acquired a new function to rescue infected cells from the fragmentation. However, this statement needs to be proven further by the single BID1E_{Bhe} expression in *Bhe ΔbepE* or *ΔbepDEF*-infected HUVECs.

How the cell fragmentation develops or the molecular mechanism used by BepE_{Bhe} to interfere with the processes are currently unknown, but we assume that the focal adhesion turnover at the rear edge of the migrating cells is impaired. Cell adhesion and migration require many spatio-temporally integrated components, all of which must be quickly and precisely regulated [42]. Focal adhesion kinase (FAK), GEFs for Rho and the Rho effector, Rho kinase II (ROCKII) are crucial for the regulation of adhesion turnover and rear edge retraction. Functional interferences to one of these components can potentially lead to the disturbed migration of the cell [43,44]. Inhibition of RhoA activity by its inhibitor, C3, leads to a strong morphological change of migrating monocytes, with frequent polarization and long tails trailed behind the cell body [45]. A phenotype that is very similar to the early stage of the cell fragmentation observed in *ΔbepE* or *ΔbepDEF*-infected HUVECs. Rho GTPases, regulate cytoskeletal dynamics and migration in many diverse cell types. RhoA signaling was shown to be coordinated at both, the leading edge and at rear during T cell migration. It is predicted that RhoA activation is independently

regulated by different GEFs in response to the unique microenvironments in each cellular region. As an example, GEF-H1 localization is restricted to the rear of crawling and transmigrating T cells, suggesting that its function is to activate RhoA locally at the back of migrating cell [46]. Interestingly, we have evidence that BepC_{Bhe} may be the effector inducing the cell fragmentation, next to its distinct function during invasome formation. This hypothesis is based on a fact that GEF-H1 can be pulled down together with BepC_{Bhe} from *Bhe*-infected cells (R. Conde, unpublished), indicating an indirect (or even direct) effect of BepC_{Bhe} on the local regulation of RhoA activity at the cell rear. To explain how the cell fragmentation develops we suggest the following possibilities. Invasome formation largely modifies the actin dynamics, inducing its rearrangements. Massive recruitment of GEF-H1 by BepC_{Bhe} to the invasomes, may result in local depletion of RhoA activity at the rear of migrating cell and thus leading to the impairment of focal adhesion turnover. Another important factor recruited by BepC_{Bhe}/BepF_{Bhe} mediated invasome formation is cofilin [47], the actin depolymerization and remodeling factor [48,]. Yet not very clear but there are some indications about an indirect regulation of cofilin by RhoA [49,50]. We propose that during migration of the infected cells cofilin may be sequestered from the rear edge of the cell, as it is involved in invasome formation. Many isoforms of tropomyosin are known to compete with ADF/cofilin proteins for binding to the actin filaments and stabilize the F-actin [51], thus stabilization of the actin filaments and impairment in depolymerization, could lead to the trouble of rear edge detachment, disturbed cell migration and subsequent fragmentation. This hypothesis is also supported by the observations from the cofilin knockdown in metastatic cancer cells. Cofilin deficient cells have rear detachment problem, forming thin elongations in the back side of the cells while moving forward [52]. These data strengthen our idea that the cell fragmentation phenomenon is induced by the Bep(s) involved in the invasome formation as a secondary effect and BepE_{Bhe} serves as a tool that interferes with this secondary effect.

We suppose that when infecting the reservoir host with *Btr* Δ bepDE, *in vivo* fragmentation or impaired migration of an infected cell is likely happening as well. The derma, where *Bartonella* is inoculated during the natural host infection, is the site where bacteria have to interact and infect innate immune cells. The *Btr* Δ bepDE cannot reach the replicative niche within the erythrocytes. The bacteria are cleared by the immune

system before appearing in the blood, (or reside in a niche for a long time and we just do not see it) this may be a result of a fragmentation of the primary infected cells in the derma or on the way to the lymphatic-blood system. The fragmented cells may be better recognized by neighboring immune cells and consequently degraded. As a result *Btr ΔbepDE* is exposed effectively to the innate immune system and is cleared on the early phase of the infection. DCs may serve as one of the candidate cell types for yet unknown “primary niche” of *Bartonella* infection. Skin migratory DCs participate in defense mechanisms against pathogens that gain access to the epidermis or dermis as a consequence of pathogen-specific skin invasion, skin lesions, or inoculation by insects. In steady state skin migratory DCs include immature epidermal DCs, langerhans cells (LCs) and immature dermal DCs [53]. The immature DCs are characterized with high phagocytic activity. They constantly sample the environment as sentinels for foreign antigens (Ag). At the same time, dendritic cells exhibit limited degradation of phagocytosed antigens, which in general favor efficient antigen presentation to T lymphocytes. Thus as professional antigen presenting cells, DCs play a central role in activation of resting T cells and initiation of primary and memory immune responses to build an effective defense mechanism and clear the organism from pathogens. While the other phagocytes neutrophils and macrophages, possess high destructive capacity of the cargo and serve as antigen non specific first line of defense [30,31]. Once become activated by taking up the Ags, DCs start directional migration towards the draining lymph nodes, upregulate MHC class II and costimulatory molecules in order to present the Ags to naive T cells within the peripheral lymph nodes and initiate the effective adaptive immune responses [36, 37]. On the way to lymph nodes DCs may serve as transporters of bacterial cargo and this in turn may be used by the bacteria as a strategy to disseminate in the host organism. These features of DCs make them attractive to be targeted and hijacked by different pathogens, with subsequent modulation their immunogenic responses with tolerogenic. *Bordetella bronchiseptica* T3SS is required for increased migration of respiratory DCs to secondary lymphoid tissues, where they stimulate immunosuppressive/tolerogenic immune responses with IL-10/low IFN- γ profile that contribute to long-term colonization of the murine respiratory tract [34]. The maturation, antigen presentation properties and cytokine profile of infected DCs are negatively regulated by *Yersinia enterocolitica* Yops [54,55] and *Brucella* Omp-25 or Btp1 [56-58]. DCs are another target cells (next to macrophages) for *Salmonella*. It infects lamina propria DCs and with the virulence factor

spvB (and possibly *spvC*) contributes to the alternative (TTSS-1 independent) pathway of gut inflammation by enhancing the transition from CD11c⁺ to CD11c⁻ host cell types and pathogen loads in the cecal mucosa [59].

We further wanted to investigate the impaired cell migration and fragmentation phenomenon in *Bartonella*-reservoir host, to understand whether these processes are affected in primary infected cells as well. The reporter tool, *Rosa 26-loxP-egfp* Balb/c transgenic mice and the infection of BMDCs from these mice with Cre-BID fusion-expressing mouse specific *Bbi* (*Bbi-Tn-cre*) gave the first evidence *in vitro* that DCs could represent one of the primary cells targeted by *Bartonella* in the reservoir host (Figure 12 and 13). We confirmed that GFP expressing BMDCs were alive; nevertheless those cells looked small in size and round in shape. The explanation why the GFP positive cells are small and having so different shape from the rest of the cells can be different: the infected cells undergo activation and morphology change; or the intensity of GFP in GFP positive cells is rather low and only the cells that are rounded up and thus have concentrated GFP signal are detectable by microscopy, and not the weaker expressors (Figure 12.A and B). With a phenotypical staining we could confirm that infected cells were indeed DCs, expressing CD11c and *Bbi* translocated the fusion effector in both of the subpopulation of BMDCs, plasmacytoid and conventional DC without any obvious preferences (Figure 14). In addition, we have preliminary evidence from *Bbi-Tn-cre i.d.* infected *Rosa 26-loxP-egfp* Balb/c transgenic mice, where we found GFP expressing cells in the draining lymph nodes. These results give a strong basement to our hypothesis that DCs are one of the cell types infected by *bartonellae in vivo* which carry the bacteria from primary infection site to the blood stream.

Taking together, in this study we provide the first understanding of the role of the *Bartonella* effector protein *in vivo*. BepE is an essential factor evolved by *Bartonella* to develop infection of a reservoir host. More specifically, we think DCs are one of the cell types infected prior blood stage infection where the BepE interferes with the function of other Beps and fine-tunes the host manipulation. As a result *Bartonellae* evade the clearance from primary immune system prior reaching the replicative niche in the blood, where it multiplies, stays hidden from host defense system and is safely transmitted further by arthropod vectors to another mammalian host. Further animal experiments are

needed to confirm the migration of primary infected cells from the derma to lymphatic-blood stream. To prove our hypothesis about *Bartonella* dissemination by DCs and the role of BepE in this process, next to wild-type *Bbi-Tn-cre*, *Bbi-Tn-cre ΔbepE* has to be used for infection of mice and BMDCs *in vitro*, which may reveal the impaired migration of primary immune cells.

Materials and methods

Ethics statement

Animals were handled in strict accordance with good animal practice as defined by the relevant European (European standards of welfare for animals in research), national (Information and guidelines for animal experiments and alternative methods, Federal Veterinary Office of Switzerland) and/or local animal welfare bodies. Animal work was approved by the Veterinary Office of the Canton Basel City on June 2003 (licence no. 1741).

Bacterial strains and growth conditions

The bacterial strains used in this study are listed in Table 1. *Bartonella* spp were grown on Columbia agar plates containing 5% defibrinated sheep blood (CBA plates) at 35°C and 5% CO₂ for 2-3 days. Strains *Btr* RSE149 [15] and *Bhe* RSE247 [21] spontaneous streptomycin-resistant strains and *Bbi* PEE0261 served as wild-type *Btr*, wild-type *Bhe* and wild-type *Bbi* respectively in this study. When indicated, media were supplemented with 30 µg/ml kanamycin, 100 µg/ml streptomycin, 10 µg/ml gentamicin, and/or 500 µM isopropyl-β-D-thiogalactoside (IPTG, <http://www.applichem.de>). *E. coli* strains were cultivated in Luria-Bertani liquid medium (LB) or on Luria-Bertani agar on plates (LA) at 37°C overnight. When indicated, media were supplemented with 50 µg/ml kanamycin, 200 µg/ml ampicillin, 20 µg/ml gentamicin, 500 µM IPTG, and/or 1 mM diaminopimelic acid (DAP).

Conjugation of *Bartonella*-expression plasmids into *Bartonella*

Conjugation of plasmids from the *E. coli* *dap*⁻ mutant b2150 (Dehio and Meyer, 1997) into *Bartonella* spp. was done by triparental mating in the presence of helper plasmid pRK2013 as described previously (Dehio *et al.*, 1998).

DNA manipulations

Plasmids used in this study are listed in Table S1, primers are listed in Table 2.

Plasmid for expression of MYC-Beps

By excising full length *bepE* from pPG105 with *NdeI* and inserting it into the respective sites in pPG180, the MYC-BepE_{Bhe} expressing vector, pPG185, was constructed. The vector expressing the two C-terminal BID domains of BepE_{Bhe} without the N-terminus, pPG172, was constructed by PCR amplifying a fragment of 1 kb from pPG105 with the primers prPG148 and prPG149. After digesting the fragment with *NdeI*, it was inserted in the respective site of pPG180.

The vector expressing the last C-terminal BID domain of BepE_{Bhe}, pRO104, was constructed by PCR amplifying a fragment of 576 bp from pPG105 with the primers prRO030 and prPG101. The PCR product was subcloned into pSC-B blunt end cloning vector (Strata clone blunt PCR cloning kit) yielding pRO010. After digesting the pRO010 with *NdeI*, it was inserted in the respective site of pPG180.

The vector expressing the BepE_{Bqu}, pRO105, was constructed by PCR amplifying a fragment of 1502 bp from boiled colony of *Bqu* RSE356 with the primers prRO033 and prRO034. The PCR product was subcloned into pSC-B blunt end cloning vector (Strata clone blunt PCR cloning kit) yielding pRO011. After digesting the pRO011 with *NdeI*, it was inserted in the respective site of pPG180.

The vector expressing the BepH_{Bgr}, pRO105, was constructed by PCR amplifying a fragment of 831 bp from boiled colony of *Bgr* CHDE142 with the primers prRO035 and prRO036. The PCR product was subcloned into pSC-B blunt end cloning vector (Strata clone blunt PCR cloning kit) yielding pRO013. After digesting the pRO013 with *NdeI*, it was inserted in the respective site of pPG180.

Plasmid for expression of proteins without an epitope tag

For constructing vector pPG110 expressing native proteins, the oligonucleotide primers prPG90 and prPG91 were used to amplify a 0.4 kb fragment from pRS40 template DNA. Using flanking *SacI* sites the generated fragment was inserted into the corresponding site of pRS40. Next, a 1.67 kb fragment containing the complete *bepD* gene and an N-terminal MYC tag was amplified using oligonucleotide primers prPG141 and prPG145 and chromosomal DNA of RSE247 as template. Using flanking *NdeI*-sites the amplified fragment was ligated into the corresponding site of pPG110, yielding pPG184. The empty

MYC tag expression vector, pPG180, was generated by cutting out *bepD* with *NdeI* from pPG184, and religating the vector.

Construction of in-frame deletions

In-frame deletion mutants of *Btr* RSE149 and *Bhe* RSE247 were generated by a two-step gene replacement procedure as described (Schulein & Dehio, 2002; Schmid *et al.*, 2004) [18,22]. The basic mutagenesis vector pTR1000 was described before (Schmid *et al.*, 2004) [22]. All mutagenesis plasmids harbour a cassette with the flanking regions of the in-frame deletion in the gene(s) of interest. This cassette was generated from two PCR fragments amplified from chromosomal DNA of *Btr* RSE149 or *Bhe* RSE247 as template, either by megaprimer PCR or by conventional cloning.

pFS20 used for generating a *Btr* Δ *bepDE* in-frame mutant was constructed as follows. Oligonucleotide primers prFS09 and prFS10 amplified fragment 1 (736 bp, containing 356 bp of 5' end of *bepC_{Btr}*) and prFS11 and prFS12 amplified fragment 2 (665 bp, containing 345 bp of 3' end of *bepH_{Btr}*). Both fragments were combined by megaprimer PCR with oligonucleotide primers prFS09 and prFS12, resulting in a fragment of 1.64 kb carrying an in-frame deletion in *bepDE_{Btr}*. By using flanking *Bam*HI sites, the fragment was inserted into the corresponding site of pTR1000, yielding pFS20. The use of pFS20 for gene replacement in RSE149 resulted in the *Btr* Δ *bepDE* mutant FS150.

Construction of the in-frame mutant *Bhe* Δ *virB4* has been described previously (Schmid *et al.*, 2004) [22].

Construction of the in-frame mutant *Bhe* Δ *bepD*, *Bhe* Δ *bepE*, *Bhe* Δ *bepF* has been described previously (Scheidegger *et al.*, 2009) [60].

pPG163 used for generating a *Bhe* Δ *bepDEF* mutant was constructed as follows. Oligonucleotide primers prTR041 and prTR051 amplified fragment 1 (853 bp, containing 321 bp of 5' end of *bepC_{Bhe}*) and prTR055 and prTR056 amplified fragment 2 (665 bp, containing 345 bp of 3' end of *bepG_{Bhe}*). Both fragments were combined by megaprimer PCR with oligonucleotide primers prTR041 and prTR056, resulting in a fragment of 1.67 kb carrying an in-frame deletion in *bepDEF_{Bhe}*. By using flanking *Bam*HI sites, the fragment was inserted into the corresponding site of pTR1000, yielding pPG163. The use of pPG163 for gene replacement in RSE247 resulted in the *Bhe* Δ *bepDEF* mutant PGE26.

Chromosomal integrations

Suicide vector pPG612 for chromosomal integration for *Bhe* was constructed in 3 sequential steps.

On the first step oligonucleotide primers prTR041 and prTR042 amplified fragment 1 (0.83 kb) and prTR043 and prTR044 amplified fragment 2 (0.83 kb) from chromosomal DNA of *Bhe* RSE247. Both fragments were combined by megaprimer PCR with oligonucleotide primers prTR041 and prTR044 resulting in a fragment of 1.68 kb. The product was digested by *Bam*HI and ligated into the corresponding site of pTR1000, yielding to pPG161. On the second step oligonucleotide primers prPG236 and prPG219 amplified fragment 1 (1.07 kb with flanking *Bcl*I and *Bam*HI sites) and prPG220 and prPG221 amplified fragment 2 (1.04 kb with flanking *Bam*HI, *Sal*I and *Xho*I sites) from chromosomal DNA of *Bhe* RSE247. Both fragments were combined by megaprimer PCR with oligonucleotide primers prPG236 and prPG221 resulting in a fragment of 2.09 kb. The product was digested by *Bcl*I and *Xho*I, and ligated into *Bam*HI/*Sal*I-digested pPG161, yielding to pPG611.

On the last step oligonucleotide primers prPG212 and prPG213 amplified the intergenic region of *Bhe* *bepC* to *bepD* with tag encoding MYC epitope and flanking *Bam*HI site as fragment 1. Oligonucleotide primers prPG214 and prPG215 amplified the *beta-lactamase* gene from pBR322 with flanking *Sac*II and *Not*I sites as fragment 2. Oligonucleotide primers prPG216 and prPG217 amplified the BID domain and terminator downstream of *bepD* from RSE247 chromosomal DNA with flanking *Not*I and *Sal*I sites as fragment 3. All three fragments were combined by megaprimer PCR with oligonucleotide primers prPG212 and prPG217 resulting in a fragment of 1.96 kb. This fragment was digested with *Bam*HI and *Sal*I and ligated into previously *Bam*HI/*Sal*I-cut pPG611, yielding pPG612.

The use of pPG612 for gene replacement in RSE247 resulted in the *Bhe* PGH75.

Suicide vector pPE0012 for chromosomal integration for *Bbi* was constructed based on pPE0010, which was used for another approach as chromosomal insertion of “CP1-Katushka-Tn” fragment into *Bbi*. pPE0010 originates from pPE002, a direct derivative of pSH003 where the direction of one of the two T7 promoter sequences at the two ends of the Transposon is modified. The oligonucleotide pair prPE427 and prPE428 amplified PCR fragment from pRS51, the product was digested with *Pac*I/*Xba*I and was ligated into the corresponding site of pPE0010, yielding pPE0012.

The use of pPE0012 for gene replacement in PEE0261 resulted in the *Bbi-Tn-cre* CMB0142.

Tyrosine to phenylalanine exchange mutant in BepE_{Bhe}

To exchange the putatively phosphorylated tyrosines to phenylalanines in the N-terminus of BepE, we applied megaprimer PCR to reamplify the sequence coding for BepE from pPG185. Briefly, using prPG190 and prPG191 binding on the plasmid pPG185 and two corresponding primers annealing to the site to be mutated, two fragments with a sequence overlap in the mutation site were amplified by PCR. In a second step, these two fragments were joined by megaprimer PCR using prPG190 and prPG191, yielding a fragment of 2.1 kb. This fragment was then cut with *NdeI* and inserted into the previously *NdeI*-cut pPG180 vector. The Y37F; Y64F; Y91F; Y106F; Y129F (BepE_{Bhe}.Y->F) mutant was generated after sequential mutation rounds using pPG185 as a template on a first round.

Western blot analysis of protein expression in *Bartonella*

Western blot analysis of expressed protein levels in *Bartonella* was performed as described previously by Schulein *et al.*, 2005 [21].

Infection of rats and mice

Female Wistar rats were obtained at the age of 10 weeks from Harlan, RCC-Füllinsdorf. *Rosa26 loxp-GFP* Balb/c mice were bred in-house, at the animal facility of Biozentrum. All animal studies were approved by the authors' institutional review boards.

The rats after two weeks of adaptation and the mice in the age between 6-12 weeks were infected with *Btr* and *Bbi* respectively. Bacterial strains were grown as described above, harvested in phosphate-buffered saline (PBS), and diluted to OD₅₉₅ = 1. Rats were anesthetized with a 2–3% Isoflurane/O₂ mixture and infected with 10 µl or 0.2 mL of the bacterial suspension in the dermis of the right ear or in the tail vein respectively. Mice were injected intradermally with 10 µl of bacterial suspension with the same concentrations mentioned above. Blood samples were taken at the tail vein and immediately mixed with PBS containing 3.8% sodium-citrate to avoid coagulation. After freezing to –70°C and subsequent thawing, undiluted and diluted blood samples were plated on Columbia agar plates containing 5% defibrinated sheep blood (CBA plates) at 35°C and 5%. CFUs were counted after 7–10 days of growth.

Cell culture

Human umbilical vein endothelial cells (HUVEC) were isolated as described before (Dehio *et al.*, 1997) and cultured in EGM medium (<http://www.promocell.com>) in a humidified atmosphere at 37°C and 5% CO₂.

Bone marrow-derived DCs (BMDCs) were differentiated *in vitro* using standard protocol [61]. Briefly bone marrow cells were flushed from the tibias and femurs of *Rosa26 loxp-GFP* Balb/c mouse with culture medium composed of DMEM medium (Invitrogen Life Technologies) supplemented with 10% FCS (Invitrogen Life Technologies). After one centrifugation, BM cells were resuspended in Tris-ammonium chloride for 2 min to lyse RBC. After one more centrifugation, BM cells were cultured for 8-10 days at 1×10^6 cells/mL in culture medium supplemented with 200 ng/ml recombinant human Flt3L (produced by 40E1 hybridoma cells, kind gift from prof. A. Rolink, not published) in 75 cm² flasks (Corning life sciences). Cultures were incubated at 37°C in 5% CO₂-humidified atmosphere.

HUVEC transfection

HUVECs were transfected using Amaxa nucleofection technology (Amaxa, <http://www.amaxa.com>) following the manufacturer's guidelines for HUVEC transfection. After transfection, cells were seeded into gelatine-coated six-well plates.

Lentiviral transformation of HUVECs

Sub-confluent (3×10^6) HEK 293T cells in 10 cm cell-culture dishes were transfected with a total of 5 µg of plasmid DNA following the FuGENE transfection protocol (FuGENE 6 Transfection Reagent, Roche). After 12 hs, the cell culture media was replaced and the cells were kept in culture for virus production in the supernatant for additional 24 hs. 7×10^4 HUVECs/well was seeded in gelatin coated 6-well plate 24 hs before the viral infection. On day of infection the viral supernatant from transfected HEK 293T cells was filtered with 0.45 µm filter and transferred onto the monolayer of HUVECs, 2 mL of viral supernatant in presence of 0.5 µg/mL Polybrene (Sigma) was applied on each well. After the first harvesting of viral supernatant the HEK 293T cells were supplemented with a fresh medium. 24 hs later the HUVECs were re-infected repeating the same procedure with followed replacement of the medium in 24hs.

Infection of HUVECs

HUVEC (passage 4-7) were plated on gelatin-coated glass slides in 24-well plates at 5×10^4 /ml using EGM or alternatively 3×10^3 /well seeded in 96-well plate. The next day cells were washed twice with M199 with Earls salts (M199, Gibco, <http://www.invitrogen.com>) supplemented with 10% fetal calf serum (FCS, <http://www.invitrogen.com>) and infected with a multiplicity of infection (MOI) of 200 bacteria per cell in M199/10% FCS/500 μ M IPTG and incubated for 24, 36 and 48 hs or 72hs for the time lapse microscopy. When necessary the infection was fixed with 3,7% paraformaldehyde.

Immunofluorescent labelling

Indirect immunofluorescent labeling was performed as described (Dehio *et al.*, 1997)[31]. Standard 96-well plate assays were stained with TRITC-phalloidin (Sigma, 100 μ g/ml stock solution, final concentration 1:400) and DAPI (Roche, 0.1 mg/ml) using a Tecan Eoware freedom pipetting robot. Glass slides for confocal microscopy were stained with Cy3- or Cy5-phalloidin (Sigma, 100 μ g/ml stock solution, final concentration 1:100), DAPI and anti-MYC antibodies (mouse anti-MYC, Invitrogen, Carlsbad, CA/USA) and/or VE-Cadherin (rabbit anti-VE-Cadherin, Bender MedSystems, Burlingame, CA/USA). Secondary antibodies for Immunofluorescence used in this study were Cy5-conjugated goat anti-rabbit Ig antibodies (Dianova, Hamburg, Germany, 1:100). For HUVECs transfected with pRO1000, Cy5-phalloidin was used for staining of F-actin and DAPI for staining of nuclei.

Image analysis and quantification of cell fragmentation

Experiments performed in 96-well plates were subjected to automated microscopy, using MD ImageXpress Micro automated microscopes. In every well, 10 sites were imaged in two different wavelengths corresponding the applied cell staining. Images were visualized using MetaExpress software (MDC) and the number of cells per image was determined automatically by MetaExpress in-build analysis modules (CountNuclei). The thin elongations of the cells and cellular fragments without nucleus were defined and counted by eye. Using the automatically determined cell number and the manual cell elongation and cell fragment counts, the percentage of elongated cells and the fragment number per cells was calculated using Microsoft Office Excel. In every condition 20 fields of

magnification 20 within the well and triplicates of the wells were analyzed. The error bars were calculated as SD within the replicas. Statistical significance was determined using Student's *t*-test. **P*<0.005, ***P*<0.001 were considered statistically significant.

For confocal laser microscopy, the stained samples were analysed using an IQ iXON spinning disc system from Andor in combination with an Olympus IX2-UCB microscope. Z-stacks with 20–30 focal planes with a spacing of 0.1–0.2 μm were recorded and xz -and yz-planes were reconstructed using Andor IQ software. Images were exported and finalized using Metamorph, ImageJ and Adobe photoshop.

Time-lapse microscopy

Time-lapse microscopy was carried out using an MD ImagXpress Micro automated microscope from Molecular devices (inside a controlled chamber held at 37°C and 5% CO₂) and images recorded using a CoolSNAP ES digital CCD camera and processed using MetaXpress software (<http://www.moleculardevices.com>). Briefly, HUVECs were infected with *Bhe* strains in 96-well format as described above. After incubating for 8h, 2 to 4 points in each well were chosen for time-lapse microscopy. The points were imaged for 72hs with 10 min lapse between each imaging. Both, red and green, fluorescence were detected at 20× magnification, and the corresponding videos were processed in MetaXpress and compiled into Quicktime (Apple, Cupertino, CA) movies.

Infection and FACS analysis of BMDCs

Day 9-10 BMDCs were harvested from the flask by vigorous pipetting followed by washing twice with room temperature PBS without Ca²⁺ or Mg²⁺ (Invitrogen Life Technologies). 2*10⁶ BMDCs were seeded in each well of 6-well plate. On the next day supernatant was replaced with the fresh M199 with Earls salts (M199, Gibco, <http://www.invitrogen.com>) supplemented with 10% fetal calf serum (FCS, <http://www.invitrogen.com>) and infected with a MOI of 50. On day 2 post infection (dpi) 20 μg/ml gentamicin was added for 2 hs and followed replacement with the fresh media. On 2 dpi and 3dpi infected BMDCs were scraped from the surface by lifter (Corning Life Science), re-suspended as single cell suspension and stained for surface markers. For staining following mAbs were used: anti-B220 (RA3-6B2) PE, anti-CD11c (HL3) APC, purchased from BD Biosciences (San Jose, CA); anti-MHC class IIb PE antibodies were purified from the hybridoma supernatant and

labeled by standard methods (kind gift from prof. Antonius Rolink). For surface phenotyping, cells were incubated in FACS buffer (PBS, 1% FBS, and 0.1% azide) for 20 min at 4°C with anti-CD11c APC and either anti-B220 PE or anti-MHCIb PE. Cells were washed and resuspended in PBS containing 2% FCS and 0.1% sodium azide (FACSwash). Propidium iodide was used at 0.5 µg/ml. Flow cytometry was performed using a FACS Calibur (BD Biosciences) and data were analyzed using the FlowJo software.

Beta-lactamase reporter assay

$3,5 \cdot 10^3$ BMDCs/well seeded in 96-well plate. On the next day the cells were infected with *Bhe* strains as described above with the MOI of 50, 100, 300. After 12, 24 and 48 hs post infection the infected cells were loaded with CCF2-AM (cephalosporin core linked 7-hydroxycoumarin) following the standard protocol (<http://www.invitrogen.com>) and translocation was determined by measuring the ratio of cleaved (460 nm) to uncleaved (530 nm) CCF2-AM. Specimens in a 96-well plate format were imaged with an MD ImagerXpress and quantification was performed with CellProfiler.

Table 1: Bacterial strains and plasmids used in this study

Strain or plasmid	Genotype or relevant characteristics	Reference
Plasmids		
pRS40	vector for expression of NLS-Cre-MobA fusion proteins	(4)
pBR322	broad host range resistance plasmid	
pPG100	<i>E.coli-Bartonella</i> shuttle vector, encoding a short FLAG tag	(4)
pTR1000	Basic mutagenesis vector to generate in-frame mutants in RSE247 and RSE149	[21]
pHS003	suicide transposon vector	[35]
pPE002	suicide transposon vector, derivative of pSH003	this study
pPE0010	Tn mutagenesis vector, derivative of pPE002	this study
pPE0012	Tn mutagenesis vector, derivative of pPE0010	this study
pPG110	<i>E.coli-Bartonella</i> shuttle vector, for tag-less expression	this study
pPG180	<i>E.coli-Bartonella</i> shuttle vector, encoding a short MYC tag	this study
pPG184	<i>E.coli-Bartonella</i> shuttle vector, encoding MYC -BepD _{Bhe}	this study
pPG163	derivative of pTR1000 to generate in-frame mutants of RSE247	this study
pPG161	derivative of pTR1000 to generate pPG611	this study
pPG611	derivative of pTR1000 to generate pPG612	this study
pPG612	derivative of pTR1000 to generate chromosomal insertion to RSE247	this study
pFS20	derivative of pTR1000 to generate in-frame mutants of RSE149	this study
pPG104	encoding FLAG-BepD _{Bhe}	[2]
pPG105	encoding FLAG-Bep _{Bhe}	[23]
pPG106	encoding FLAG-BepF _{Bhe}	[23]

Table 1 continued

Strain or plasmid	Genotype or relevant characteristics	Reference
pPG185	encoding MYC-BepE _{Bhe}	this study
pPG185.M118	encoding MYC-BepE_FFFFF _{Bhe}	this study
pPG172	encoding MYC-BID1/2 _{Bhe}	this study
pRO104	encoding MYC-BID2 _{Bhe}	this study
pRO105	encoding MYC-BepE _{Bqu}	this study
pRO107	encoding MYC-BepH _{Bgr}	this study
pFS31	encoding BepD _{Btr}	this study
pFS32	encoding BepE _{Btr}	this study
pFS33	encoding BepD _{Btr} , BepE _{Btr}	this study
pFS01	encoding FLAG-BepD _{Btr}	this study
pFS02	encoding FLAG-BepE _{Btr}	this study
pPG213	encoding MYC-BepD _{Btr}	this study
pPG214	encoding MYC-BepE _{Btr}	
pCMV-FLAG2	eukaryotic expression vector, encoding a short FLAG tag	Eastman Kodak, New Haven
pWAY21	plasmid for ectopic expression of N-terminal eGFP fusion proteins	Molecular Motion Montana lab
pRO1000	eukaryotic expression, encoding FLAG-GFP-BepE	this study

Lenti Viral plasmids

pLenti-mCherryLifeact	encoding mCherry LifeAct	O. Pertz, unpublished
pMDL	packaging vector for plenty	O. Pertz, unpublished
pREV	packaging vector for plenty	O. Pertz, unpublished
pVSVG	packaging vector for plenty	O. Pertz, unpublished

Table 1 continued

Strain or plasmid	Genotype or relevant characteristics	Reference
<i>E. coli</i> strains		
NovaBlue	endA1 hsdR17(r K12–m K12+) supE44 thi-1 recA1 gyrA96 relA1 lac[F' proA+B+ lacIqΔM15::Tn10 (Tc ^R)]	Novagen, Madison
β2150	F' lacZDM15 lacIq traD36 proA+B+ thrB1004 pro thi strA hsdS lacZΔM15 ΔdapA::erm (Erm ^R) pir	[31]
<i>Bartonella henselae</i> strains		
RSE247	Spontaneous Sm ^R strain of ATCC 49882T, serving as wild-type <i>Bhe</i>	[21]
RSE242	Δ <i>virB4</i> mutant, derivative of RSE247	[22]
TRB106	Δ <i>bepB-G</i> mutant, derivative of RSE247	[21]
PGC80	Δ <i>bepD</i> mutant, derivative of RSE247	[60]
PGD20	Δ <i>bepE</i> mutant, derivative of RSE247	[60]
TRB222	Δ <i>bepF</i> mutant, derivative of RSE247	[60]
PGE26	Δ <i>bepDEF</i> mutant, derivative of RSE247	this study
PGD21	Δ <i>bepE</i> mutant, containing pPG185	this study
ROB109	Δ <i>bepE</i> mutant, containing pPG172	this study
ROB111	Δ <i>bepE</i> mutant containing pRO104	this study
ROB113	Δ <i>bepE</i> mutant containing pRO105	this study
ROB117	Δ <i>bepE</i> mutant containing pRO107	this study
ROB119	Δ <i>bepE</i> mutant containing pPG214	this study
ROB121	Δ <i>bepE</i> mutant containing pPG213	this study
PGD67	Δ <i>bepDEF</i> mutant, containing pPG185	this study
ROB141	Δ <i>bepDEF</i> mutant containing pPG172	this study
ROB143	Δ <i>bepDEF</i> mutant containing pRO104	this study
ROB145	Δ <i>bepDEF</i> mutant containing pRO105	this study
ROB149	Δ <i>bepDEF</i> mutant containing pRO107	this study

Table 1 continued

Strain or plasmid	Genotype or relevant characteristics	Reference
ROB151	$\Delta bepDEF$ mutant containing pPG214	this study
ROB153	$\Delta bepDEF$ mutant containing pPG213	this study
PGH75	chromosomal integration of Bla-BIDBepD _{Bhe} , derivative of RSE247	this study
<i>Bartonella tribocorum</i> strains		
RSE149	Spontaneous Sm ^R strain, serving as wild-type <i>Btr</i>	[15]
FS150	$\Delta bepDE$ mutant, derivative of RSE149	this study
FS179	$\Delta bepDE$ mutant, containing pFS32	this study
FS180	$\Delta bepDE$ mutant, containing pFS33	this study
ROA150	$\Delta bepDE$ mutant, containing pPG105	this study
ROA158	$\Delta bepDE$ mutant, containing pPG185.M118	this study
ROA168	$\Delta bepDE$ mutant, containing pPG172	this study
<i>Bartonella quintana</i> strain		
RSE356	Spontaneous Sm ^R strain, serving as wild-type <i>Bqu</i>	[25]
<i>Bartonella grahamii</i> strain		
CHDE142	No 376, isolated from <i>Microtus</i> sp. serving as wild-type <i>Bgr</i>	[27]
<i>Bartonella Birtlesii</i> strains		
PEE0261	IBS325T serving as wild-type <i>Bbi</i>	[28]
CMB0142	<i>Bbi-Tn-cre</i> , derivative of PEE0261	this study

Table 2: Oligonucleotides used in this study

Name	Sequence ^a	Restriction sites
prTR15	ATAAGAAT <u>GCGGCCG</u> GATGAAAAGAAATCAACCACCCC	<i>NotI</i>
prTR16	CGGGATCCTTAGATGGCGAAAAGCTATTGCC	<i>BamHI</i>
prTR041	CGGGATCCGCACACTCTGTGGAAAAACC	<i>BamHI</i>
prTR042	CGGGATCCTTAGCTGGCAATAGCAAGCG	<i>BamHI</i>
prTR043	ATAAGAAT <u>GCGGCCG</u> GATGTTAGAGCATAATTATCTGTAT	<i>NotI</i>
prTR044	ATAAGAAT <u>GCGGCCG</u> GATGAAAAAAAAACAACCAGCCC	<i>NotI</i>
prTR051	CAACCATCCCCTCCGACTCCCACAAATCAAAAAGGA	
prTR055	CACAAAAAATGGTGCTGGC	
prTR056	GCTCTAGAGGCGTTACACAGGGAAGAG	<i>XbaI</i>
prFS09	CGGGATCCGCTTTCGTCGTTGGGCACA	<i>BamHI</i>
prFS10	ATCTGTTTTATGTTTATGCCACTTTAGCCTGTAAGA GCCAGTG	
prFS11	CACTGGCTCTTACAGGCTAAAGTGGCATAAACATAA AACAGAT	
prFS12	CGGGATCCTTTGAATTCCTGCATTTTTTCTT	<i>BamHI</i>
prFS01	CGGGATCCGGAATTCCCATATGAAAAAACATCATCCACACCCA	<i>BamHI, NdeI</i>
prFS02	CGGGATCCGGAATTCCCATATGTTACATGGCATAAGCCATTCC	<i>BamHI, NdeI</i>
prFS17	CGGGATCCGGAATTCCCATATGGTGAAAAAAGTCACCCACAAC	<i>BamHI, NdeI</i>
prFS18	CGGGATCCGGAATTCCCATATGTTACATGGCATAAGACATTCCT	<i>BamHI, NdeI</i>
prPG90	CGCGAGCTCTTTAAGAAGGAGATATACATATGGG GATGCCTGGCAGTTTAT	<i>SacI, NdeI</i>
prPG91	CGCGAGCTCTAAATCAGAACGCAGAAGCG	<i>SacI</i>
prPG101	GGAATTCATATGTTAGATGGCGAAAGCTATTGC	<i>NdeI</i>
prPG141	CGCGCTTATTAATGGAACAAAAACTTATTTCTGAA GAAGATCTTCATATGAAAAAATCGACCATCCCCT	<i>AseI, NdeI</i>

^aRestriction endonuclease cleavage sites are underlined

Table 2: continued

Name	Sequence ^a	Restriction sites
prPG142	CGCGCTT <u>ATTAATCATATG</u> TTACATACCAAAGGCCA TTCC	<i>AseI, NdeI</i>
prPG190	GCTCCGCCATCGCCGCT	
prPG191	GGATTGAACGTTGCGAAGC	
prPG212	CGCGGATCCACACGTGAGATATCTATAATTCTCTCTG	<i>BamHI</i>
prPG213	AG <u>CCGCGG</u> CAAGATCTTCTTCAGAAATAAGTTTTTGTTCCATGCATGCTTCCTTTCAAGC	<i>SacII</i>
prPG214	CTTATTTCTGAAGAAGATCTTG <u>CCGCGG</u> CTCACCCAGAAA CGCTGGTG	<i>SacII</i>
prPG215	TG <u>CGGCCGCC</u> CAATGCTTAATCAGTGAGGCAC	<i>NotI</i>
prPG216	GATTAAGCATTGGG <u>CGGCCG</u> CTGGAGTTGGCCC AGGAAGG	<i>NotI</i>
prPG217	ACGCGT <u>CGACAC</u> ATTTTCATAA <u>CACTTCTTGGCGCAC</u>	<i>SalI</i>
prPG219	<u>GGATCC</u> CAAGCTTTCTCAATAGCAATATTTGTTTTG AAAGC	<i>BamHI</i>
prPG236	CCGAATTCTGATCAAGAAATAATTCCACCTCTTAGT TACGTGG	
prPE247	CCGTTA <u>ATTAAT</u> ATTCTGAAATGAGCTGTTGAC	<i>PacI</i>
prPE248	CCGT <u>CTAGAC</u> CAGAACGCAGAAAGCGGTCTG	<i>XbaI</i>
prRO030	GGAATT <u>CCATATGC</u> ATCCTGAAAGGGAGAGAC	<i>NdeI</i>
prRO033	GGAATT <u>CCATATG</u> AAAAAAAAACCAACCATCCTC	<i>NdeI</i>
prRO034	GGAATT <u>CCATATG</u> TTAGCTGGCGAAAGCTATTGC	<i>NdeI</i>
prRO037	GGAATT <u>CCATATG</u> AAAAACATCATCCACACCC	<i>NdeI</i>
prRO038	GGAATT <u>CCATATG</u> TTACATGGAATAAGCCATACC	<i>NdeI</i>

^aRestriction endonuclease cleavage sites are underlined

Figure Legends

Figure 1: Invasion of red blood cells (RBCs) with *Btr* is delayed for 4 days in *i.d.* infection compared to *i.v.* route.

Groups of rats ($n = 5$) were injected with phosphate-buffered saline (PBS) solution containing *Btr* wild type either intravenously (*i.v.*) in the tail vein or intradermally (*i.d.*) on the ear (200 μ l and 10 μ l respectively bacterial suspension, $OD_{595}=1$). Blood samples were collected from the tail vein with 10% sodium-citrate supplementation at the time points indicated on the graphs. The blood cells were lysed by freezing the whole blood. Undiluted and serial dilutions of thawed blood in PBS were plated on sheep blood supplemented columbia agar plates (CBA) for counting colony forming units (CFU) per mL of blood. Plotted graphs represent an average of bacterial number/mL of blood in animals groups from which bacteria were recovered at the given time points post-infection. The error bars represent standard deviation for the groups of animals.

Figure 2: Rats infected with *Btr* $\Delta bepDE$ do not develop blood stage infection.

Groups of rats ($n= 5$) were injected *i.d.* with PBS solution containing *Btr* wild-type or *Btr* $\Delta bepDE$ (10 μ l bacterial suspension in PBS, $OD_{595}= 1$). Blood samples were collected from the tail vein with 10% sodium-citrate supplementation at the time points indicated on the graphs. The blood was frozen to lyse red blood cells, undiluted and serial dilutions of thawed blood in PBS were plated on CBA for counting CFUs per mL of blood. Plotted graphs represent time course of single animals from which bacteria were recovered at a given time point post-infection. Each value corresponds to an average acquired from serial dilutions. One animal out of 5 (out of 13 in combined results from 3 independent experiments) infected with $\Delta bepDE$ detected in the blood with few days delay compared to wild-type infected rats. However, after reaching the blood stream the knockout strain was as successful as wild-type in colonization of blood showing high titers of bacteria.

Figure 3: Complementation of abacteremic phenotype of *Btr ΔbepDE*.

Groups of rats ($n = 3$ for *i.v.*, $n = 5$ for *i.d.*) were injected with PBS solution containing *Btr* corresponding strains depicted on the graph ($200 \mu\text{l}$ and $10 \mu\text{l}$ of $\text{OD}_{595} = 1$ for *i.v.* and *i.d.* respectively). Blood samples were collected from the tail vein with 10% sodium citrate supplementation at 16 days post infection (dpi). The blood cells were lysed by freezing the whole blood. Undiluted and serial dilutions of thawed blood in PBS were plated on sheep blood supplemented CBA for counting CFU per mL of blood. Plotted graph represents data of single animals (circles) with an average (line) of the values from serial dilutions within the group of animals, (similar observation was obtained after 10 dpi). *Btr ΔbepDE* behaved as wild-type when directly delivered in the blood (*i.v.*) and reached the same high titers but was not detectable in the blood using the *i.d.* route of infection. The blood abacteremic phenotype of *Btr ΔbepDE* could be rescued by over expression of plasmid encoded BepD_{Btr} and BepE_{Btr} or BepE_{Btr} alone *in trans*. BepE_{Bhe} could functionally replace BepE_{Btr} and enabled *Btr ΔbepDE* to colonize the blood.

Figure 4: Tyrosine containing motives of BepE are not essential for *Bartonella* to reach the blood.

A. Groups of rats ($n = 3$ for control groups, $n = 5$ for complementation strains) were injected *i.d.* with PBS solution containing $10 \mu\text{l}$ of $\text{OD}_{595} = 1$ of *Btr* corresponding strains depicted on the graph. Blood samples were collected from the tail vein with 10% citrate supplementation at the time points indicated on the graph. The blood was frozen to lyse red blood cells, undiluted and serial dilutions of thawed blood in PBS were plated on CBA for counting CFU/mL of blood. Plotted graph represents data of single animals with an average of serial dilutions, at 16 days post-infection. Both mutants of BepE_{Bhe} are complementing *Btr ΔbepDE* phenotype, showing no essential role of the tyrosine containing motives and the N-terminal part of BepE_{Bhe} in colonization of natural host.

B. Protein levels of BepE_{Bhe} and BepE_{Bhe} mutant expressions by heterologous complementation in *Btr ΔbepDE*. $\alpha\text{-BepE}_{Bhe}$ western blot of bacterial total lysate ($\text{OD}_{595} = 2$) is presented.

Figure 5: Infection with *Bhe* $\Delta bepE$ or $\Delta bepDEF$ leads to the fragmentation of HUVECs.

A. The monolayer of HUVECs was infected for 24 h, 36 h and 48 h with MOI=200 of *Bhe* wild-type, *Bhe* $\Delta bepE$ or *Bhe* $\Delta bepDEF$ mutants followed by fixation, immunocytochemical staining and confocal laser scanning microscopy. F-actin is represented in red and bacterial DNA and cell nucleus in blue (scale bar = 25 μ m). Panel for *Bhe* $\Delta bepE$ and *Bhe* $\Delta bepDEF$ shows the cell elongation starting at 24 hpi, going from dramatic to extreme on 36 and 48 hpi and forming fragments without nucleus.

B. Cell fragmentation was quantified in semi-automated manner. HUVECs in 96-well format were infected with *Bhe* strains depicted on the graph. 20 fields per well were imaged by MD ImageXpress Micro automated microscopes. The number of cells per image was determined automatically by MetaExpress in-build analysis modules (CountNuclei). The thin elongations of the cells were defined and counted by eye. The percentage of elongated cells is shown on the figure. In every condition 20 fields of magnification 20 within the well and triplicates of the wells were analysed. The error bars were calculated as SD within the replicas. Statistical significance was determined using Student's *t*-test. * $P < 0.005$, ** $P < 0.001$ were considered statistically significant

Figure 6: Multiple fragmentation of *Bhe* $\Delta bepE$ infected HUVEC in time-lapse

Prior to infection, HUVECs of an early passage were infected with lentiviral vectors encoding *mCherry LifeAct*. F-actin fluorescent HUVECs in 96 well format were infected with MOI=200 of *Bhe* $\Delta bepE$. At 8 hpi infected cells were exposed to MD ImageXpress Micro automated microscope for live cell imaging. Snapshots of gray scale images with 30 min intervals are presented on the figure. The scale bar is for 25 μ m. The errors are pointing to the regions of the cell where the fragmentation is taking place.

Figure 7: By providing BepE_{Bhe} *in-trans* on a plasmid, the Δ bepDEF-infected HUVECs do not undergo cell fragmentation.

A. The monolayer of HUVECs was infected for 24 h, 36 h and 48 h with MOI=200 of single effector complemented *Bhe* Δ bepDEF-pbepD_{Bhe}, *Bhe* Δ bepDEF-pbepE_{Bhe} and *Bhe* Δ bepDEF-pbepF_{Bhe} strains followed by fixation, immunocytochemical staining and confocal laser scanning microscopy (scale bar = 25 μ m). F-actin is represented in red and bacterial DNA and cell nucleus in blue. Panel for *Bhe* Δ bepDEF-pbepD_{Bhe} and *Bhe* Δ bepDEF-pbepF_{Bhe} shows that the cell elongation followed by fragmentation is not rescued; only BepE_{Bhe} was able to complement the cell fragmentation.

B. Cell fragmentation was quantified in semi-automated manner as described above for Figure 5.

Figure 8: The BID domains of BepE_{Bhe} are sufficient to inhibit the fragmentation of ECs.

A. The monolayer of HUVECs was infected for 24h, 36h and 48h with MOI=200 of Δ bepE complemented with either both BID domains or the last C-terminal BID domain followed by fixation, immunocytochemical staining and confocal laser scanning microscopy (scale bar = 25 μ m). F-actin is represented in red and bacterial DNA and cell nucleus in blue. Panels for *Bhe* Δ bepE-pBID1/2E_{Bhe} and *Bhe* Δ bepE-pBID2E_{Bhe} show that the cell elongation followed by fragmentation could not be rescued by the last BID domain of BepE_{Bhe} only, showing an intermediate phenotype. The two BIDs together were needed to inhibit the effect of the knock out strains.

B. Alignment of two BID domains of BepE_{Bhe} shows 53.3% of pair wise identity. Geneious 5.3.4. Software was used for the amino acid sequence alignment.

C. Cell fragmentation was quantified in semi-automated manner as described for Figure 5.

D. Protein levels of the two BIDs and the last C term BID of BepE_{Bhe} by over expression of pBID1/2E and pBID2E in *Bhe* Δ bepE and *Bhe* Δ bepDEF. The α -BepE_{Bhe} western blot was obtained from total lysate of (OD₅₉₅= 2) wild-type *Bhe* and plasmid complemented strains.

Figure 9: BepE_{Bhe} homologs are able to inhibit fragmentation of HUVECs caused by *Bhe* Δ bepDEF.

A. HUVECs were infected for 24 h, 36 h and 48 h with MOI=200 of *Bhe* mutant strain complemented with the indicated Beps followed by fixation, immunocytochemical staining and confocal laser scanning microscopy. F-actin is represented in red and bacterial DNA and cell nucleus in blue (scale bar = 25 μ m). Compared to BepE_{Btr}, BepE_{Bqu} and BepH_{Bgr}, Bep_{Btr} revealed the lowest potency to inhibit the fragmentation. The time point 36 hpi is presented on the figure.

B. Cell fragmentation was quantified in semi-automated manner as described for Figure 5.

C. Protein levels of the BepE_{Bhe} homologs, BepE_{Bqu}, BepE_{Btr}, BepD_{Btr} and BepH_{Bgr} by over expression in *Bhe* Δ bepE and *Bhe* Δ bepDEF. The α -FLAG (M2) and α -Myc western blots were obtained from total lysate of (OD₅₉₅ = 2) *Bhe* wild-type and plasmid complemented strains.

Figure 10: Ectopic expression of GFP-BepE_{Bhe} in HUVECs

HUVECs of an early passage were electroporated according to the Amaxa nucleofection protocol with the plasmid encoding for CMV promoter driven GFP-BepE_{Bhe}. 24 hours post transfection (hpt) GFP-BepE_{Bhe} expressing cells were quantified by flow cytometry (A) and analysed by scanning confocal microscopy (B). Around 50 % of HUVECs expressed GFP-BepE_{Bhe} and BepE_{Bhe} localized to the plasma membrane.

Figure 11: Ectopic expression of BepE_{Bhe} in HUVECs preserves the cells from fragmentation

HUVECs of an early passage were transfected with the plasmid encoding CMV-promoter driven GFP or GFP-BepE_{Bhe} using the Amaxa nucleofection kit. After 24 hpt cells were infected with *Bhe* wild-type and *Bhe* Δ bepE. The infection was stopped at several time points as depicted on the figure followed by fixation, immunocytochemical staining and

confocal laser scanning microscopy (scale bar = 25 μm). F-actin is represented in red, bacterial DNA and cell nucleus in blue, GFP and GFP-BepE_{Bhe} in green.

Figure 12: Effector translocation in *Bbi* infected BMDCs.

BMDCs, cultured *in vitro* from *Rosa26-loxP-egfp* Balb/c transgenic mouse bone marrow in presence of Flt3L for 10 days, were infected with MOI=50 of either *Bbi* wild-type or *Bbi-Tn-cre* strain (expressing a NLS-cre-BID fusion) for two days.

A. GFP expression in infected cell culture was detected using a Leica DM-IRBE inverted fluorescence microscope.

B. GFP-expressing cells from the live population on day 2 post infection of MBDC culture as analysed by flow cytometry. Upper panel of dot plots corresponds to the results obtained from *wild-type Bbi* infection of BMDCs. The lower panel shows the results for *Bbi-Tn-cre* infection.

C. Quantification of GFP-expressing cells from the live population on day 2 and day 3 post infection of MBDC culture analysed by flow cytometry. The data are normalized, GFP⁺ cells quantified either in CD11c⁺ or CD11c⁻ cell-population. Results from 2 *independent experiments with duplicates* are shown.

Figure 13: *Bbi* infected cells are CD11c⁺ dendritic cells.

BMDCs from *Rosa26 loxp-GFP* Balb/c mice were infected with MOI=50 of either with *Bbi* wild type or *Bbi-Tn-cre*, after 3 days post infection infected cell culture was stained for CD11c and analysed by flow cytometry.

A. Distribution of GFP and CD11c expressing cells in the whole population of BMDCs. UR (Upper Right) dot plot is an unstained wild-type infected control sample, LL (Lower Left) – stained for CD11c *wild-type Bbi* infected and LR (lower Right) – CD11c stained *Bbi-Tn-cre* infected . Results of *one representative* experiment out of 2 are shown.

B. Quantification of GFP-expressing CD11c⁺ and CD11c⁻ cells in BMDCs population. Error bars denote SD within replicas and different experiments. Results of 2 *different experiments with duplicates* are quantified.

Figure 14: *Bbi* infects pDCs and cDCs *in vitro*.

BMDCs from *Rosa26 loxp-GFP* Balb/c mice were infected with MOI=50 of either *Bbi* wild type or *Bbi-Tn-cre*, after 3 days post infection infected cell culture was stained for CD11c in combination with either α -MHCIlb or α -B220 antibodies. The stained and unstained samples were analysed by flow cytometry.

A. Distribution of GFP/MHCIlb and GFP/B220 expressing cells in the CD11c⁺ cell population of BMDCs is shown in the middle panel of dot plots. Results of *one representative* experiment out of 2 are shown.

B. Quantification of MHCIlb/GFP-expressing infected DCs. The data are normalized to CD11c⁺MHCIlb⁺ and CD11c⁺MHCIlb⁻ population.

C. Quantification of GFP-expressing infected pDCs and cDCs. The data are normalized to CD11c⁺B220⁺ and CD11c⁺B220⁻ population.

Error bars denote standard deviation within replicas and different experiments. Results of 2 *different experiments with duplicates* are quantified.

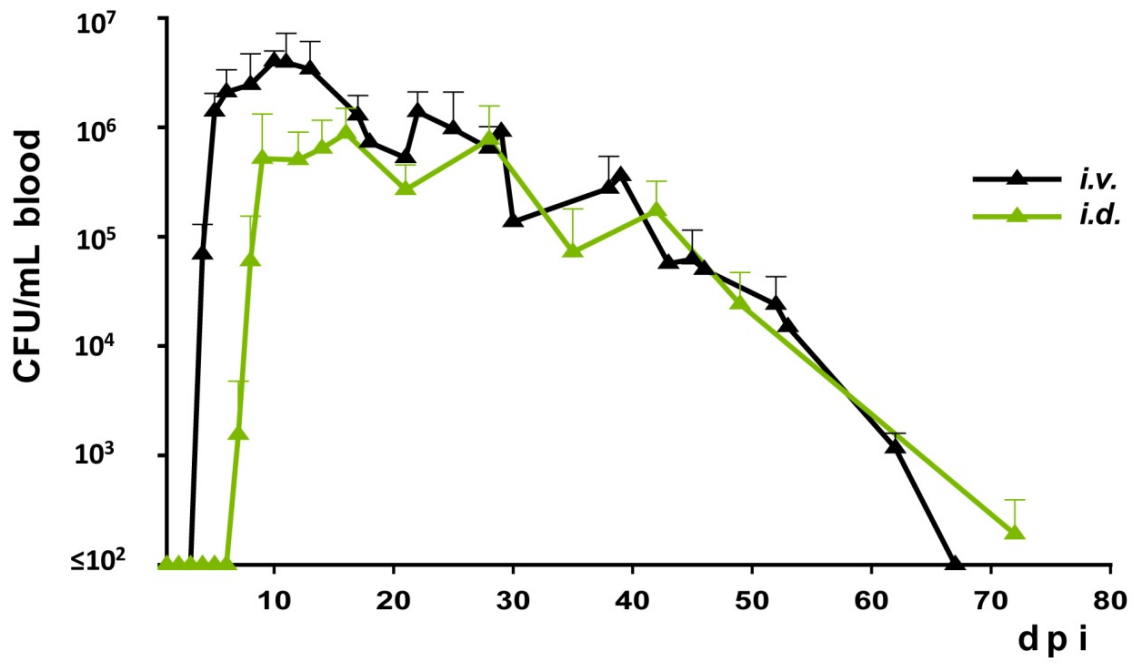


Figure 1.

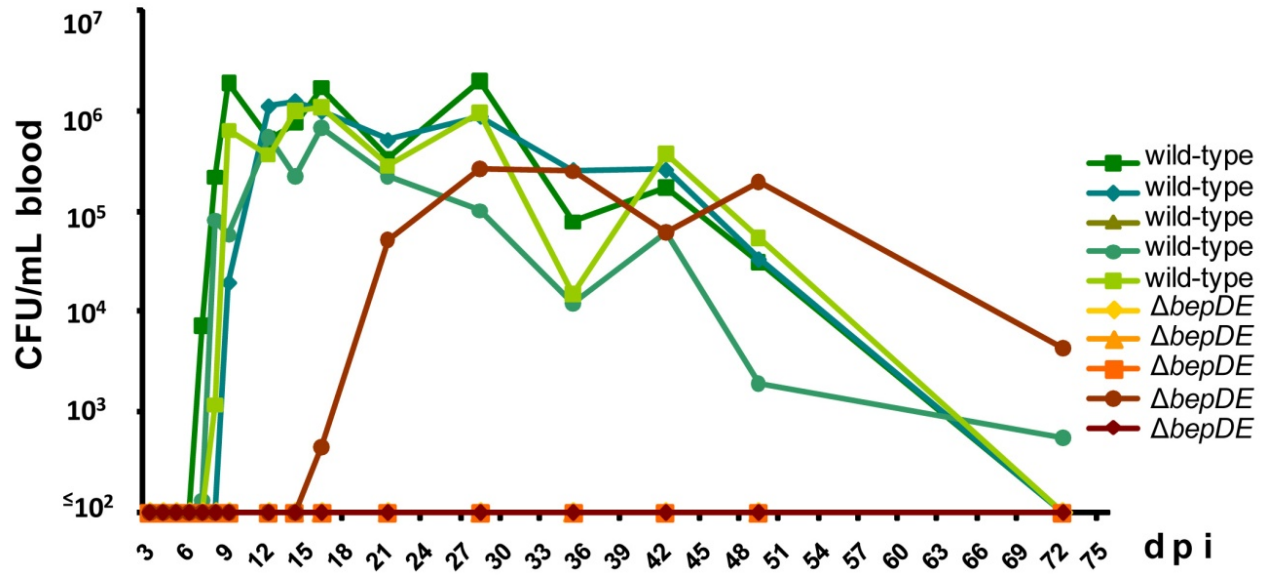


Figure 2.

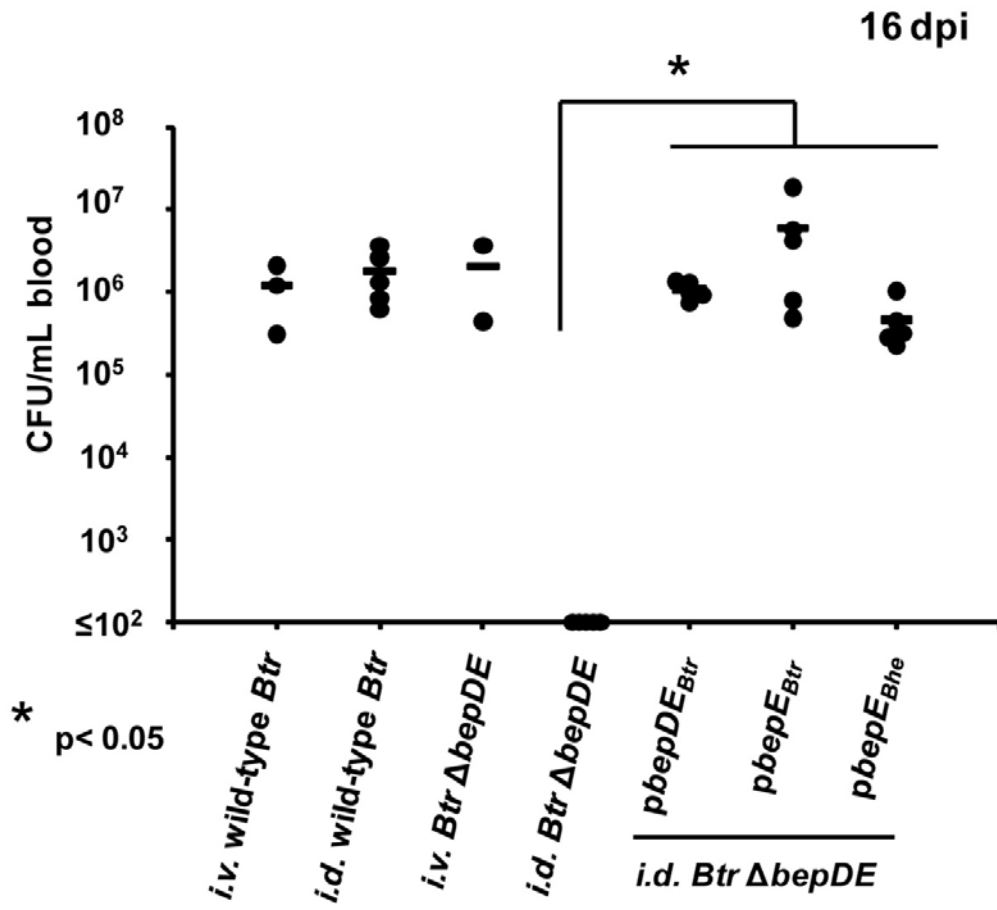


Figure 3.

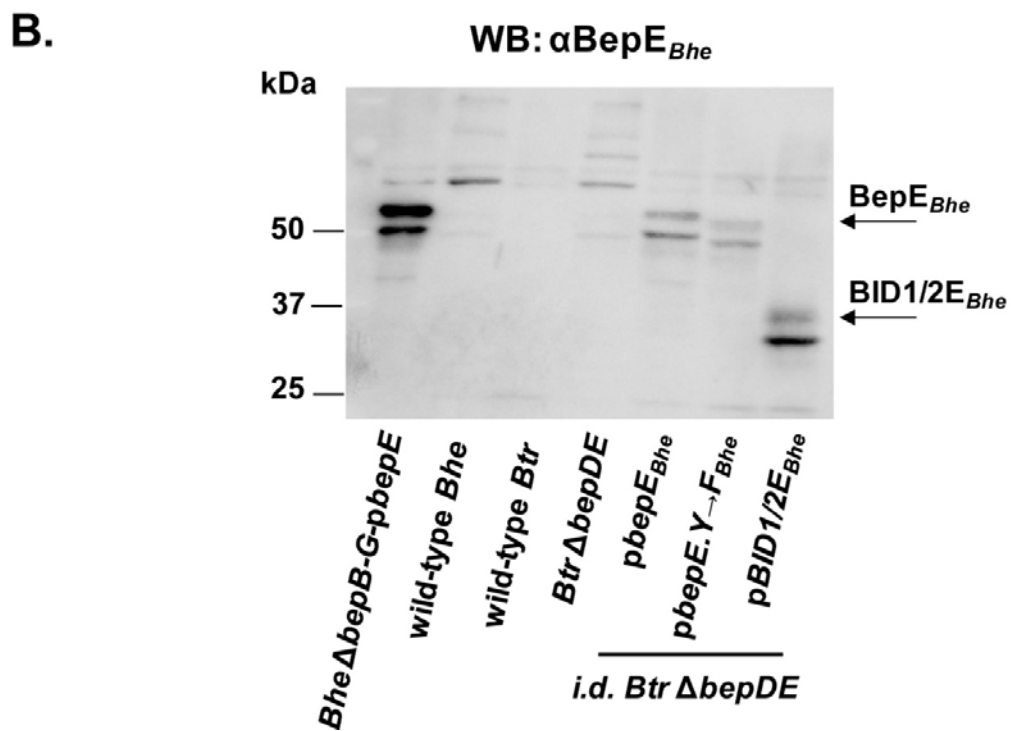
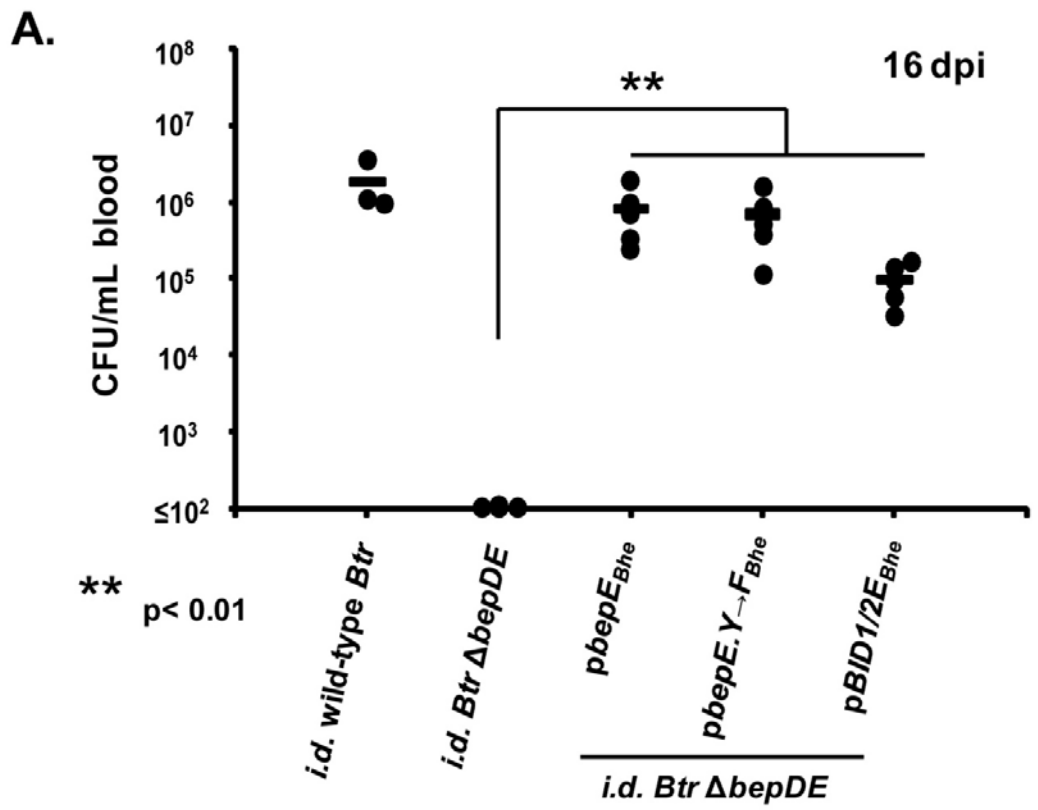


Figure 4.

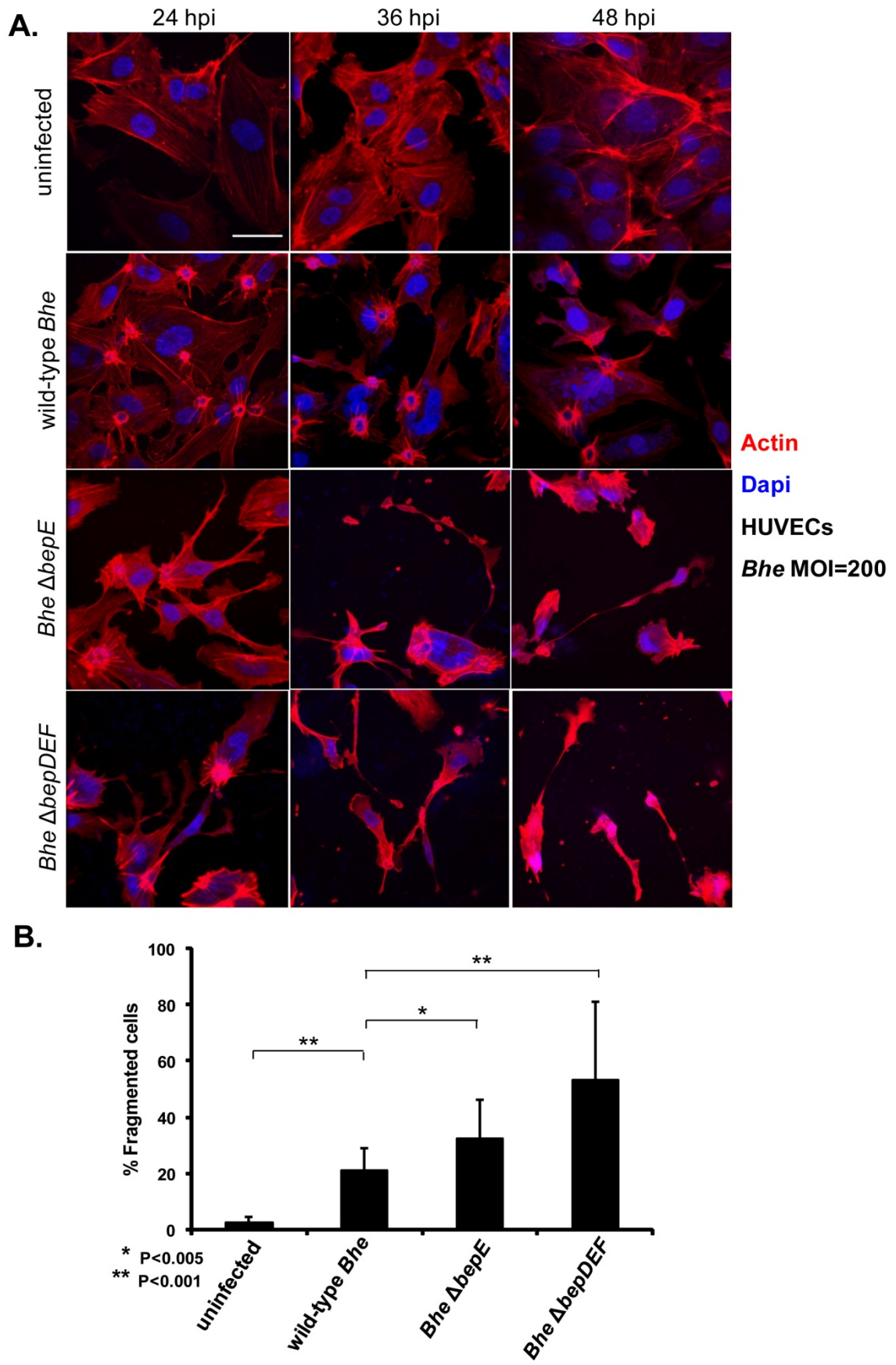


Figure 5.

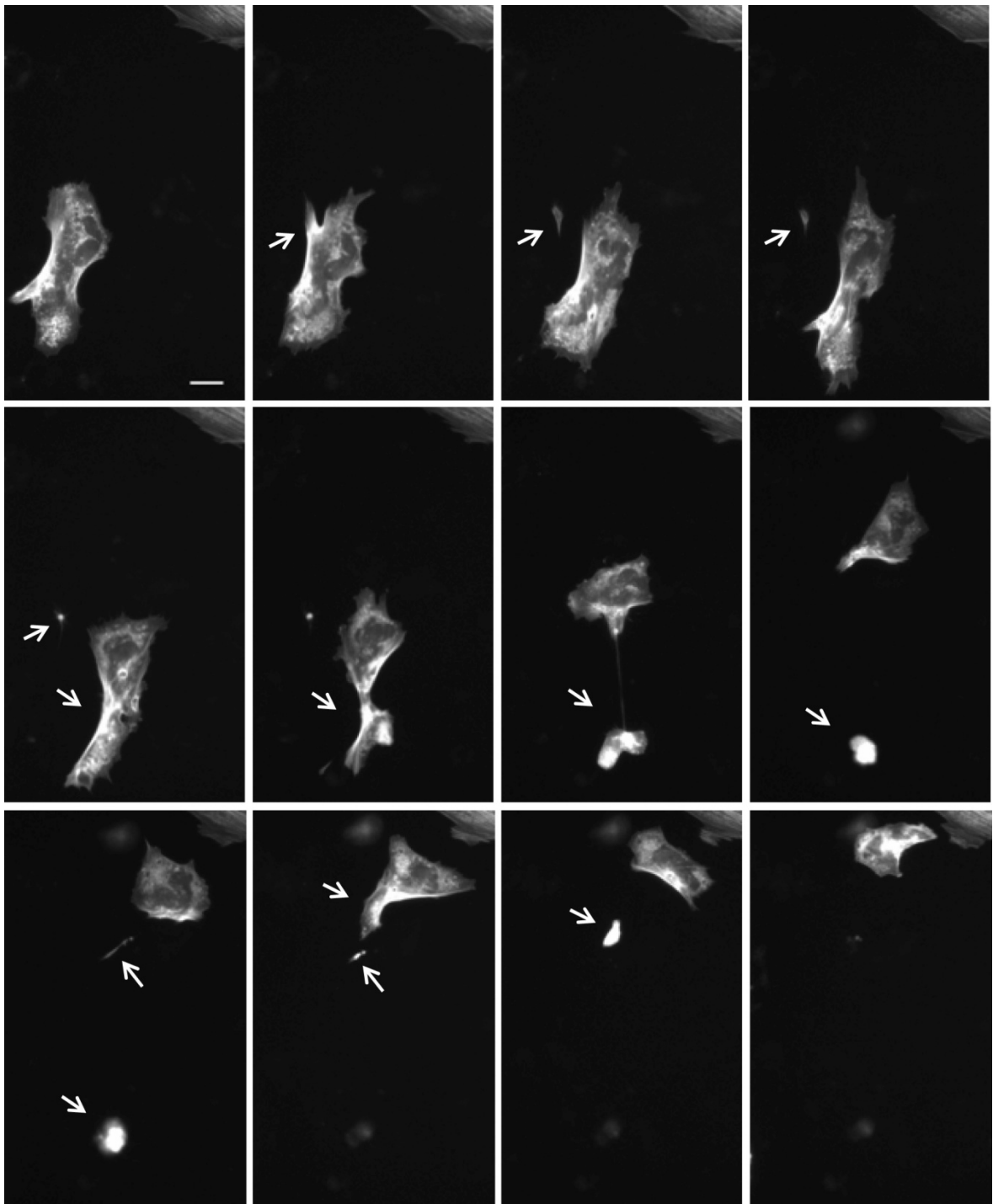


Figure 6.

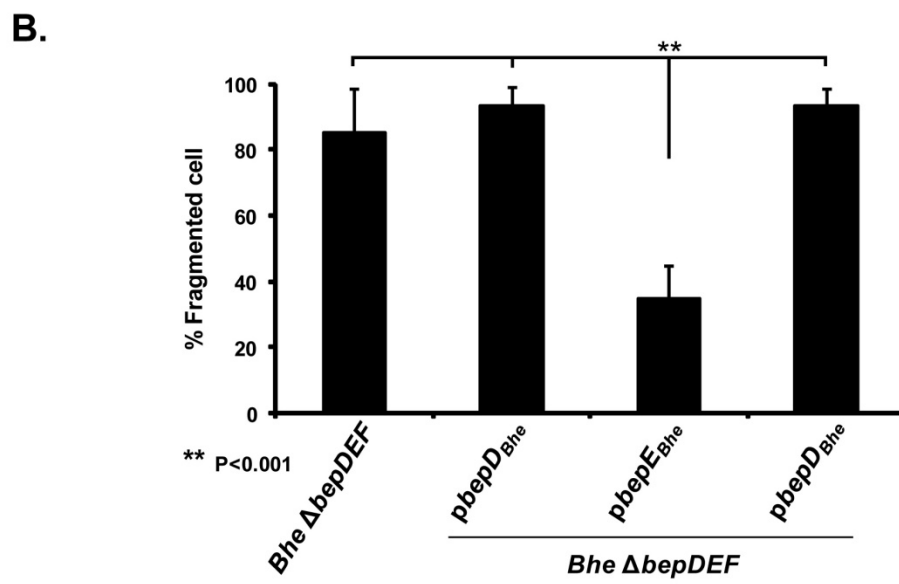
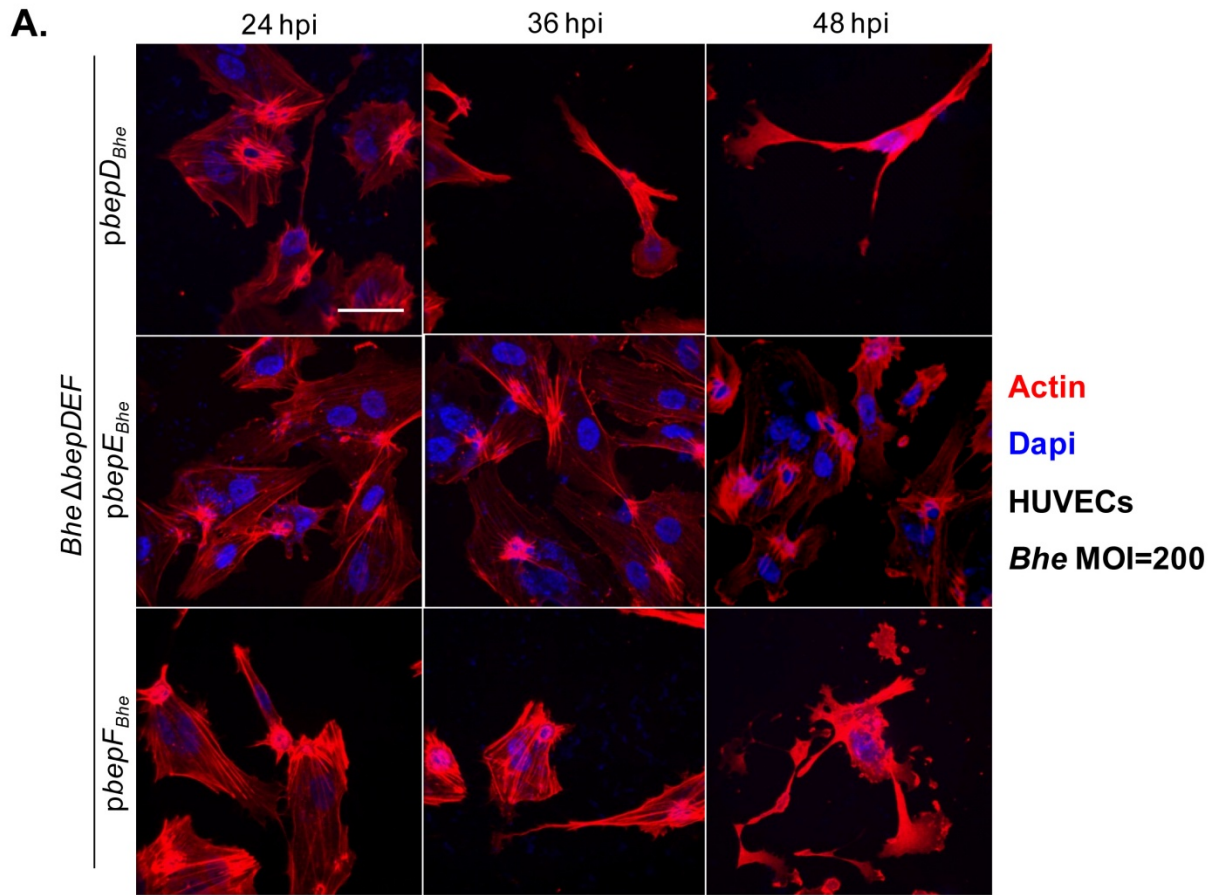


Figure 7.

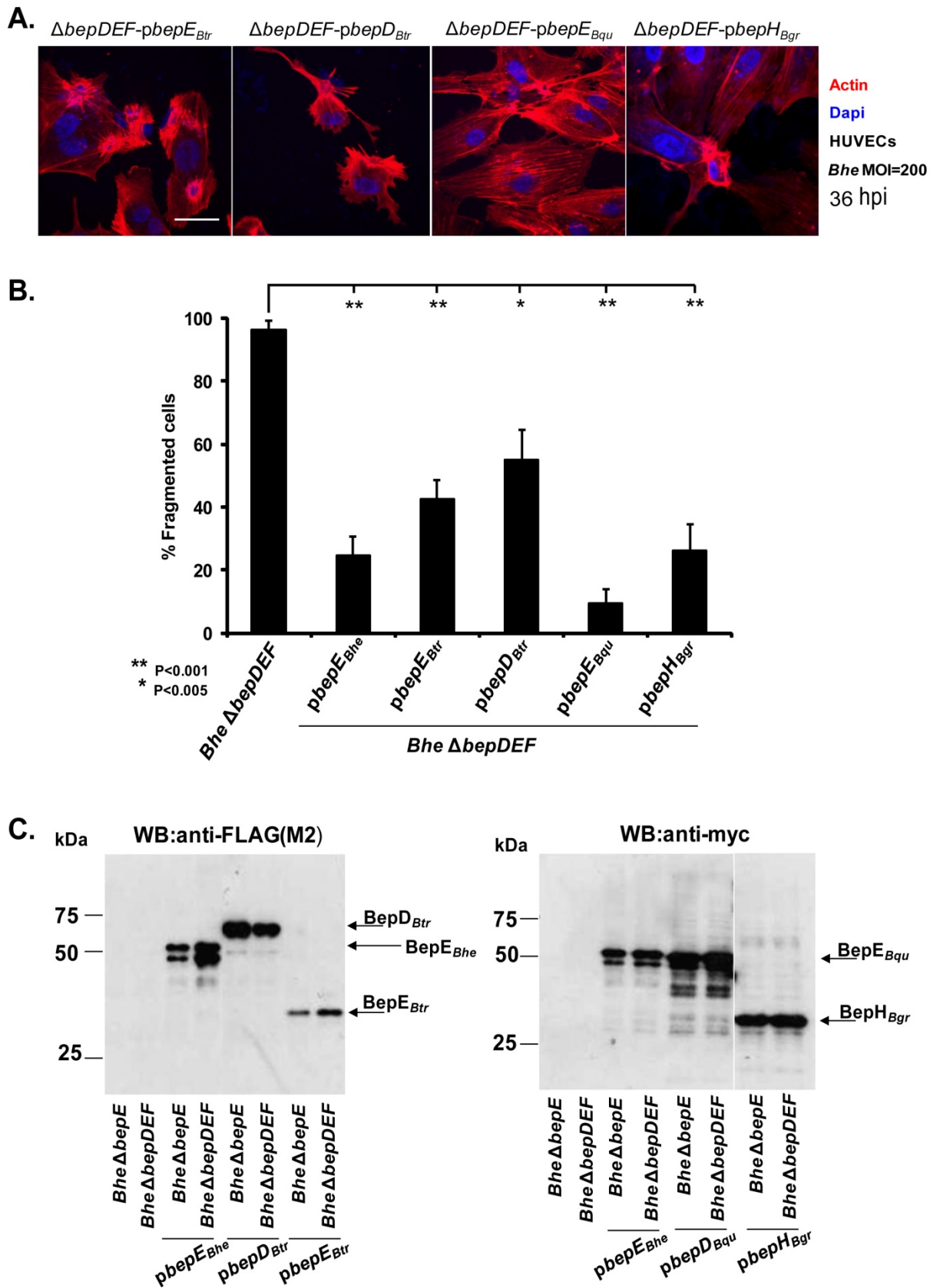


Figure 9.

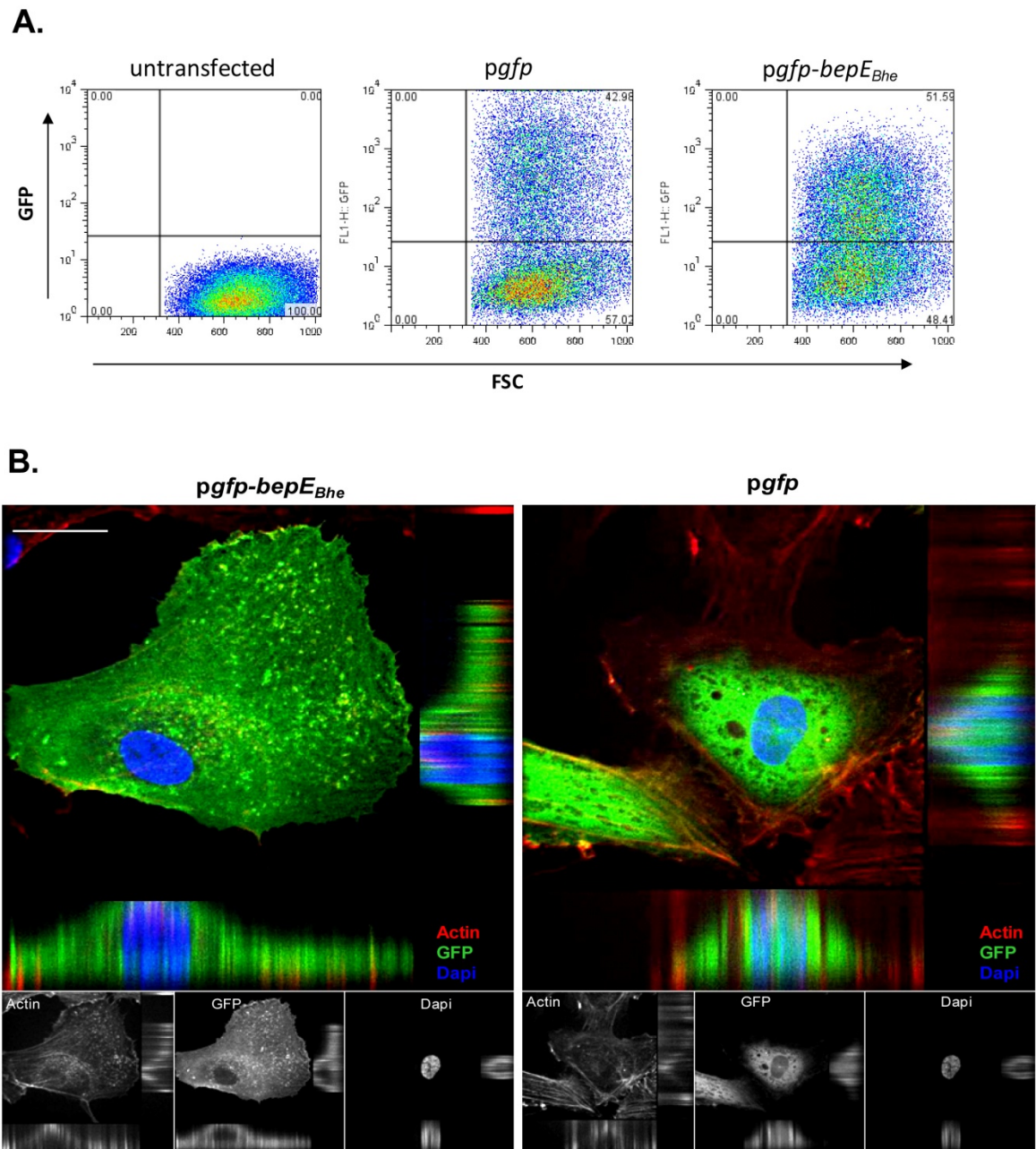


Figure 10.

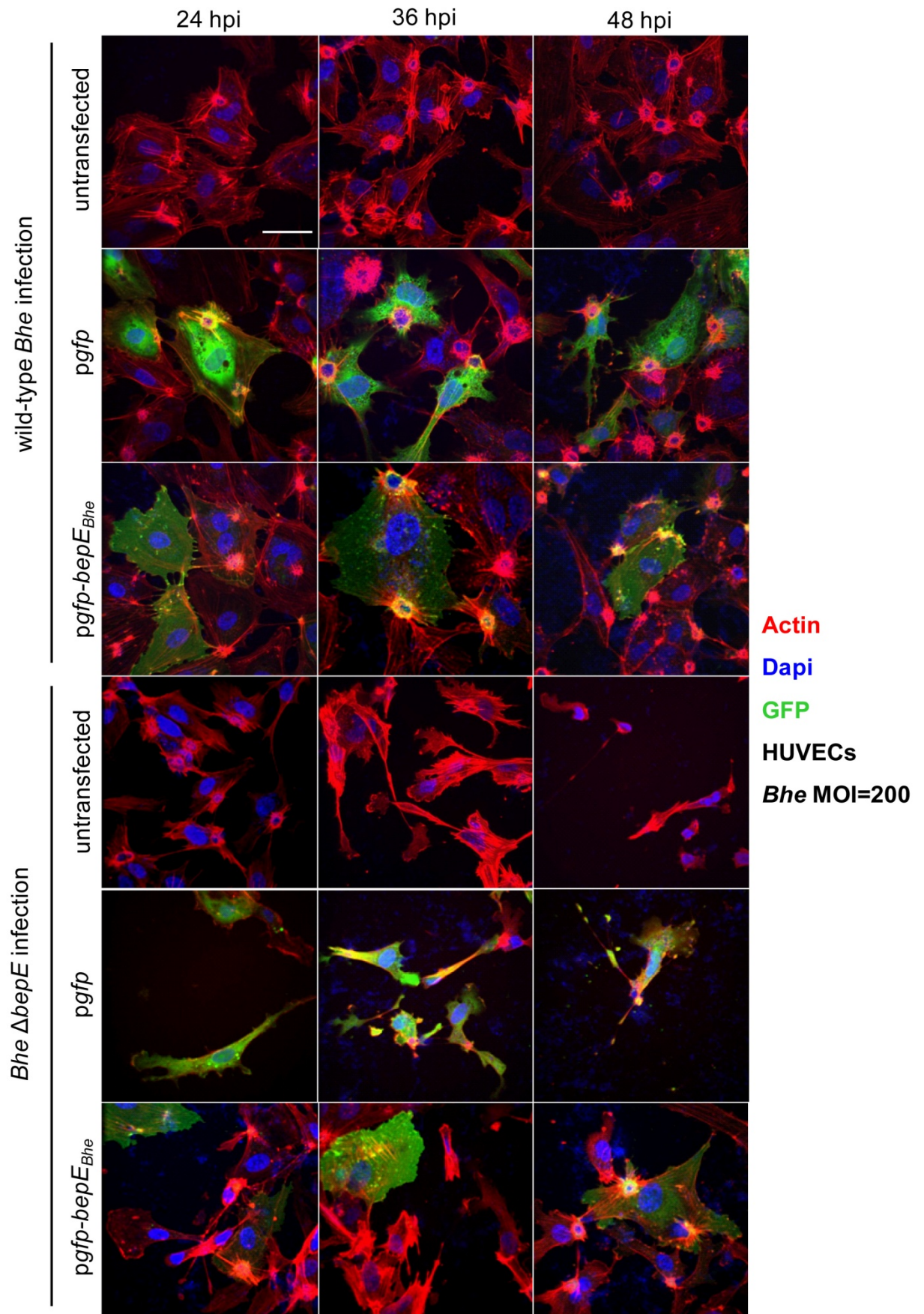


Figure 11.

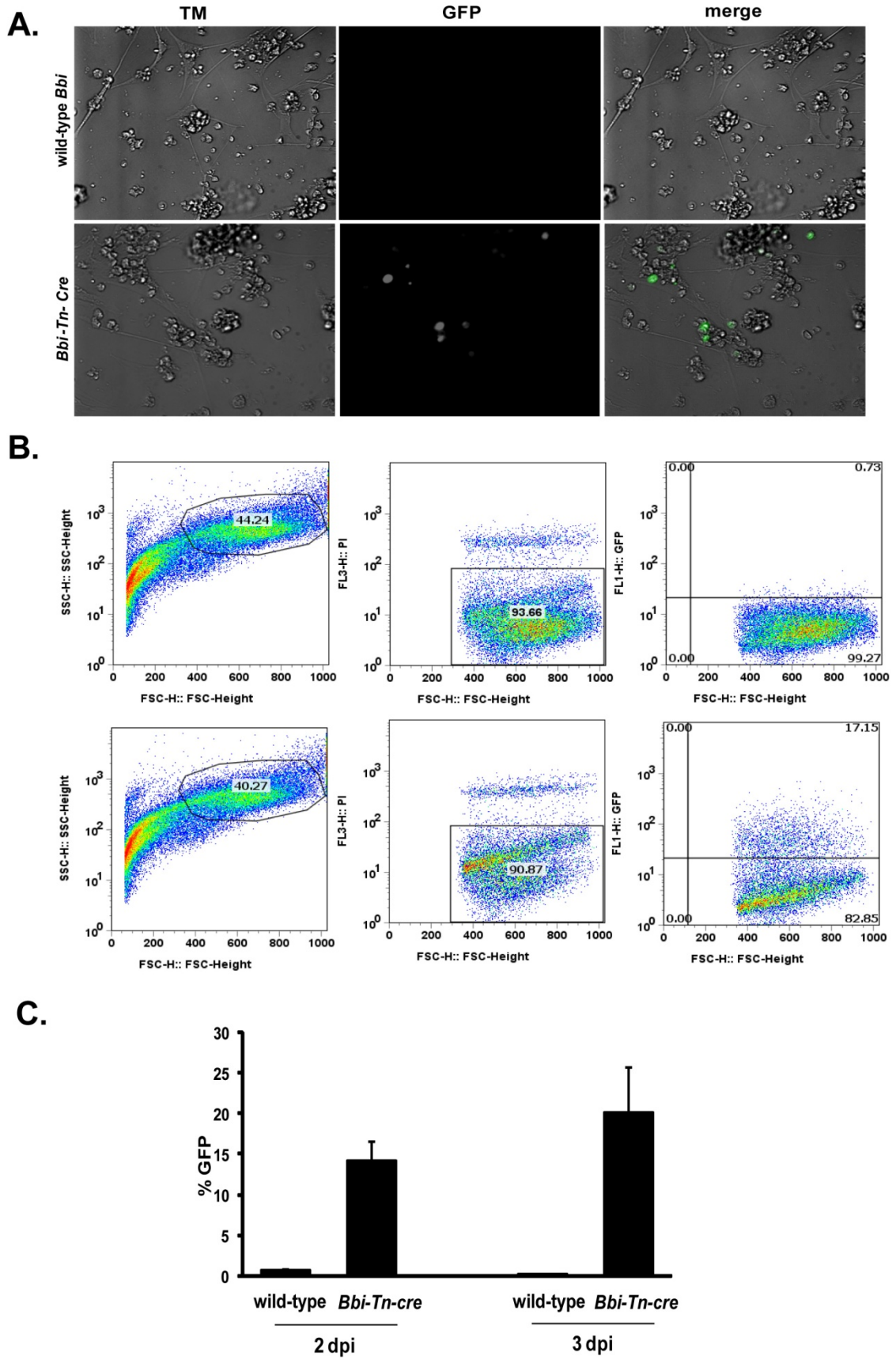


Figure 12.

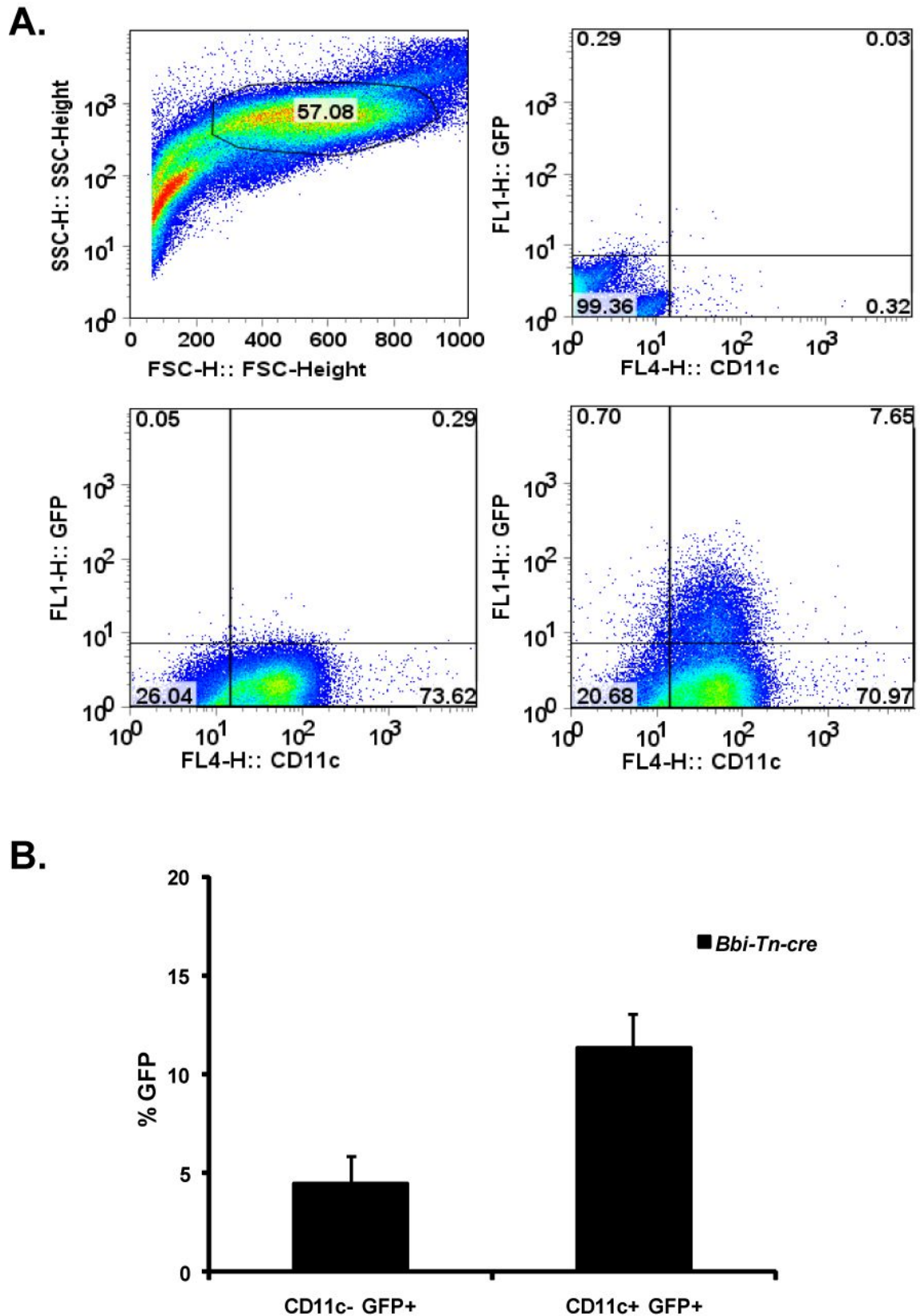


Figure 13.

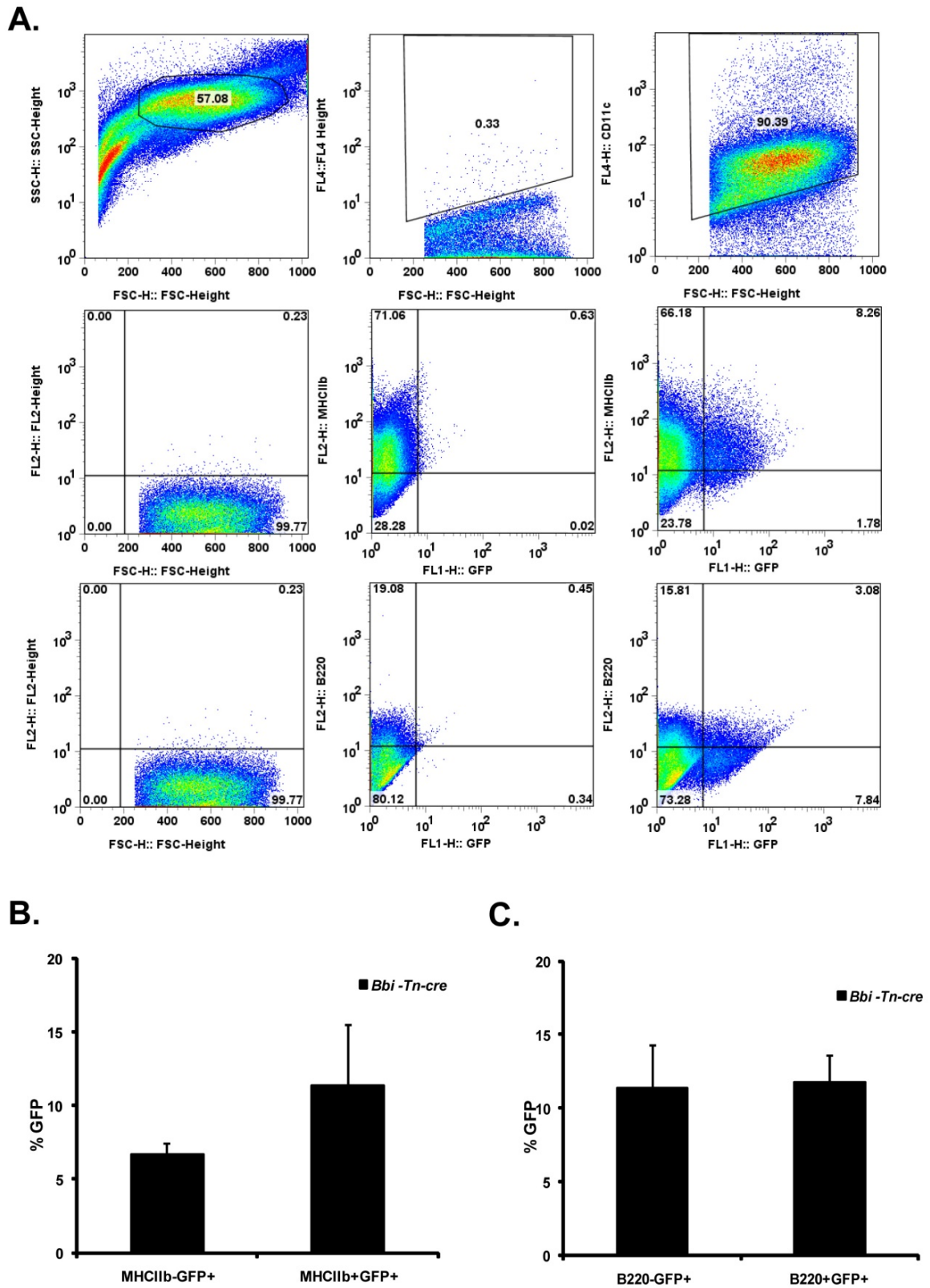


Figure 14.

Supplementary Figure Legends

Suppl. Figure 1: BepE_{Bhe} localizes to the membrane of HELA cells and to the membrane and cell-cell contacts of infected HUVECs.

A. Full-length MYC tagged BepE_{Bhe} (MYC-BepE_{Bhe}) and the two MYC tagged C-terminal BID domains (MYC-BID1/2E_{Bhe}). The (+++) indicates the positively charged tail sequence C-terminally to the BID, required for the VirB/VirD4-dependent translocation.

B. The two C-terminal BID domains of BepE_{Bhe} are sufficient to achieve localization to the plasma membrane. HELA cells were infected for 48 h with MOI= 150, fixed, permeabilized, and stained for f-actin (red), MYC-tag (green), and total bacteria (blue). 1) uninfected cells, 2) empty vector control, 3) MYC-BepE_{Bhe}, 4) MYC-BID1/2E_{Bhe}. The scale bar represents 20 μm .

C. Myc tagged BepE_{Bhe} localization to cell-cell contacts, co-localization with VE-cadherin. HUVECs were infected for 48 h with MOI= 150, fixed, permeabilized, and stained for VE-Cadherin (red), MYC-tag (green), and f-actin (blue). 1) uninfected cells, 2) empty vector control, 3) MYC-BepE_{Bhe}, 4) MYC- BID1/2E_{Bhe}. The scale bar represents 20 μm .

Suppl. Figure 2: The amino acid sequence similarity of BepE_{Bhe} homologs from different species of *Bartonellae*

The BepE homologs from *Bartonella* species depicted on the figure (BepE_{Bhe}, BepD_{Btr}, BepE_{Btr}, BepE_{Bqu} and BepH_{Bgr}) were aligned with the software Geneious Pro 5.3.4 . The amino acid sequence alignment with pair wise % identity is displayed here. The tyrosine-containing N-termini and BID domains were aligned independently.

Suppl. Figure 3: PCR screen of the outcome clones from rats infected with *Btr*.

The primer sets, prFS13/14 and prFS15/16, were used to amplify either BepD_{Btr} or BepE_{Btr} respectively from boiled colonies of the strains depicted on the graph. Neither BepD_{Btr} nor BepE_{Btr} PCR signal was detected from the clone recovered from the one rat infected with *Btr* Δ bepDE (rat # 606) that developed bacteremia starting at 16 dpi.

Suppl. Figure 4: Complementation of the blood abacteremic phenotype of *Btr* Δ bepDE.

Groups of rats (n = 3 for *i.v.*, n = 5 for *i.d.*) were injected with PBS solution containing *Btr* corresponding strains 200 μ l and 10 μ l of OD₅₉₅= 1 for *i.v.* and *i.d.* respectively. Blood samples were collected from the tail vein with 10% sodium citrate supplementation at day 10 p.i. The blood was frozen to lyse red blood cells, undiluted and serial dilutions of thawed blood in PBS were plated on defibrinated sheep blood supplemented CBA plates for counting CFU per mL of blood. Plotted graph represent data of single animals (circles) with an average (line) of the values from serial dilutions within the group of animals, (similar observation was obtained after day 16 post-infection). *Btr* Δ bepDE behaves as wild-type when directly delivered in the blood (*i.v.*), reaches the same high titers but is not detectable in the blood with *i.d.* route of infection. The blood abacteremic phenotype of *Btr* Δ bepDE can be rescued by over expression of plasmid encoded BepD_{Btr} and BepE_{Btr} or BepE_{Btr} alone *in trans*. BepE_{Bhe} can functionally replace BepE_{Btr} and enable *Btr* Δ bepDE to colonize the blood.

Suppl. Figure 5: Maintenance of the plasmid in the blood of infected rats.

Groups of rats (n = 5) were intradermally injected with PBS solution containing *Btr* corresponding strains, 10 μ l of OD₅₉₅= 1. Blood samples were collected from the tail vein with 10% citrate supplementation at the time points indicated on the graph. The blood was frozen to lyse red blood cells, undiluted and serial dilutions of thawed blood in PBS

were plated on plain CBA or CBA containing the resistance marker for the corresponding plasmid used for effector complementation in *Btr ΔbepDE*. The bar graph above shows the percentage of plasmid containing *Bartonella* within the pool of *Btr* recovered from the animal blood. The data are represented as average of the group of animals and serial dilutions of blood in PBS. *Bartonella* tend to lose plasmid during the infection, suggesting that there is no selection pressure to maintain it at the stage of blood infection.

Suppl. Figure 6: Tyrosine containing motives of BepE_{Bhe} are not essential for *Bartonella* to reach the blood.

Groups of rats (n = 3 for control groups, n= 5 for complementation strains) were *i.d.* injected with PBS solution containing *Btr* corresponding strains, 10 μl of OD₅₉₅= 1. Blood samples were collected from the tail vein with 10% sodium citrate supplementation at the time points indicated on the graph. The blood was frozen to lyse red blood cells, undiluted and serial dilutions of thawed blood in PBS were plated on CBA for counting CFU per mL of blood. Plotted graph represents data of single animals (circles) with an average of serial dilutions within the group of animals (lines) at 10 days post-infection (similar observation was obtained after 16 dpi). Both mutants of BepE_{Bhe} are complementing *Btr ΔbepDE* phenotype, showing no essential role of tyrosine containing motives and BepE_{Bhe} N-terminal part in colonization of natural host.

Suppl. Figure 7: The *Bhe* strains have the similar growth rates in infected cell culture.

The monolayer of HUVECs was infected for 24 h, 48 h with MOI=200 of different strains of *Bhe* depicted on the graph above. The infected cell culture was lysed with 0.5% Saponin in PBS. The lysate and serial dilutions in PBS were plated on CBA plates to enumerate the CFUs per well. Plotted graphs represent an average of serial dilutions and duplicates per time point. Error bars denote SD within serial dilutions. Results of one representative experiment out of 3 are shown.

No major difference was detected in growth of different *Bhe* strains used for *in vitro* infections that could potentially explain the different toxicity of strains to the infected cells and earlier fragmentation process as compared to wild-type

Suppl. Figure 8: Ectopic expression of BepE_{Bhe} in HUVECs preserves the cells from fragmentation

HUVECs on an early passage were transfected with the plasmid encoding CMV-promoter driven *GFP* or *GFP-BepE_{Bhe}* using Amaxa nucleofection kit. After 24 h post transfection cells were infected with *Bhe wild-type* and Δ *bepDEF*. The infection was stopped at several time points depicted on the figure above followed by fixation, immunocytochemical staining and confocal laser scanning microscopy. F-actin is represented in red, bacterial DNA and cell nucleus in blue, GFP and GFP-BepE_{Bhe} in green. T4SS independent delivery of BepE_{Bhe} in HUVECs proves that interference of BepE_{Bhe} with other Beps and inhibition of fragmentation is a specific function and not the out competition in translocation when over expressed by plasmid in *Bartonella*.

Suppl. Figure 9: Time course of bacteremia in *Bbi* infected Balb/c mice.

The group of (n=7) Balb/c mice was intradermally injected with 10 μ l of PBS containing *Bbi* wild-type bacteria (OD₅₉₅=1). Blood samples were collected from the tail vein with 10% citrate supplementation at the time points indicated on the graphs. The blood was frozen to lyse red blood cells and undiluted and serial dilutions of thawed blood in PBS were plated on sheep blood supplemented CBA for counting CFU per mL of blood. Plotted graphs represent single animals from which bacteria were recovered at a given time point post-infection.

Suppl. Figure 10: Translocation of Bla-BID fusion by *Bhe* into infected bone marrow derived dendritic cells (BMDCs) from C57/BL6/J mice.

BMDCs, cultured *in vitro* from C57/BL6/J mouse bone marrow in the presence of Flt3L for 10 days, were infected with either *Bhe* wild-type or *Bhe* strain expressing Bla-BID fusion with the different MOIs described on the graph. Infected cells were loaded with CCF2-AM (cephalosporin core linked 7-hydroxycumarin) and translocation was determined by measuring the ratio of cleaved (460 nm) to uncleaved (530 nm) CCF2-AM. The plotted graph shows the percentage of cells that got translocation of Bla-BID fusion at given time points of the infection. Specimens in a 96-well plate format were imaged with an MD ImagXpress and quantification was performed with CellProfiler. The results shown represent the average of triplicate wells. Error bars denote standard deviation within the triplicates.

Suppl. Figure 11: Comparison of the *virB* T4SS loci of *B. birtlesii*, *B. henselae* and *B. tribocorum*

Sequence similarity is shown for genes having more than 30% amino acid identities over a sequence stretch of more than 250 amino acids. VirB T4SS genes are shown in yellow and VirB T4SS effector genes in green.

Suppl. Movie 1: Random cell migration of uninfected and wild-type *Bhe*-infected HUVECs. HUVECs express LifeAct and wild-type *Bhe* expresses GFP. The acquisition started at 8 hpi. Cells were imaged for 72hs with. The movie with 30 min time-lapse between images is presented.

Suppl. Movie 2: Cell fragmentation induced by *Bhe* Δ *bepE*. HUVECs expressing LifeAct are infected either with *Bhe* Δ *bepE* (left side) or with *Bhe* Δ *bepE*-*pbepE* (right side). The acquisition started at 8 hpi. Cells were imaged for 72hs with. The movie with 30 min time-lapse between images is presented.

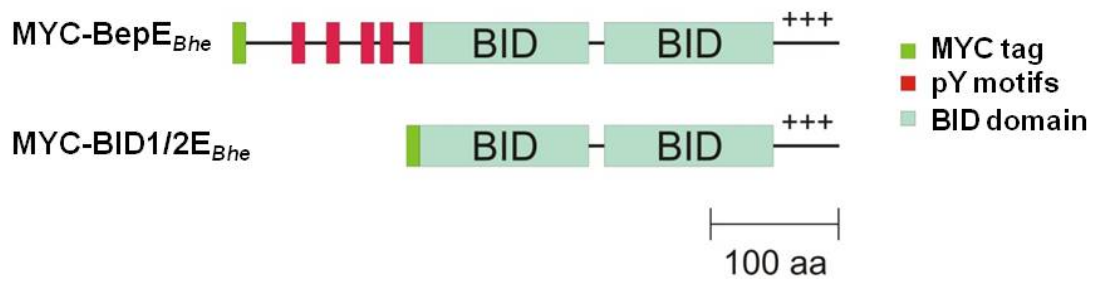
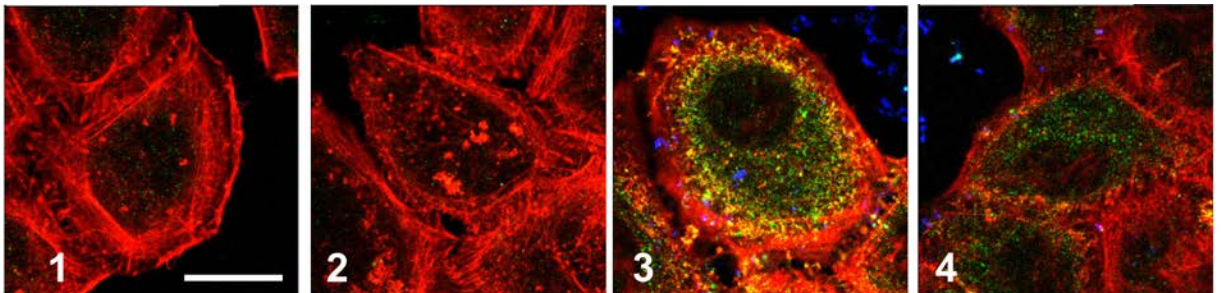
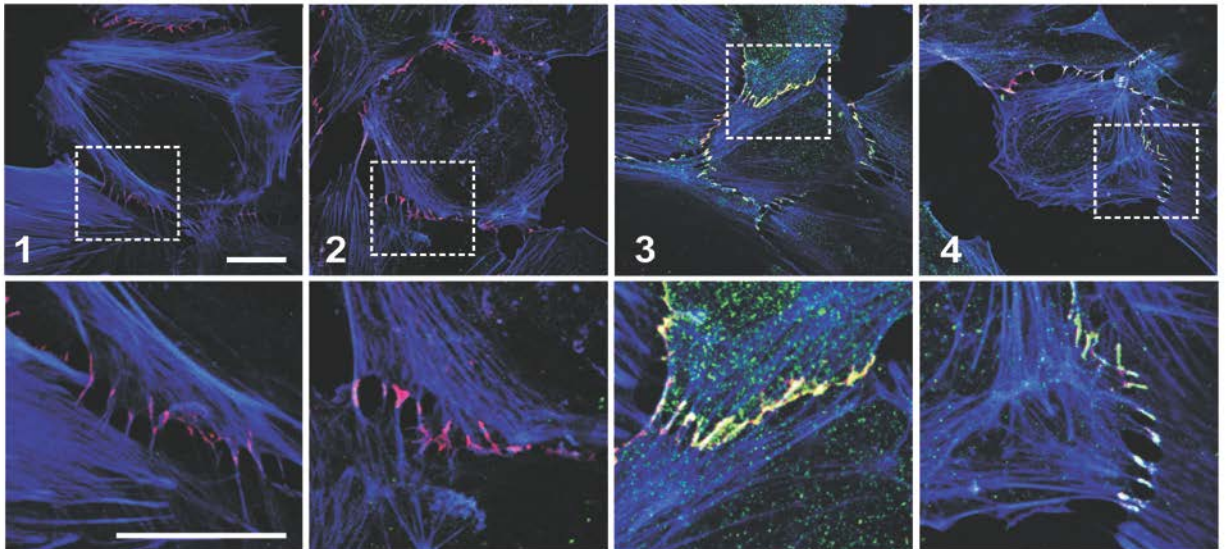
Suppl. Movie 3: Multiple cell fragmentation induced by *Bhe* Δ *bepDEF*. HUVECs expressing LifeAct are infected either with *Bhe* Δ *bepDEF* (left side) or with *Bhe*

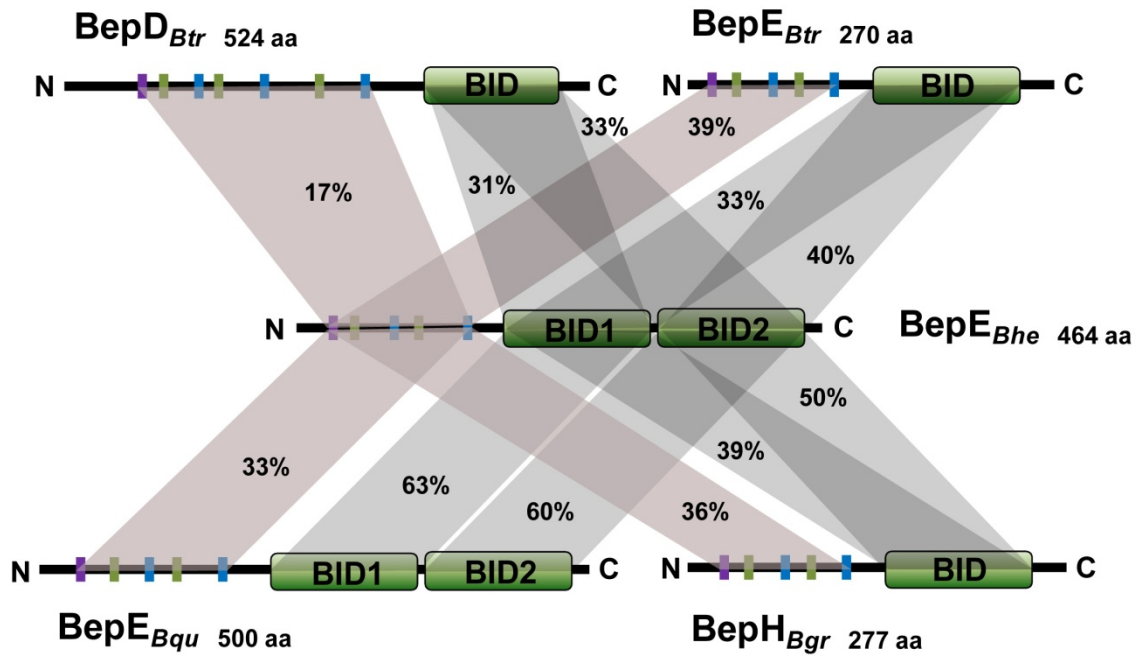
ΔbepDEF-pbepE (right side). The acquisition started at 8 hpi. Cells were imaged for 72hs with. The movie with 30 min time-lapse between images is presented.

Suppl. Movie 4: Cell fragmentation induced by *Bhe ΔbepE*. HUVECs expressing LifeAct (uninfected, upper left), HUVECs expressing LifeAct infected with wild-type *Bhe* (upper right), with *Bhe ΔbepE* (left below) and *ΔbepE-pbepE* (right below). The acquisition started at 8 hpi. Cells were imaged for 72hs with. The movie with 30 min time-lapse between images is presented.

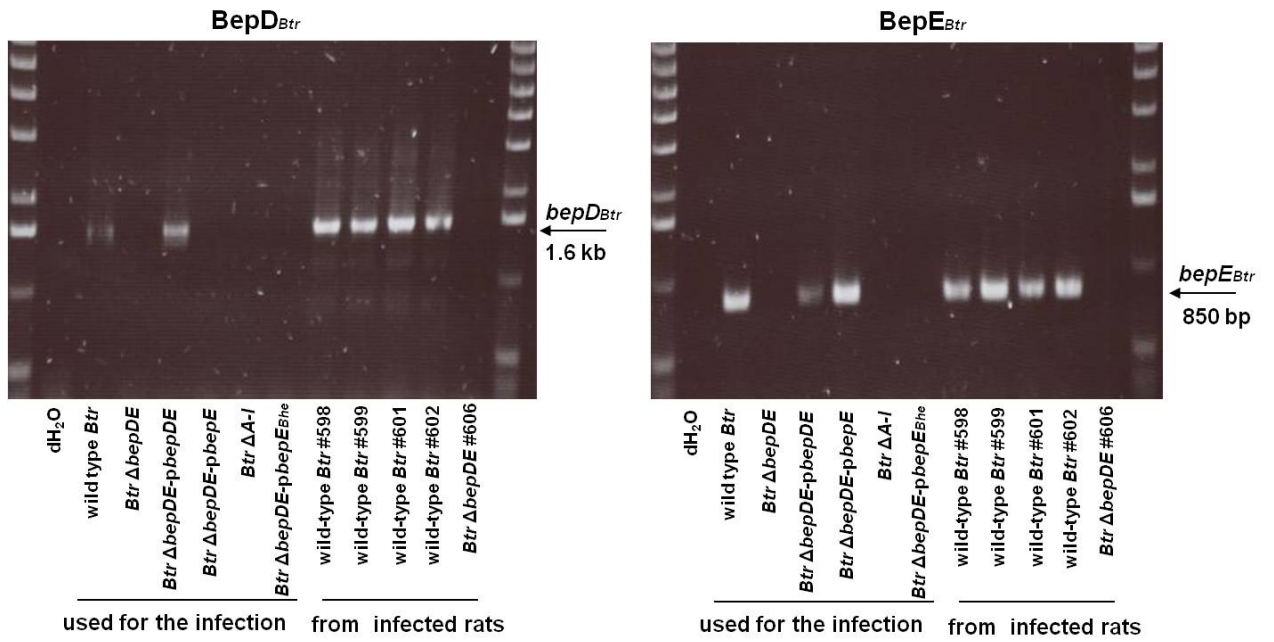
Suppl. Movie 5: Cell fragmentation is T4SS-dependent. Phase contrast movies of HUVECs infected with wild-type *Bhe* (upper left), HUVECs infected with *Bhe ΔvirB4* (upper right), with *Bhe ΔbepE* (left below) and uninfected HUVEC (right below). The acquisition started at 8 hpi. Cells were imaged for 72hs with. The movie with 15 min time-lapse between images is presented.

Supplementary Figures

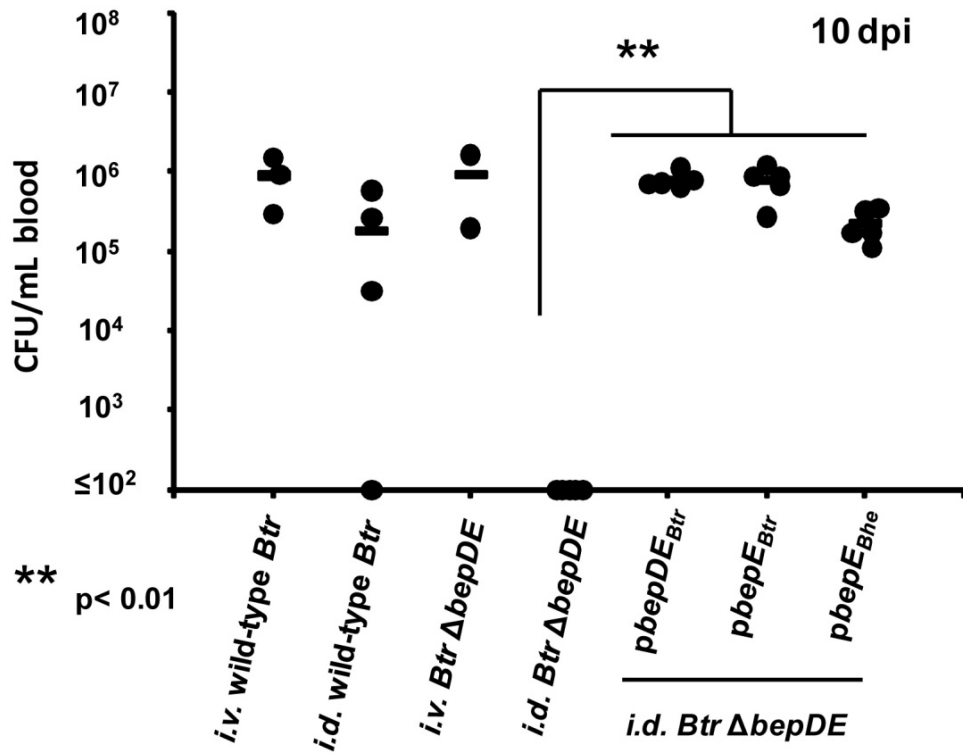
A.**B.****C.****Suppl. Figure 1.**



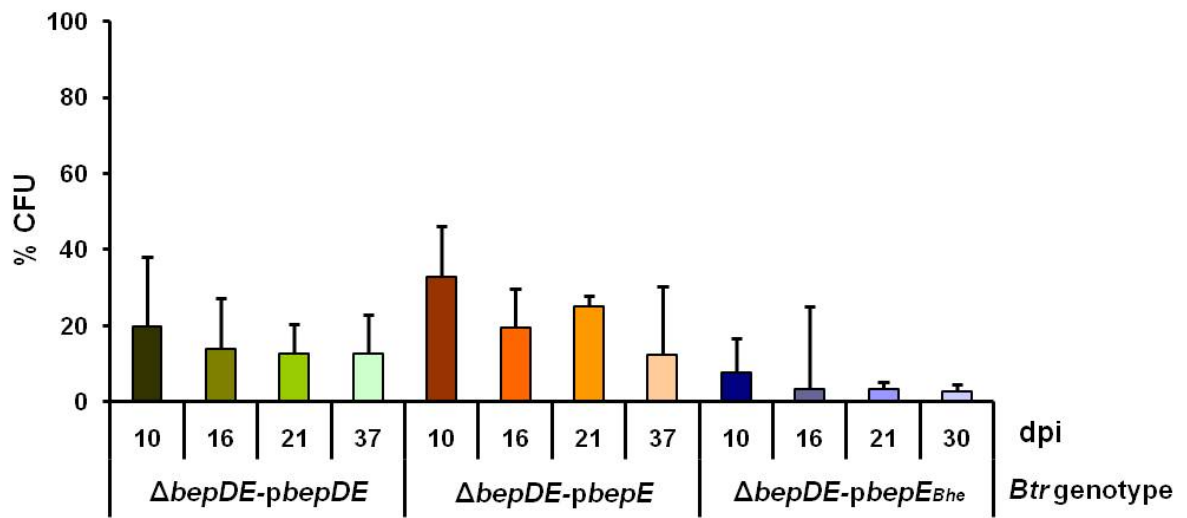
Suppl. Figure 2



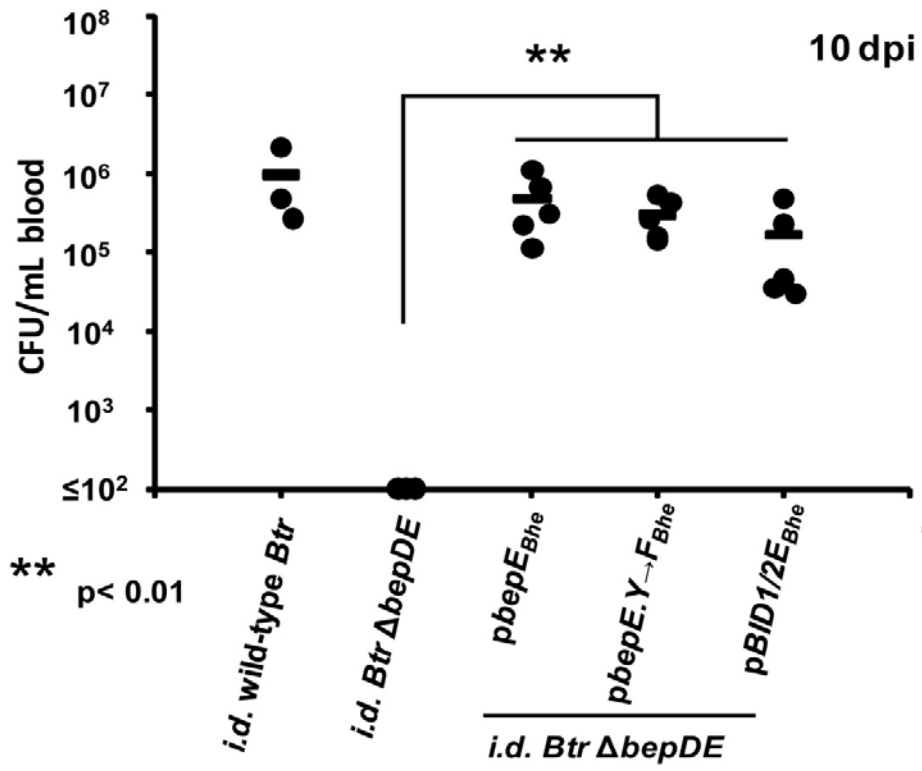
Suppl. Figure 3.



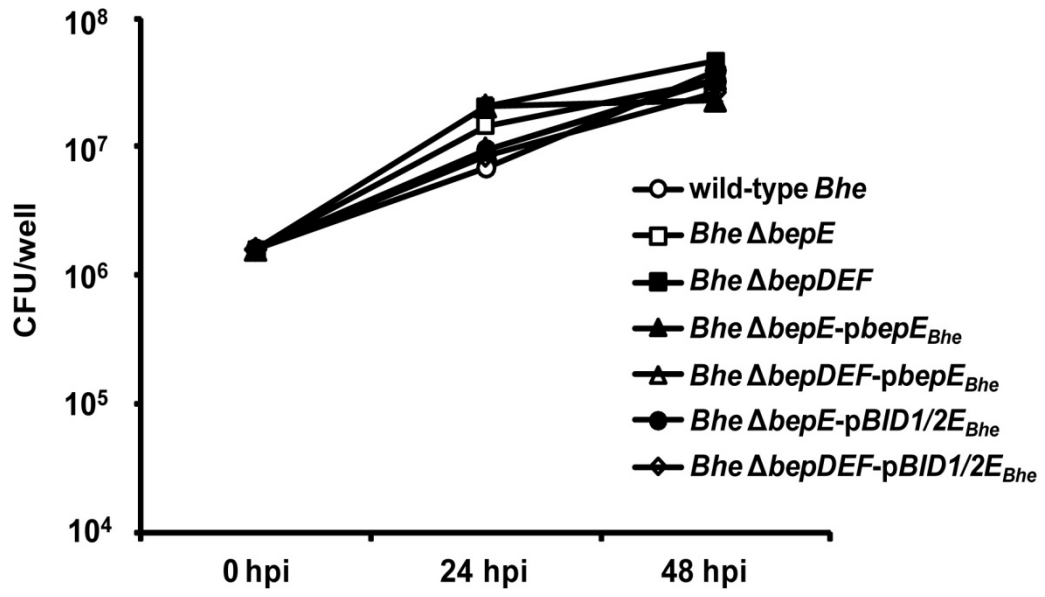
Suppl. Figure 4.



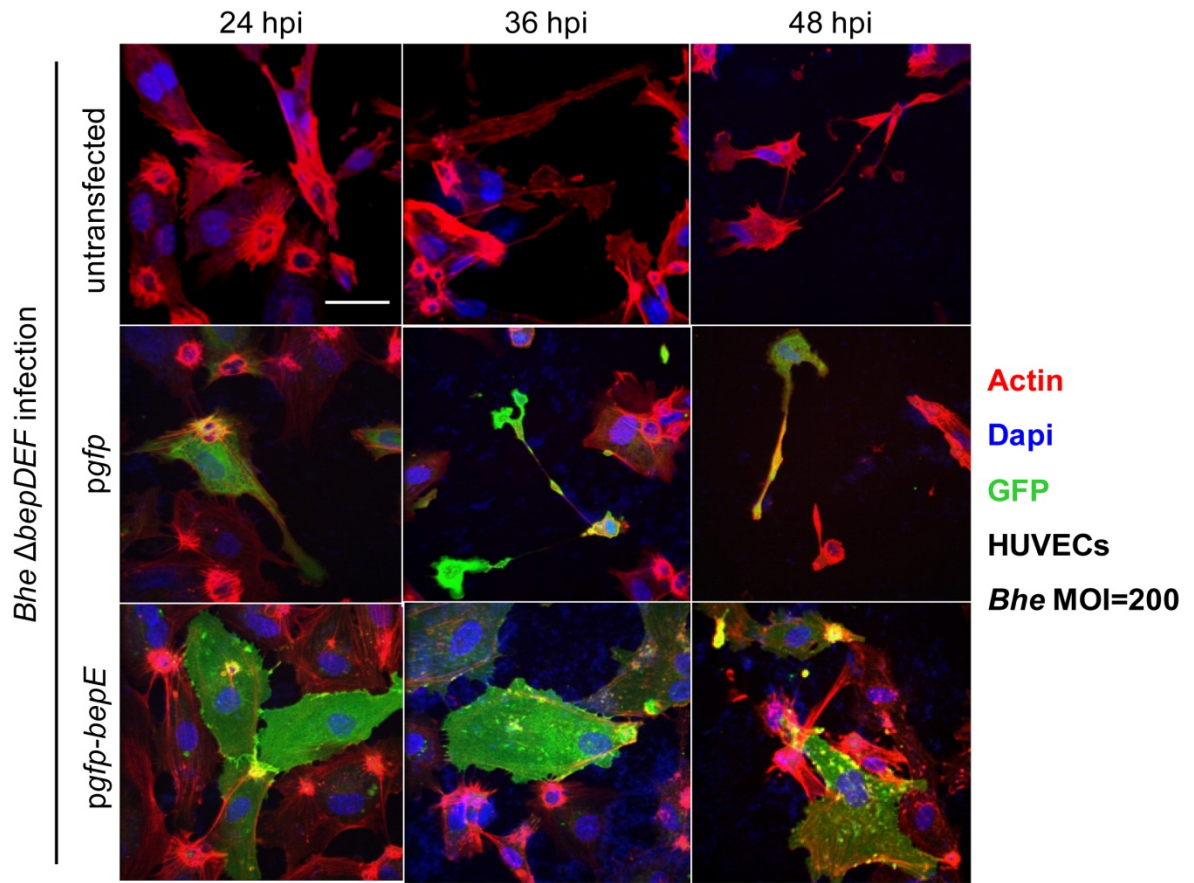
Suppl. Figure 5.



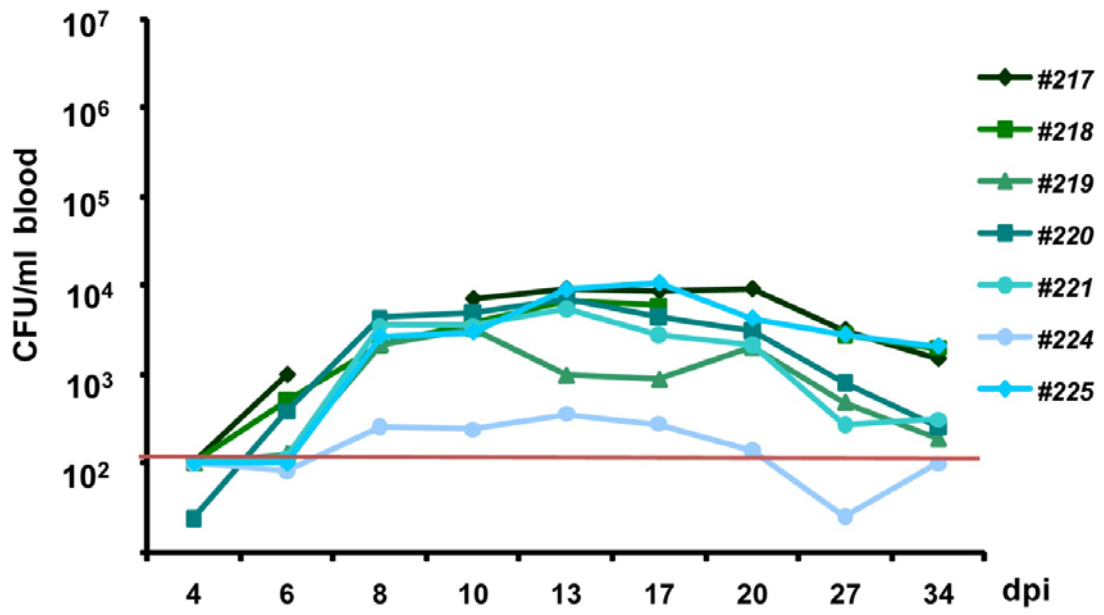
Suppl. Figure 6.



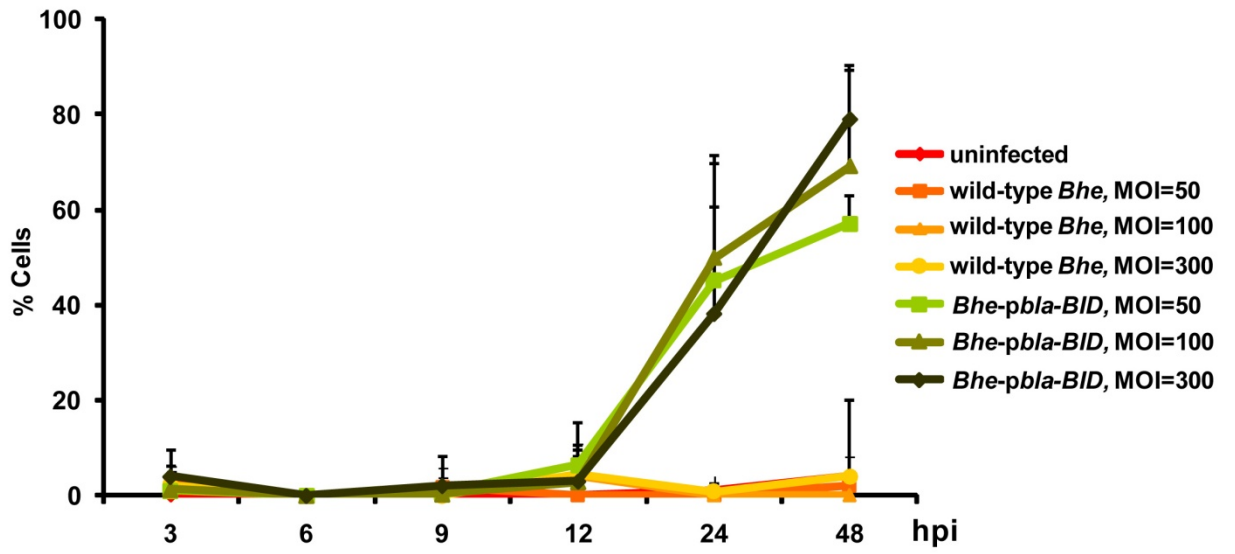
Suppl. Figure 7.



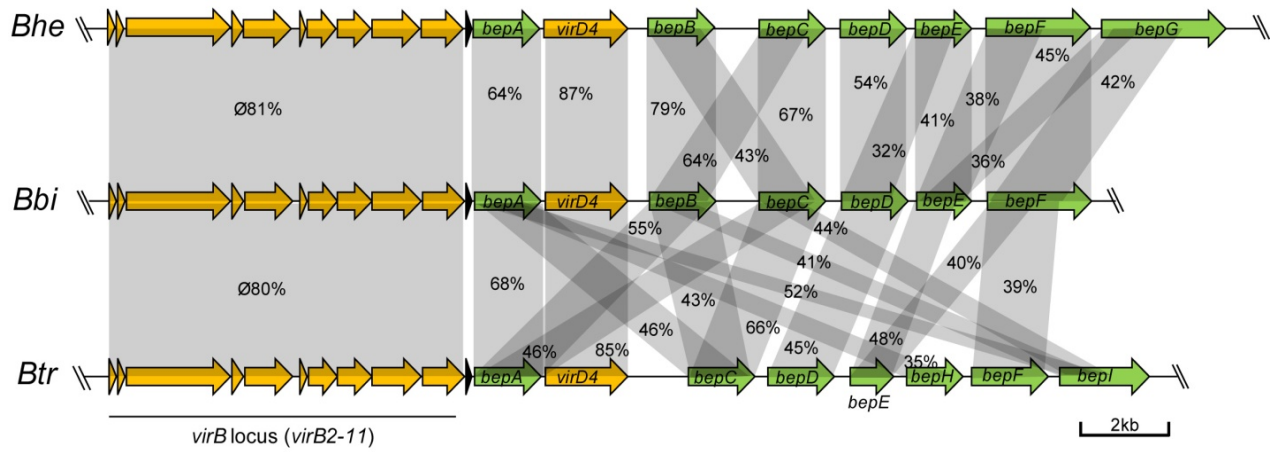
Suppl. Figure 8.



Suppl. Figure 9.



Suppl. Figure 10.



Suppl. Figure 11.

References:

1. Monack, D. M., A. Mueller, et al. (2004). "Persistent bacterial infections: the interface of the pathogen and the host immune system." Nat Rev Microbiol **2**(9): 747-765.
2. Hong, P. C., R. M. Tsolis, et al. (2000). "Identification of genes required for chronic persistence of *Brucella abortus* in mice." Infect Immun **68**(7): 4102-4107.
3. Celli, J., C. de Chastellier, et al. (2003). "Brucella evades macrophage killing via VirB-dependent sustained interactions with the endoplasmic reticulum." J Exp Med **198**(4): 545-556.
4. Hervet, E., X. Charpentier, et al. (2011). "The protein kinase LegK2 is a T4SS effector involved in endoplasmic reticulum recruitment and intracellular replication of *Legionella pneumophila*." Infect Immun.
5. Schroeder, G. N. and H. Hilbi (2008). "Molecular pathogenesis of *Shigella* spp.: controlling host cell signaling, invasion, and death by type III secretion." Clin Microbiol Rev **21**(1): 134-156.
6. Diacovich, L. and J. P. Gorvel (2010). "Bacterial manipulation of innate immunity to promote infection." Nat Rev Microbiol **8**(2): 117-128.
7. Chomel BB, Boulouis HJ, Maruyama S, et al. *Bartonella* spp. in pets and effect on human health. Emerg Infect Dis 2006; **12**: 389–394.
8. Boulouis HJ, Chang CC, Henn JB, et al. Factors associated with the rapid emergence of zoonotic *Bartonella* infections. Vet Res 2006; **36**:383–410.
9. Chomel BB, Boulouis HJ, Breitschwerdt EB, et al. Ecological fitness and strategies of adaptation of *Bartonella* species to their hosts and vectors. Vet Res 2009; **40**:29
10. Breitschwerdt, E. B., R. G. Maggi, et al. (2010). "Bartonellosis: an emerging infectious disease of zoonotic importance to animals and human beings." J Vet Emerg Crit Care (San Antonio) **20**(1): 8-30
11. Dehio, C. (2004). "Molecular and cellular basis of *Bartonella* pathogenesis." Annu Rev Microbiol **58**: 365-390.
12. Dehio, C. (2005). "Bartonella-host-cell interactions and vascular tumour formation." Nat Rev Microbiol **3**(8): 621-631.
13. Foil L., Andress E., Freeland R.L., Roy A.F., Rutledge R., Triche P.C., O'Reilly K.L., Experimental infection of domestic cats with *Bartonella henselae* by inoculation of *Ctenocephalides felis* (Siphonaptera: Pulicidae) feces, J. Med. Entomol. (1998) **35**: 625–628
14. Raoult D., Roux V., The body louse as a vector of reemerging human diseases, Clin. Infect. Dis. (1999) **29**:888–911.
15. Schulein, R., A. Seubert, C. Gille, C. Lanz, Y. Hansmann, Y. Piemont, and C. Dehio. 2001. Invasion and persistent intracellular colonization of erythrocytes. A unique parasitic strategy of the emerging pathogen *Bartonella*. J Exp Med **193**:1077-1086.
16. Engel, P., W. Salzburger, et al. (2011). "Parallel Evolution of a Type IV Secretion System in Radiating Lineages of the Host-Restricted Bacterial Pathogen *Bartonella*." PLoS Genet **7**(2): e1001296.
17. Seubert, A., R. Hiestand, F. de la Cruz, and C. Dehio. 2003. A bacterial conjugation machinery recruited for pathogenesis. Mol Microbiol **49**:1253-1266.

18. Schulein, R. and C. Dehio (2002). "The VirB/VirD4 type IV secretion system of Bartonella is essential for establishing intraerythrocytic infection." Mol Microbiol **46**(4): 1053-1067.
19. Vayssier-Taussat, M., D. Le Rhun, et al. (2010). "The Trw type IV secretion system of Bartonella mediates host-specific adhesion to erythrocytes." PLoS Pathog **6**(6)
20. Nystedt, B., A. C. Frank, et al. (2008). "Diversifying selection and concerted evolution of a type IV secretion system in Bartonella." Mol Biol Evol **25**(2): 287-300.
21. Schulein, R., P. Guye, et al. (2005). "A bipartite signal mediates the transfer of type IV secretion substrates of Bartonella henselae into human cells." Proc Natl Acad Sci U S A **102**(3): 856-861.
22. Schmid, M. C., R. Schulein, et al. (2004). "The VirB type IV secretion system of Bartonella henselae mediates invasion, proinflammatory activation and antiapoptotic protection of endothelial cells." Mol Microbiol **52**(1): 81-92.
23. Rhomberg, T. A., M. C. Truttmann, et al. (2009). "A translocated protein of Bartonella henselae interferes with endocytic uptake of individual bacteria and triggers uptake of large bacterial aggregates via the invasome." Cell Microbiol **11**(6): 927-945.
24. Truttmann, M. C., T. A. Rhomberg, et al. (2011). "Combined action of the type IV secretion effector proteins BepC and BepF promotes invasome formation of Bartonella henselae on endothelial and epithelial cells." Cell Microbiol **13**(2): 284-299.
25. Schmid, M. C., F. Scheidegger, et al. (2006). "A translocated bacterial protein protects vascular endothelial cells from apoptosis." PLoS Pathog **2**(11): e115.
26. Selbach, M., F. E. Paul, et al. (2009). "Host cell interactome of tyrosine-phosphorylated bacterial proteins." Cell Host Microbe **5**(4): 397-403.
27. Koesling, J., T. Aebischer, C. Falch, R. Schulein, and C. Dehio. 2001. Cutting edge: antibody-mediated cessation of hemotropic infection by the intraerythrocytic mouse pathogen Bartonella grahamii. J Immunol **167**:11-14.
28. Marignac, G., F. Barrat, et al. (2010). "Murine model for Bartonella birtlesii infection: New aspects." Comp Immunol Microbiol Infect Dis **33**(2): 95-107.
29. Angelov, G. S., M. Tomkowiak, et al. (2005). "Flt3 ligand-generated murine plasmacytoid and conventional dendritic cells differ in their capacity to prime naive CD8 T cells and to generate memory cells in vivo." J Immunol **175**(1): 189-195.
30. Diao, J., E. Winter, et al. (2004). "Characterization of distinct conventional and plasmacytoid dendritic cell-committed precursors in murine bone marrow." J Immunol **173**(3): 1826-1833.
31. Dehio, C., M. Meyer, et al. (1997). "Interaction of Bartonella henselae with endothelial cells results in bacterial aggregation on the cell surface and the subsequent engulfment and internalisation of the bacterial aggregate by a unique structure, the invasome." J Cell Sci **110 (Pt 18)**: 2141-2154.
32. Savina, A. and S. Amigorena (2007). "Phagocytosis and antigen presentation in dendritic cells." Immunol Rev **219**: 143-156.
33. Shortman, K. and S. H. Naik (2007). "Steady-state and inflammatory dendritic-cell development." Nat Rev Immunol **7**(1): 19-30.
34. Skinner, J. A., M. R. Pilione, et al. (2005). "Bordetella type III secretion modulates dendritic cell migration resulting in immunosuppression and bacterial persistence." J Immunol **175**(7): 4647-4652.

35. Saenz, H. L., P. Engel, et al. (2007). "Genomic analysis of Bartonella identifies type IV secretion systems as host adaptability factors." Nat Genet **39**(12): 1469-1476.
36. Randolph, G. J., J. Ochando, et al. (2008). "Migration of dendritic cell subsets and their precursors." Annu Rev Immunol **26**: 293-316.
37. Alvarez, D., E. H. Vollmann, et al. (2008). "Mechanisms and consequences of dendritic cell migration." Immunity **29**(3): 325-342.
38. Popa, C., S. Abdollahi-Roodsaz, et al. (2007). "Bartonella quintana lipopolysaccharide is a natural antagonist of Toll-like receptor 4." Infect Immun **75**(10): 4831-4837.
39. Matera, G., M. C. Liberto, et al. (2008). "The Janus face of Bartonella quintana recognition by Toll-like receptors (TLRs): a review." Eur Cytokine Netw **19**(3): 113-118.
40. Capo, C., N. Amirayan-Chevillard, et al. (2003). "Bartonella quintana bacteremia and overproduction of interleukin-10: model of bacterial persistence in homeless people." J Infect Dis **187**(5): 837-844.
41. Edelman, G. M. and J. A. Gally (2001). "Degeneracy and complexity in biological systems." Proc Natl Acad Sci U S A **98**(24): 13763-13768.
42. Larsen, M., M. L. Tremblay, et al. (2003). "Phosphatases in cell-matrix adhesion and migration." Nat Rev Mol Cell Biol **4**(9): 700-711
43. Iwanicki, M. P., T. Vomastek, et al. (2008). "FAK, PDZ-RhoGEF and ROCKII cooperate to regulate adhesion movement and trailing-edge retraction in fibroblasts." J Cell Sci **121**(Pt 6): 895-905.
44. Rid, R., N. Schiefermeier, et al. (2005). "The last but not the least: the origin and significance of trailing adhesions in fibroblastic cells." Cell Motil Cytoskeleton **61**(3): 161-171.
45. Worthylake, R. A., S. Lemoine, et al. (2001). "RhoA is required for monocyte tail retraction during transendothelial migration." J Cell Biol **154**(1): 147-160.
46. Heasman, S. J., L. M. Carlin, et al. (2010). "Coordinated RhoA signaling at the leading edge and uropod is required for T cell transendothelial migration." J Cell Biol **190**(4): 553-563.
47. Truttmann, M. C., T. A. Rhomberg, et al. (2011). "Combined action of the type IV secretion effector proteins BepC and BepF promotes invasome formation of Bartonella henselae on endothelial and epithelial cells." Cell Microbiol **13**(2): 284-299.
48. Bamburg, J. R. and B. W. Bernstein (2010). "Roles of ADF/cofilin in actin polymerization and beyond." F1000 Biol Rep **2**: 62
49. Eiseler, T., H. Doppler, et al. (2009). "Protein kinase D1 regulates cofilin-mediated F-actin reorganization and cell motility through slingshot." Nat Cell Biol **11**(5): 545-556
50. Marshall, T. W., H. L. Aloor, et al. (2009). "Coronin 2A regulates a subset of focal-adhesion-turnover events through the cofilin pathway." J Cell Sci **122**(Pt 17): 3061-3069.
51. Kuhn, T. B. and J. R. Bamburg (2008). "Tropomyosin and ADF/cofilin as collaborators and competitors." Adv Exp Med Biol **644**: 232-249.
52. Sidani, M., D. Wessels, et al. (2007). "Cofilin determines the migration behavior and turning frequency of metastatic cancer cells." J Cell Biol **179**(4): 777-791.
53. Lopez-Bravo, M. and C. Ardavin (2008). "In vivo induction of immune responses to pathogens by conventional dendritic cells." Immunity **29**(3): 343-351.

54. Autenrieth, S. E., T. R. Linzer, et al. (2010). "Immune evasion by *Yersinia enterocolitica*: differential targeting of dendritic cell subpopulations in vivo." PLoS Pathog **6**(11): e1001212.
55. Autenrieth, S. E., I. Soldanova, et al. (2007). "Yersinia enterocolitica YopP inhibits MAP kinase-mediated antigen uptake in dendritic cells." Cell Microbiol **9**(2): 425-437.
56. Skendros, P., G. Pappas, et al. (2011). "Cell-mediated immunity in human brucellosis." Microbes Infect **13**(2): 134-142.
57. Gorvel, J. P. (2008). "Brucella: a Mr "Hide" converted into Dr Jekyll." Microbes Infect **10**(9): 1010-1013.
58. Salcedo, S. P., M. I. Marchesini, et al. (2008). "Brucella control of dendritic cell maturation is dependent on the TIR-containing protein Btp1." PLoS Pathog **4**(2): e21.
59. Kappeli, R., P. Kaiser, et al. (2011). "Roles of spvB and spvC in *S. Typhimurium* colitis via the alternative pathway." Int J Med Microbiol **301**(2): 117-124.
60. Scheidegger, F., Y. Ellner, et al. (2009). "Distinct activities of Bartonella henselae type IV secretion effector proteins modulate capillary-like sprout formation." Cell Microbiol **11**(7): 1088-1101.
61. Brasel, K., T. De Smedt, et al. (2000). "Generation of murine dendritic cells from flt3-ligand-supplemented bone marrow cultures." Blood **96**(9): 3029-3039.
62. Clifton, D. R., K. A. Fields, et al. (2004). "A chlamydial type III translocated protein is tyrosine-phosphorylated at the site of entry and associated with recruitment of actin." Proc Natl Acad Sci U S A **101**(27): 10166-10171.
63. Backert, S., E. Ziska, et al. (2000). "Translocation of the Helicobacter pylori CagA protein in gastric epithelial cells by a type IV secretion apparatus." Cell Microbiol **2**(2): 155-164.
64. Lamalice, L., F. Le Boeuf, et al. (2007). "Endothelial cell migration during angiogenesis." Circ Res **100**(6): 782-794.
65. Lopez-Bravo, M. and C. Ardavin (2008). "In vivo induction of immune responses to pathogens by conventional dendritic cells." Immunity **29**(3): 343-35
66. Insall, R. H. and L. M. Machesky (2009). "Actin dynamics at the leading edge: from simple machinery to complex networks." Dev Cell **17**(3): 310-322.
67. Ponti, A., M. Machacek, et al. (2004). "Two distinct actin networks drive the protrusion of migrating cells." Science **305**(5691): 1782-1786.
68. Zaidel-Bar, R., C. Ballestrem, et al. (2003). "Early molecular events in the assembly of matrix adhesions at the leading edge of migrating cells." J Cell Sci **116**(Pt 22): 4605-4613.
69. Wood, W. and P. Martin (2002). "Structures in focus--filopodia." Int J Biochem Cell Biol **34**(7): 726-730.
70. Miao, L., O. Vanderlinde, et al. (2003). "Retraction in amoeboid cell motility powered by cytoskeletal dynamics." Science **302**(5649): 1405-1407.

Additional work (results unrelated to the manuscript)

In this part I will describe my work unrelated to the manuscript (in preparation), mainly the work that has been carried out to characterize transgenic mouse line C57BL/6-TgN(BepE-pPG2001)2001, the expression of BepE_{Bhe} under the promoter of CD11c⁺. Additionally, I bring the results of *in vitro* secretion of IL-10 upon BMDC infection with *Bhe* and introduce the *i.d.* infection of C57/BL6/J mice with *Bartonella taylorii*.

The plasmids used for generation of transgenic (Tg) mice were constructed by Dr. Patrick Guye during his last year of PhD study. Tg mice were generated by Daniela Klewe-Nebenius, Transgenic Mice Core Facility (TMCF), Biozentrum. Tg mice analysis was performed by me, during my first year of PhD study, with the help of Dr. Lee Kim Swee at the laboratory of Prof. Antonius Rolink at DBM, University of Basel.

1. Ectopic expression of BepE in CD11c⁺ cells of transgenic mice - C57BL/6-TgN(BepE-pPG2001)2001

Bhe BepE is injected into infected eukaryotic cells as diverse as primary endothelial or dendritic cells (DCs). Upon injection into these cells, it localizes to the plasma membrane and to cell-cell contacts (P. Guye, Thesis work, 2006). BepE is tyrosine – phosphorylated by host cell kinases on its ITIMs, ITSMs and a Csk binding-like site. Upon phosphorylation these motifs interact with SHP1/2, Grb2/7 and Csk (within ITIM/ITSM and Csk-like binding motives respectively) [1]. The data accumulated so far, the localization and the cellular interaction partners, suggests that BepE mimics inhibitory immune receptors. The ability to control the activation of various immune cells by such mimicry might be one of the key factors in the success of *Bartonella* to cause long-term persistent infections. To assess the impact of this putative immunomodulatory protein on the immune response Tg mice, C57BL/6-TgN(BepE-pPG2001)2001, expressing BepE ectopically in DCs were generated.

Tg mice were produced by microinjection of transgene DNA into fertilized murine oocytes. Transgene DNA was obtained from the plasmid construct - pPG2001, which encoded *bepE*

from *Bhe* under the control of CD11c promoter (Figure 1.A). Tg mice were bred heterozygously and the offspring was genotyped by PCR for the presence of trans gene with the primer pair prPG256/257 (Figure 1.B). The expression of BepE in Tg mice was analyzed by flow cytometry in Flt3-differentiated BMDCs. Around 6% of BMDCs from Tg mice expressed BepE protein. (Figure 1.C).

1.1. Maturation and Ag presentation properties of BMDCs from Tg mice

DCs have a dual role to prime adaptive immune responses and to induce self-tolerance. Two important properties of DCs underlie their ability to exert these activities. First, the antigen sampling and migratory capacities of DCs effectively allow naive T cells to come into contact with peripheral antigens. Second, the ability of DCs to sense and translate environmental cues dictates, to a large extent, the fate of T cells that respond to such antigens. The mechanisms that are used by DCs to translate their environment for the benefit of lymphocytes are embodied in the concept of DC maturation. DCs can exist in two functional states, immature and mature. Only a mature DC has the ability to prime an immune response. High cell-surface levels of MHC molecules, CD40, CD80, CD83 and CD86 correlate with T-cell-priming ability, it is generally assumed that DCs that are mature by phenotypic criteria are also functionally mature, that is, immunogenic. However, phenotypically mature DCs do not always promote T-cell immunity and can, in fact, induce tolerance [24]. Thus DCs fine-tune immune responses by instructing T-cell differentiation and polarization. DCs transmit a distinct set of instructions to T cells that is based on their state of differentiation or maturation, and these instructions programme outcomes that range from humoral to cytolytic to suppressive (regulatory) T-cell responses [26].

Considering such a pivotal role of Ag presentation properties of DCs for the development of an effective immune response, we decided to investigate whether BepE expression has modulated these features in BMDCs of Tg mice. BMDCs were differentiated from the bone marrow of Tg and wild-type C57BL/6 mice in the presence of Flt3 ligand for 10 days. Differentiated BMDCs were stained for CD11c, B220, CD86, MHCII surface molecules; which allowed to distinguish cDCs and pDCs (Figure 2.A), and to characterize the activation status of these subpopulations (Figure 2.B). Mixed leukocyte reaction assay

was used to examine the allo-stimulation activity of BMDCs from wild-type Tg mice. Carboxyfluorescein diacetate, succinimidyl ester (CFSE) - labeled lymphocytes from the lymph nodes of Balb/c mouse were mixed with BMDCs obtained from C57BL/6 (wild-type and Tg) mice in different ratios: 5:1, 10:1, 50:1 and 100:1. One sample contained plain lymphocytes as a negative control. 5 days after stimulation the leukocyte mixture was stained with anti-CD4 Abs and propidium iodide (PI). The stained samples were acquired by flow cytometry. The data were analyzed by Flowjo 7.2.4 software (Figure 2.C and 2.D).

1.2. DCs in T cell development in the thymus

DCs are involved in T cells development in the thymus. In more details, bone marrow-derived MHCII⁺ thymic DCs at corticomedullary junction of thymus present circulatory Ags to the double positive (CD4⁺CD8⁺) thymocytes that have already undergone differentiation from double negative to double positive phenotype and positive selection in the cortex. Ag recognition and strong TCR signaling after contact with thymic DCs drives the double positive thymocytes to apoptosis. Thus DCs negatively select self Ag-recognizing T cells and only about 1% of self tolerant thymocytes go on further maturation to single positive (CD4⁺ and CD8⁺) T cells [2,3].

We wanted to assess the impact of BepE expression on thymic DCs during T cell development. Thus, we analyzed the thymus from Tg mice for double negative and double positive thymocytes and single positive T cells.

As compared to wild-type, the thymus from Tg mice did not display any differences in the composition of all four cell types (Figure 3). Next to it we examined also peripheral lymphoid organs for the composition of T cell sub-populations.

1.3. DCs in regulatory T cells (T regs) development

T regs are characterized by expression of the transcription factor Foxp3 and they play key roles in the maintenance of lymphoid homeostasis in a number of immune circumstances. These cells maintain tolerance to self and control autoimmune deviation [4,5] prevent runaway responses to pathogens or allergens, help to maintain a balance with obligate

microbial flora [6], and facilitate tumors' escape from immune monitoring. Two origins have been described for Foxp3⁺ cells. The first is the thymus, where Foxp3⁺ cells are generated roughly in sync with positive selection of CD4⁺ T cells. The second is the periphery, where a number of triggers induce the expression of Foxp3 in T cells [7]. In both of the cases DCs are the cells driving T cells to Foxp3⁺ cells as they serve as Ag-presenting cells during the process. We assumed the putative inhibitory effect of BepE could influence on the proportion of T regs in thymus and peripheral lymphoid organs, such as spleen and lymph nodes.

1.4. The impact of DCs on Natural Killer (NK) T cell development

NK T cells have characteristics of both T and NK cells. They have TCRs like T cells and possess CD16, other typical receptors and killer activity like NK cells. NK T cells belong to a subset of T cells that has unique characteristics [8]. These cells are considered to be innate T lymphocytes that are restricted by MHC class I-like CD1d antigen-presenting molecules and recognize lipids and glycolipids as antigens [9]. The activated, NKT-cell population rapidly secretes large amounts of cytokines, especially interleukin IL-4 and IFN- γ . Because of their rapid response to the activation, NKT cells can regulate early immunological events in diverse situations, such as the control of autoimmune diseases in humans and mice, tumor rejection and especially they are involved in different bacterial, parasitic, fungal and viral infections [10,11]. Although the NK T cell development is poorly understood, it is believed that they develop in the thymus alongside mainstream T cells and that corticomedullar DCs are required for the negative selection during the differentiation of thymocytes into NK T cells [12]. Thus, considering the role of DCs in NK T cell development, we decided to analyze the spleen of Tg mice for NK T cells as well.

1.5. Summary

Based on our results we can summarize that no significant differences in different compartments of immune system of Tg and wild-type mouse were observed. BepE ectopic expression did not impair maturation and Ag presentation properties of DCs (*in*

vitro) and the development of T cells populations in thymus; or their composition in peripheral lymphoid organs. We speculate that the expression of BepE on protein level may not be high enough to result in obvious phenotypes, or some other compensatory mechanisms in the Tg mice avoid functional interference of BepE within the processes investigated above.

Assuming that BepE, more specifically the BID domains of BepE, revealed a critical importance for the establishment of *Bartonella* infection *in vivo* and based on our hypothesis that DCs are the cells that deliver *Bartonella* from inoculation site, derma to the lymphatic-blood system, I plan to *i.d.* infect Tg mice (next to wild-type) with *Bbi* Δ BepE (I am currently constructing the mutant) and monitor the blood bacteremia of the infected animals. I am interested to investigate whether the ectopic expression of BepE in DCs may restore the bacteremia of *Bbi* Δ BepE infected reservoir host, based on the fact that BepE_{Btr} and BepE_{Bhe} were able to complement the abacteremic phenotype of *Btr* Δ BepDE.

Figure Legends

Figure 1: Genotyping and BepE expression in transgenic (Tg) mice

A. Plasmid map of the construct, pPG2001, was used for the generation of Tg mice, where *Bhe bepE-gene* is under the control of CD11c promoter (by Geneious 5.3.4 software).

B. prPG256/257 primer-pair were used to amplify the *bepE* trans gene on the genomic DNA extracted from the toe of Tg mouse. The genotyping PCR included amplification of *NCAM* gene as a control for genomic DNA. As a positive control for *bepE* gene pPG2001 plasmid template was taken. Three out of 8 mice were positive for trans gene in the screen depicted on the figure.

C. BMDCs were obtained from wild-type and Tg mice by Flt3 ligand treatment of bone marrow cells for 10 days. The cytoplasmic staining of differentiated BMDCs was performed with primary rabbit anti-BepE polyclonal antibodies and mouse anti-rabbit Alexa633 Abs were used as secondary Abs. The stained BMDC samples were acquired by flow cytometry and the cytoplasmic expression of BepE protein was analyzed by WinMDI 2.8 software.

Figure 2: Ag presentation and T cell stimulation by DCs

BMDCs were obtained from wild-type (n=3) and Tg (n=3) mice by Flt3 ligand differentiation of bone marrow cells for 10 days. Differentiated BMDCs were stained for CD11c, B220, CD86, MHCII surface molecules; which allowed to distinguish cDCs and pDCs (A), and to characterize the activation status of these subpopulations (B). Samples were acquired by FACS and analyzed by Flowjo 7.2.4 software. The error bars denote standard deviation within the groups of animals.

C. Mixed leukocyte reaction assay was used to examine the allo-stimulation activity of BMDCs from wild-type (n=3) and Tg (n=3) mice. Carboxyfluorescein diacetate, succinimidyl ester (CFSE) - labeled lymphocytes from the lymph nodes of Balb/c mouse were mixed with BMDCs obtained from C57BL/6 (wild-type and Tg) mice in different ratios depicted on the graph. One sample contained plane lymphocytes as a negative control. 5 days after stimulation the leukocyte mixture was stained with anti-CD4 Abs and propidium iodide (PI). The stained samples were acquired by flow cytometry. The data

were analyzed by Flowjo 7.2.4 software. The cells were gated on CD4⁺ population within live (PI negative) region and successive generations of proliferated T cells were observed by decreasing intensity of CFSE .

D. Quantification of T cell proliferation is presented on bar graph. The error bars stand for the standard deviation within the groups of animals analyzed.

Figure 3: BepE expression in DCs does not impair CD4 and DC8 development

Single cell suspensions were obtained by homogenization of thymus, spleen and lymph nodes from wild-type (n=3) and Tg (n=3) mice. Cell suspension was double-stained for CD4 and CD8 with anti-CD4 FITC and anti-CD8 PE respectively. The data were acquired by flow cytometry and analyzed by WinMDI2.8 software.

A. T cell development in thymus. A Representative dot plots for T cell distribution and quantification graphs are presented. The error bars denote standard deviation within the groups of animals.

B. CD4 and CD8 T cell composition in spleen. A Representative dot plots for T cell distribution and quantification graphs are presented. The error bars denote standard deviation within the groups of animals.

C. CD4 and CD8 T cell proportion in lymph nodes. A Representative dot plots for T cell distribution and quantification graphs are presented. The error bars denote standard deviation within the groups of animals.

Figure 4: Regulatory T (T regs) cell-distribution in the organs is not impaired in Tg mice

Single cell suspensions were obtained by homogenization of thymus, spleen and lymph nodes from wild-type (n=3) and Tg (n=3) mice. Cell suspension was double-stained for surface CD25 and intracellular Foxp3 with anti-CD25 and anti-Foxp3 respectively. The data were acquired by flow cytometry and analyzed by WinMDI 2.8 software.

A. T regs in the thymus. A Representative dot plots for T cell distribution and quantification graphs are presented. The error bars denote standard deviation within the groups of animals.

B. T regs in the spleen. A Representative dot plots for T cell distribution and quantification graphs are presented. The error bars denote standard deviation within the groups of animals.

C. T regs in lymph nodes. A Representative dot plots for T cell distribution and quantification graphs are presented. The error bars denote standard deviation within the groups of animals.

Figure 5: The numbers NK T cells are not impaired in Tg mice

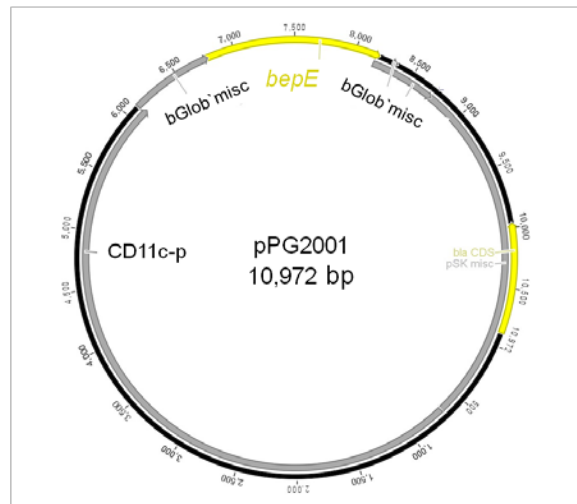
Single cell suspensions were obtained by homogenization of thymus, spleen and lymph nodes from wild-type (n=3) and Tg (n=3) mice. Cell suspension was double stained for CD4 and CD8 with anti-CD4 FITC and anti-CD8 PE respectively. The data were acquired by flow cytometry and analyzed by WinMDI2.8 software.

A. T cell development in thymus. Representative dot plots for T cell distribution and quantification graphs are presented. The error bars denote standard deviation within the group of animals.

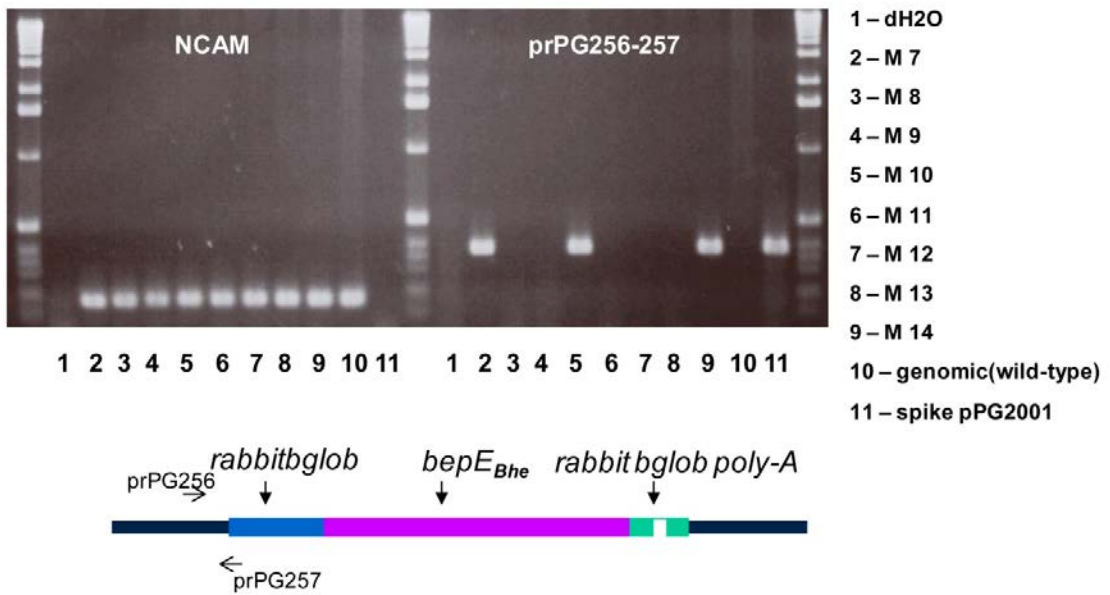
B. CD4 and CD8 T cells composition in spleen. Representative dot plots for T cell distribution and quantification graphs are presented. The error bars denote standard deviation within the group of animals.

C. CD4 and CD8 T cells proportion in lymph nodes. Representative dot plots for T cell distribution and quantification graphs are presented. The error bars denote standard deviation within the group of animals.

A.



B.



C.

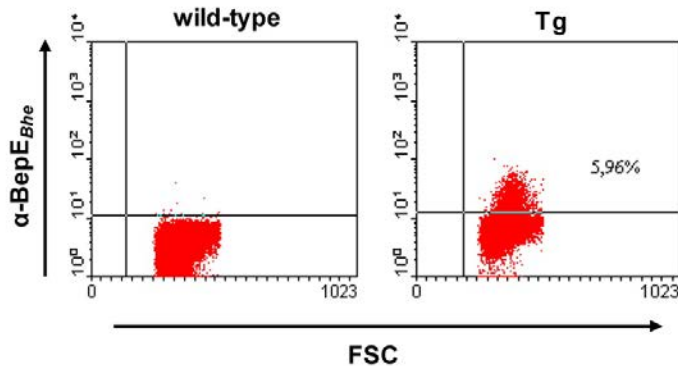


Figure 1.

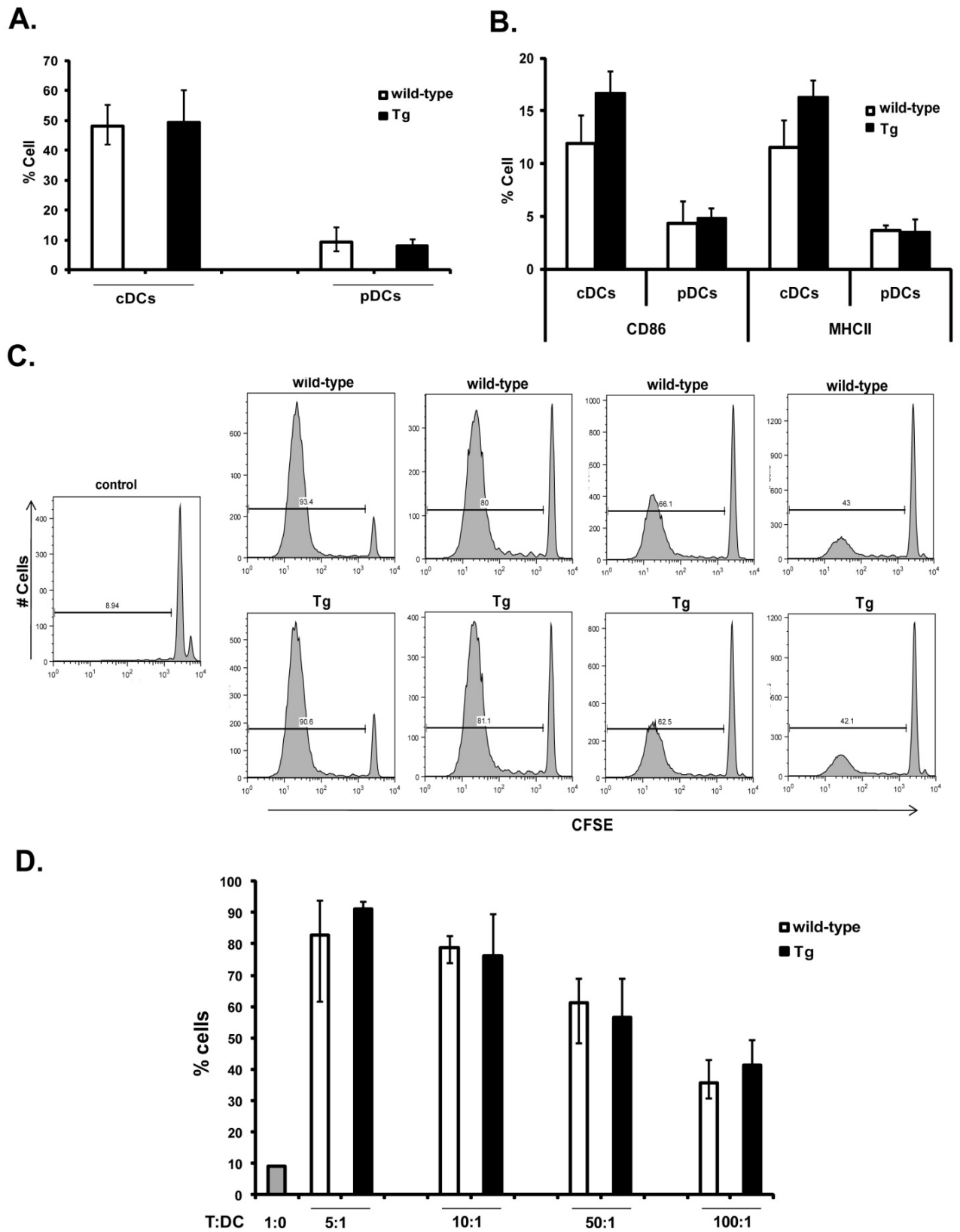


Figure 2.

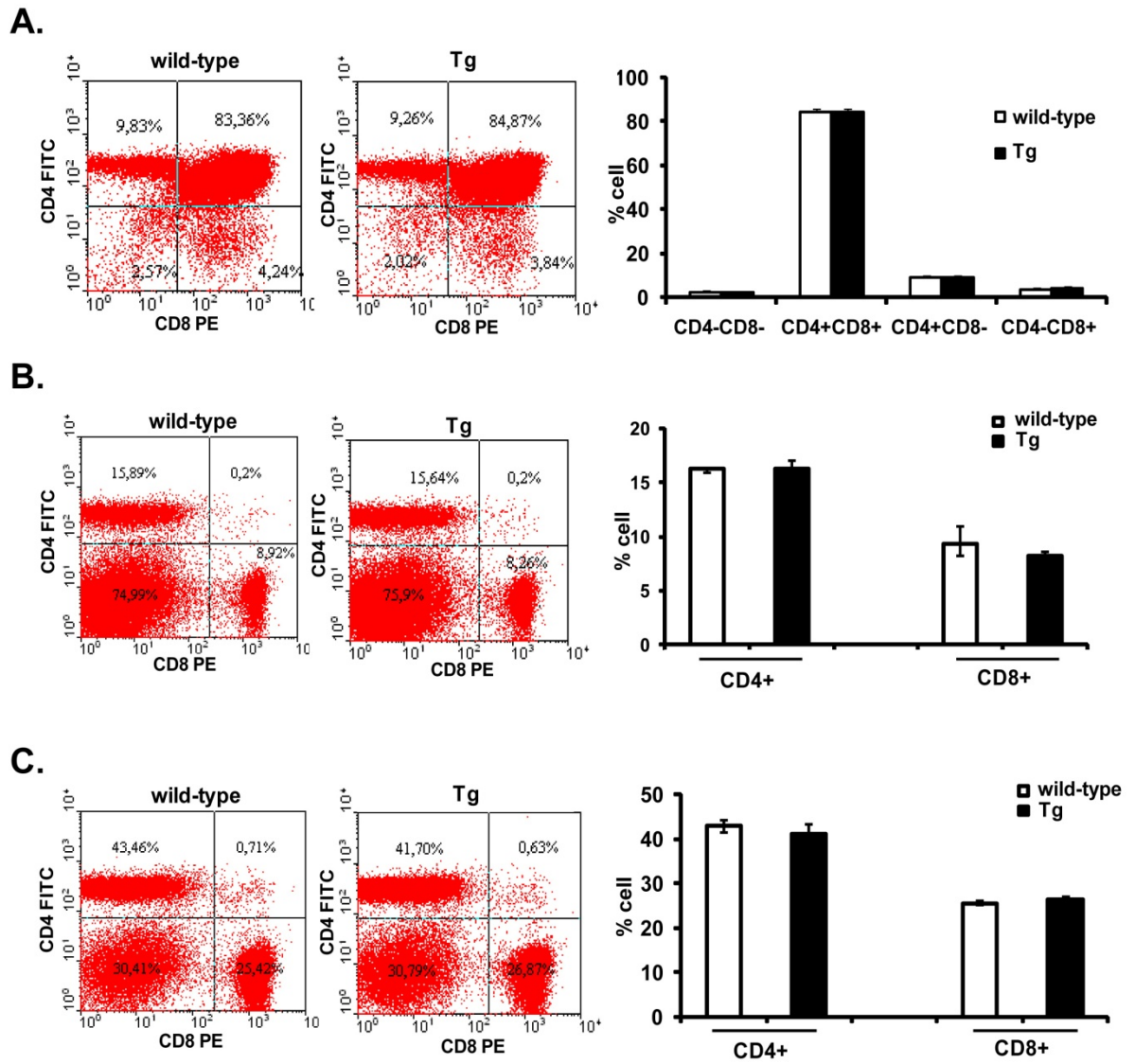


Figure 3.

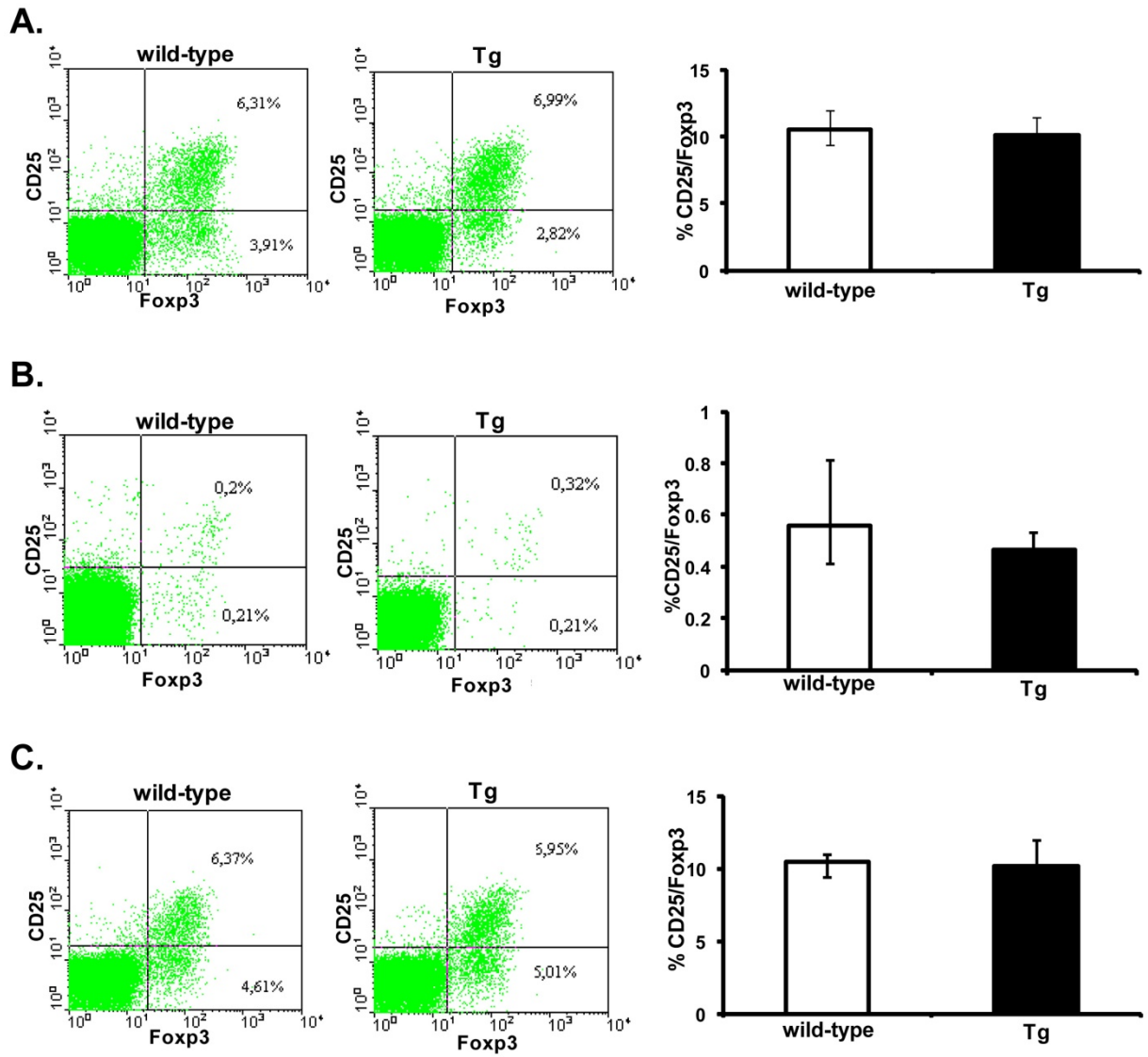


Figure 4.

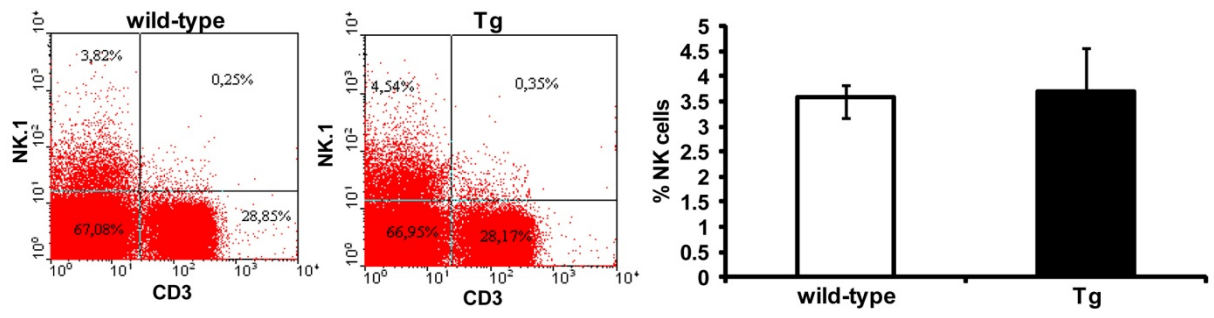


Figure 5.

2. Tolerance to *Bartonella* during long-term persistent infection

The immune response has evolved to protect the host from a wide range of potentially pathogenic microorganisms, but parallel mechanisms to control over-exuberant immune responses and prevent reactivity to self are required to limit host damage. Interleukin-10 (IL-10) is an anti-inflammatory cytokine with a crucial role in preventing inflammatory and autoimmune pathologies. IL-10 supports the differentiation of tolerogenic and anergic T cells by directly inhibiting the phosphorylation of CD28 and subsequent downstream signalling and efficiently inhibits the proliferation and cytokine production of those cells. Interleukin-10 is also recognized as stimulating the production of T cells with regulatory function that can suppress effector T-cell proliferation [27-30]. A number of cells of the innate and adaptive immune response produce IL-10, including DC and macrophages, Th1, Th2, Th17 and T regs [13].

Many chronic pathogens subvert host immunity by upregulating the expression of anti-inflammatory cytokines, such as IL-10. Some viruses capable of establishing chronic infections produce viral homologues to IL-10. Although, no bacteria-encoded IL-10 homologues have been described, bacteria can induce the secretion of endogenous IL-10 and/or TGF- β from innate immune cells that respond to the infection [14]. DCs exposed to filamentous hemagglutinin (FHA) from *Bordetella pertussis* secrete IL-10 and inhibit LPS-induced inflammatory cytokine production. Furthermore, these IL-10-secreting DCs induce the clonal expansion of T reg1 cells that are capable of suppressing the *Bordetella*-specific Th1 immune response [15,16]. *Chlamydia trachomatis* induces the expression of IL-10 indirectly, by increasing prostaglandin E₂ (PGE₂) secretion levels. By this mechanism it encourages T reg function to interfere with the delivery of anti-chlamydial Th1 responses and minimize destructive inflammation of the infected genital tract tissue [27].

Bqu infection of homeless people (human is the only host known for *Bqu*) known as trench fever with recurrent fever, headaches and leg pain, is usually resolved within the month but 5-10% of the cases develop chronic bacteremia for longer times. *Bqu* bacteremia exhibited high IL-10 production and an attenuated inflammatory response, which may favor bacterial persistence [17]. The dependence of bacterial persistence on the elevated levels of IL-10 was confirmed experimentally by infecting IL-10^{-/-} mice with

Bbi, where infected animals did not develop bacteremia [18]. Even more, IL-10 secretion and interference with the Th1 response against *Bhe* was observed in mouse, an incidental host infection model for *Bhe* [19].

In this regard, I was interested to investigate whether IL-10 production is connected to *Bartonella* effector proteins, especially to BepE as it shows a molecular mimicry to immune inhibitory receptors and bares putative ITIM/ITSM and Csk-like binding domain on the N term [1]. Potentially this molecule could modulate the immune response against *Bartonella* by inducing anti-inflammatory cytokine production and by this bacteria could favor in the establishment of long term infection. First, I decided to infect BMDCs, BMDCs and T lymphocytes as a co-culture with the ratio 1:5 and T lymphocytes from Balb/c mouse with wild-type and different mutant strains of *Bhe* at MOI of 50. After 24 hpi I measured the secretion of IL-10 in the supernatant of infected cells by indirect ELISA. As a result, I did not observe any clear dependence of IL-10 secretion on BepE. The IL-10 secretion was BMDC specific and infections with the mutant *Bhe* showed high perturbations within independent experiments (Figure 6 and 7). In both conditions of BMDC infection, BMDCs alone or co-cultured with T cells, IL-10 was detected in the supernatant. However, infected T cells did not produce any IL-10. It is noteworthy to mention that I did not have a careful look whether effector translocation takes place in T cells.

Next, I infected BMDCs from Myd88^{-/-} mouse with the same pattern of *Bhe* strains, in order to confirm that IL-10 production is induced rather by TLRs signaling after *Bartonella* recognition than by BepE translocation via T4SS. Myd88 is a TIR domain-containing adaptor and associates with the cytoplasmic TIR domain of TLRs [20], thus it is in a very beginning of TLR signaling and if BepE has a potential to mimic even the TLR signaling, the IL-10 production would be observed. In addition, it is known that *Bartonella* has a modified LPS and it is not recognized by TLR4 [21,22], the only TLR receptor within the TLR-family, that has a Myd88-independent pathway next to Myd88-dependent signaling [23]. As a result, infected Myd88 BMDCs did not produce IL-10 (Figure 7), indicating that indeed, IL-10 production during *Bartonella* infection is TLR mediated and we speculate it is rather via TLR2 recognition of *Bartonella* lipopeptides, in line with the fact that heat killed *Bqu* is activating TLR2 signaling [21].

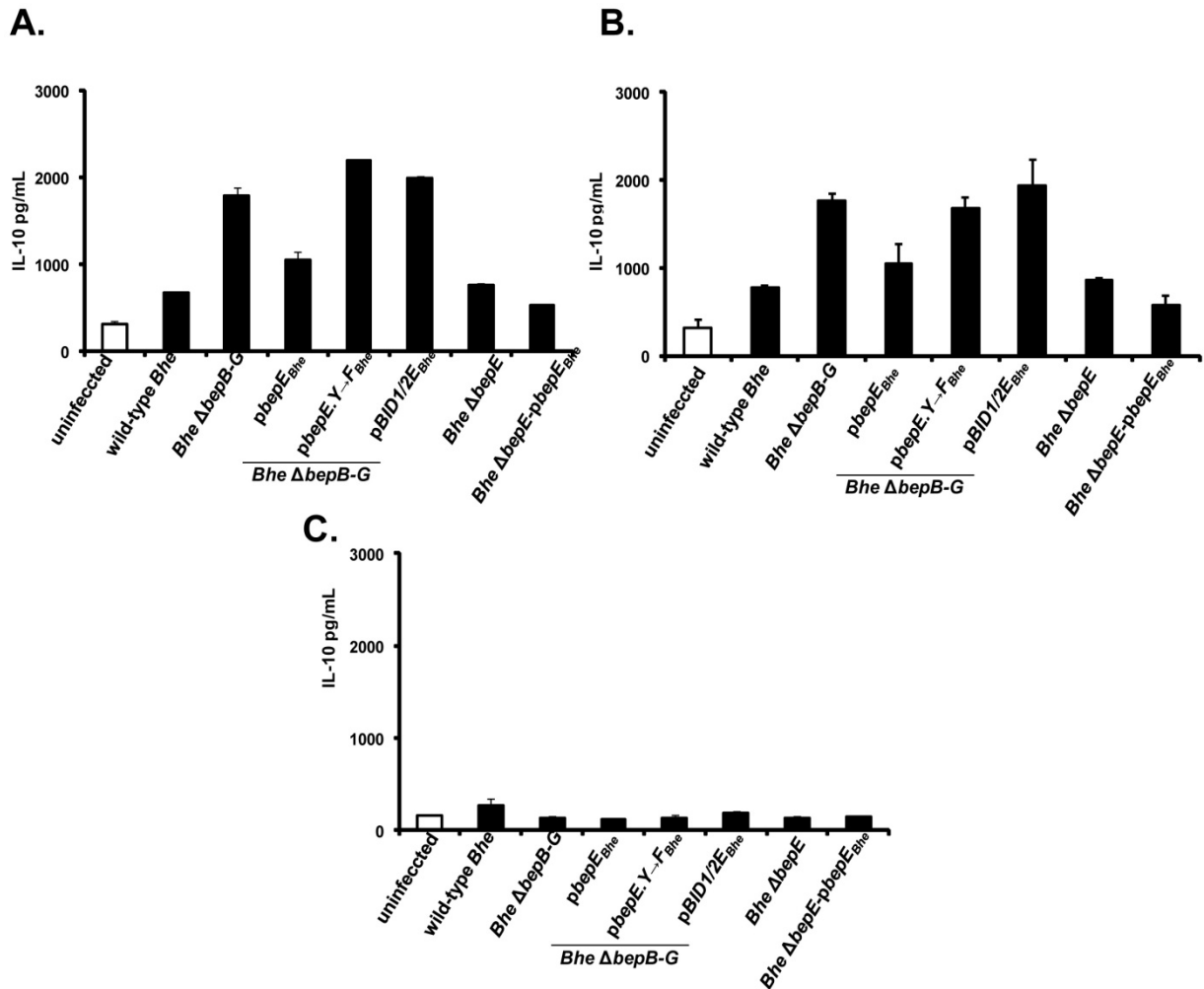


Figure 1: IL-10 is secreted by infected BMDCs but not by infected T cells alone

BMDCs (A), BMDC-T cell co-culture (the ratio 1 to 5 respectively) (B) and T cells (C) cultured *in vitro* from wild-type Balb/c mouse were infected (MOI=50) with either wild-type *Bhe* or the mutant strains depicted on the graph. After 24 hpi the secreted IL-10 was detected in the supernatant of infected cell culture by indirect ELISA. BMDCs were cultured from the bone marrow in the presence of Flt3L for 10 days; the T cells were obtained from the lymph nodes. The bar graph shows the amount of secreted IL-10 per mL of supernatant from infected cell culture. The error bars denote standard deviation within triplicates.

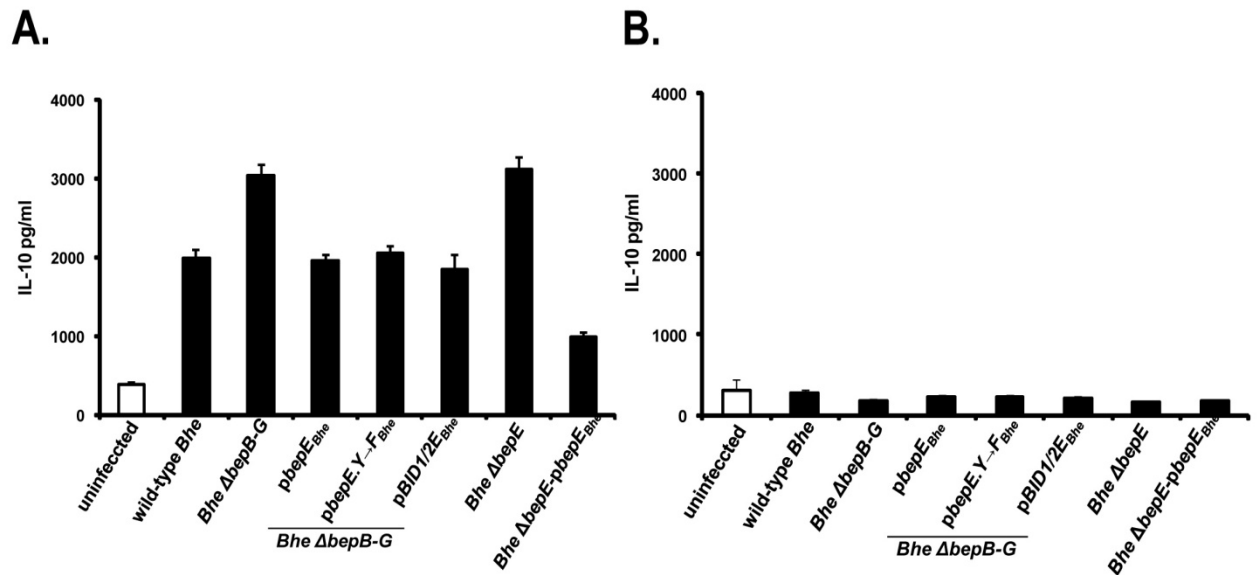


Figure 2: IL-10 secretion by *Bhe* infected BMDCs is mediated via TLR receptors and is not Bep dependent

BMDCs, cultured *in vitro* from Balb/c wild-type (A) or Balb/c Myd88^{-/-} mouse bone marrow in the presence of Flt3L for 10 days, were infected (MOI=50) with either wild-type *Bhe* or mutant strains depicted on the graph. After 24 hpi the secreted IL-10 was detected in the supernatant of infected BMDC culture by indirect ELISA. The bar graph shows the amount of secreted IL-10 per mL of supernatant from infected cell culture. The similar results were observed from the later time points of BMDC infection with wild-type *Bhe* and the *Bhe* mutants. The error bars denote standard deviation within triplicates.

3. Infection of C57/BL6/J mice with *Bartonella taylorii*

During the establishment of a mouse infection model for *Bartonella*, one of the candidates, with consideration of natural host specificity, was *Bartonella taylorii* (*Bta*). We wanted to characterize *i.d.* infection in C57/BL6/J mice, comparing *Bta* infection in two routes, *i.d.* versus *i.v.* and the following bacteremia in blood from the tail vein. The animals with the *i.d.* injection of C57/BL6/J (*Bta*) underwent unusual signs that were not observed in any previous cases of *Bartonella in vivo* infections. Most of the *i.v.* infected mice had damaged tails with necrotic areas few days after infection (4 dpi). Starting from day 10 *i.d.* infected mice developed necrotic tissues on the ear, but not only at the site of infection. These observations are not *Bartonella* strain specific; the similar observations were seen in a parallel experiment with *Btr* infection of C57/BL6/J mice (data not shown). I assume this is rather mouse line specific phenomenon [25]. C57/BL6/J mice with stronger TH1 response and strong cytotoxic effect against *Bartonella* containing cells developed tissue necrosis. The phenomenon described here has not been investigated further.

Although the bacteremia in C57/BL6/J mice reaches high titers, more than 10^7 bacteria per mL of blood, the system is not convenient to study long term infection of *Bartonella* because the animals with the necrotic lesions have to be sacrificed.

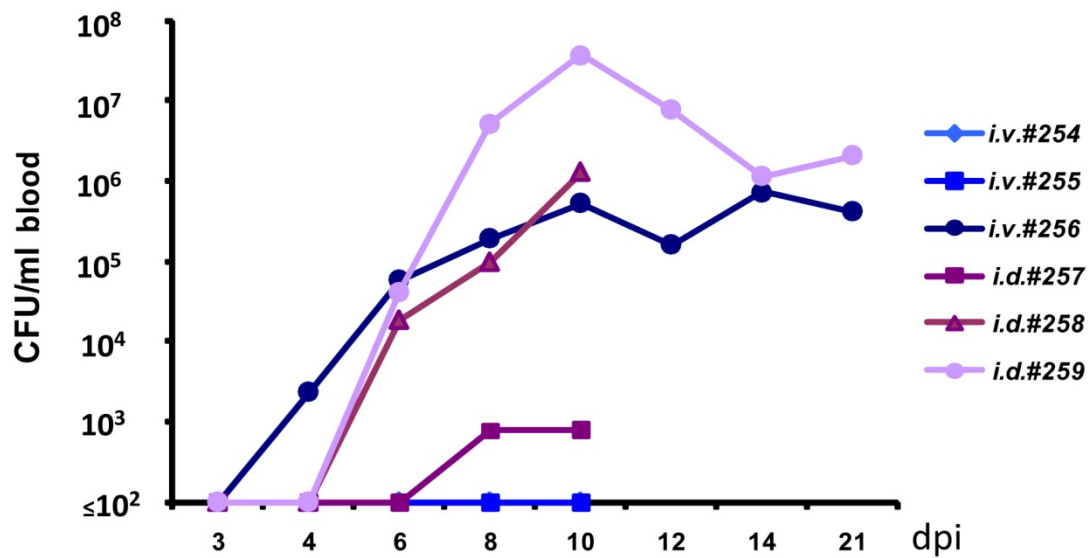


Figure : The time course of bacteremia in *Bta* infected C57/BL6/J mice

The group of (n=3) C57/BL6/J mice were either *i.v.* or *i.d.* injected with PBS containing wild-type *Bta* bacteria (200 μ l and 10 μ l of OD₅₉₅=1 respectively). Blood samples were collected from the tail vein with 10% citrate supplementation at the time points indicated on the graphs. The blood was frozen to lyse red blood cells and undiluted and serial dilutions of thawed blood in PBS was plated on sheep blood supplemented CBA for counting colony forming units (CFU) per mL of blood. Plotted graphs represent a single animal from which bacteria were recovered at a given time point post-infection. Mice #254, 255, 257, 258 were sacrificed because of necrotic lesions on the tail and the ear.

References:

1. Selbach, M., F. E. Paul, et al. (2009). "Host cell interactome of tyrosine-phosphorylated bacterial proteins." *Cell Host Microbe* **5**(4): 397-403.
2. Bommhardt, U., M. Beyer, et al. (2004). "Molecular and cellular mechanisms of T cell development." *Cell Mol Life Sci* **61**(3): 263-280.
3. Sprent, J. and H. Kishimoto (2002). "The thymus and negative selection." *Immunol Rev* **185**: 126-135.
4. Sakaguchi, S., M. Ono, et al. (2006). "Foxp3+ CD25+ CD4+ natural regulatory T cells in dominant self-tolerance and autoimmune disease." *Immunol Rev* **212**: 8-27.
5. Sakaguchi, S., T. Yamaguchi, et al. (2008). "Regulatory T cells and immune tolerance." *Cell* **133**(5): 775-787.
6. Yamaguchi, T. and S. Sakaguchi (2006). "Regulatory T cells in immune surveillance and treatment of cancer." *Semin Cancer Biol* **16**(2): 115-123.
7. Feuerer, M., J. A. Hill, et al. (2009). "Foxp3+ regulatory T cells: differentiation, specification, subphenotypes." *Nat Immunol* **10**(7): 689-695.
8. Yang, Y., A. Ueno, et al. (2003). "Control of NKT cell differentiation by tissue-specific microenvironments." *J Immunol* **171**(11): 5913-5920.
9. Bendelac, A., M. N. Rivera, et al. (1997). "Mouse CD1-specific NK1 T cells: development, specificity, and function." *Annu Rev Immunol* **15**: 535-562.
10. Skold, M. and S. M. Behar (2003). "Role of CD1d-restricted NKT cells in microbial immunity." *Infect Immun* **71**(10): 5447-5455.
11. Stenstrom, M., M. Skold, et al. (2005). "Natural killer T-cell populations in C57BL/6 and NK1.1 congenic BALB.NK mice—a novel thymic subset defined in BALB.NK mice." *Immunology* **114**(3): 336-345.
12. Berzins, S. P., A. P. Uldrich, et al. (2004). "Parallels and distinctions between T and NKT cell development in the thymus." *Immunol Cell Biol* **82**(3): 269-275.
13. Saraiva, M. and A. O'Garra (2010). "The regulation of IL-10 production by immune cells." *Nat Rev Immunol* **10**(3): 170-181.
14. Skinner, J. A., M. R. Pilione, et al. (2005). "Bordetella type III secretion modulates dendritic cell migration resulting in immunosuppression and bacterial persistence." *J Immunol* **175**(7): 4647-4652.
15. McQuirk, P., C. McCann, et al. (2002). "Pathogen-specific T regulatory 1 cells induced in the respiratory tract by a bacterial molecule that stimulates interleukin 10 production by dendritic cells: a novel strategy for evasion of protective T helper type 1 responses by Bordetella pertussis." *J Exp Med* **195**(2): 221-231.
16. McQuirk, P. and K. H. Mills (2002). "Pathogen-specific regulatory T cells provoke a shift in the Th1/Th2 paradigm in immunity to infectious diseases." *Trends Immunol* **23**(9): 450-455.
17. Capo, C., N. Amirayan-Chevillard, et al. (2003). "Bartonella quintana bacteremia and overproduction of interleukin-10: model of bacterial persistence in homeless people." *J Infect Dis* **187**(5): 837-844.
18. Marignac, G., F. Barrat, et al. (2010). "Murine model for Bartonella birtlesii infection: New aspects." *Comp Immunol Microbiol Infect Dis* **33**(2): 95-107.
19. Kabeya, H., A. Yamasaki, et al. (2007). "Characterization of Th1 activation by Bartonella henselae stimulation in BALB/c mice: Inhibitory activities of interleukin-10 for the production of interferon-gamma in spleen cells." *Vet Microbiol* **119**(2-4): 290-296.

20. Takeda, K. and S. Akira (2004). "TLR signaling pathways." Semin Immunol **16**(1): 3-9.
21. Popa, C., S. Abdollahi-Roodsaz, et al. (2007). "Bartonella quintana lipopolysaccharide is a natural antagonist of Toll-like receptor 4." Infect Immun **75**(10): 4831-4837.
22. Matera, G., M. C. Liberto, et al. (2008). "The Janus face of Bartonella quintana recognition by Toll-like receptors (TLRs): a review." Eur Cytokine Netw **19**(3): 113-118.
23. Kawai, T., O. Takeuchi, et al. (2001). "Lipopolysaccharide stimulates the MyD88-independent pathway and results in activation of IFN-regulatory factor 3 and the expression of a subset of lipopolysaccharide-inducible genes." J Immunol **167**(10): 5887-5894.
24. Reis e Sousa, C. (2006). "Dendritic cells in a mature age." Nat Rev Immunol **6**(6): 476-483.
25. Mitaka, K., Y. Miyazaki, et al. (2011). "Th2-biased immune responses are important in a murine model of chronic hypersensitivity pneumonitis." Int Arch Allergy Immunol **154**(3): 264-274.
26. Randolph, G. J., J. Ochoa, et al. (2008). "Migration of dendritic cell subsets and their precursors." Annu Rev Immunol **26**: 293-316.
27. Liu, W. and K. A. Kelly (2008). "Prostaglandin E2 modulates dendritic cell function during chlamydial genital infection." Immunology **123**(2): 290-303.
28. Moore, K. W., R. de Waal Malefyt, et al. (2001). "Interleukin-10 and the interleukin-10 receptor." Annu Rev Immunol **19**: 683-765.
29. Igiertseme, J. U., G. A. Ananaba, et al. (2000). "Suppression of endogenous IL-10 gene expression in dendritic cells enhances antigen presentation for specific Th1 induction: potential for cellular vaccine development." J Immunol **164**(8): 4212-4219.
30. Joss, A., M. Akdis, et al. (2000). "IL-10 directly acts on T cells by specifically altering the CD28 co-stimulation pathway." Eur J Immunol **30**(6): 1683-1690.

4 - Conclusions

4. Conclusions

To summarize, my PhD thesis aimed investigation of the role of BepE in reservoir host infection. The *in vitro* analysis served to understand the cellular bases of the *in vivo* findings. Here, I will draw the conclusions on the main findings of my work.

The establishment of rat *intra-dermal* infection model

In order to closely mimic the reservoir host infection by *Bartonella* I have established the rat *intra-dermal* (*i.d.*) infection model, inoculation of *B. tribocorum* in the ear dermis of the animal. This route of infection reflects the natural way of *Bartonella* transmission by arthropods when the bacteria are inoculated in the skin of a mammal via the feces of a vector after animal scratches [1]. The *i.d.* infected animals develop blood stage infection, which starts around 7-8 days post infection and lasts for 10 weeks. It is a long-term bacteremic infection without obvious clinical manifestations, a hallmark of the reservoir host infection by *Bartonellae*. The time delay that *Btr* is taking to appear in blood corresponds to the way that bacteria need to pass from the derma to the lymphatic-blood system and to the possible interaction with the innate immune system. In summary, the rat *i.d.* model enables us to distinguish *Bartonella* factors involved on two different phases of the infection: early phase, prior seeding into the blood and the blood stage. On those two stages bacteria have different environment to interact with, and assumably different strategies to cope with the host immune system.

In vivo relevance for BepE

The rat *i.d.* infection model revealed BepE as a critical factor in the establishment of reservoir host bacteremia. The expression of BepE_{Btr} could rescue the abacteremic phenotype of *Btr* Δ bepDE mutant and enabled the strain to reach the blood. Heterologous complementation of *Btr* Δ bepDE phenotype with BepE_{Bhe} suggests that this function of BepE is conserved between different species of *Bartonellae*. Even more, I could demonstrate that the C-terminal BID domains are having the specific function but putative phosphotyrosine-containing N-term of BepE does not play an essential role in the establishment of long-term bacteremic infection of the natural host by *Bartonella*.

BepE a fine-tune mechanism of host cell manipulation by *Bartonella*

Another phenotype of BepE but *in vitro* was observed during the infection of HUVECs with *Bhe* Δ bepE (and Δ bepDEF) mutant(s). HUVECs infected with *Bhe* strain that lacked BepE_{Bhe} revealed disturbed rear edge detachment during migration and followed with the fragmentation of cell body. This phenomenon was inhibited by pbepE_{Bhe} expression in *Bhe* Δ bepE (and Δ bepDEF) as well as, by T4SS independent expression of pbepE_{Bhe} in HUVECs by transfection prior the infection with *Bhe* Δ bepE (and Δ bepDEF). We found that the cell fragmentation of infected HUVECs is T4SS dependent and is a secondary effect of translocated Beps, potentially the Beps involved in the invasome formation. Further we conclude that the C-terminal BID domains of BepE_{Bhe} are sufficient to interfere with the fragmentation process. From this we could hypothesize that primary infected cells in *i.d.* infection model of rats may also undergo fragmentation or impaired migration when infected with *Btr* Δ bepDE and then *Bartonella* does not succeed to reach the blood system and colonize red blood cells.

Potential “primary niche” cells for *Bartonella* in the reservoir host

I introduced the *i.d. in vivo* infection of *Rosa 26-loxP-egfp* Balb/c mice and *in vitro* mouse Bone Marrow-derived Dendritic Cells (BMDCs) with *B. birtlesii* (*Bbi*) strain that is expressing Cre-BID fusion protein. The *in vitro* model showed for the first time *Bartonella* effector protein translocation in primary immune cells of the reservoir host. This finding builds a strong basis for the hypothesis that primary infected cells *in vivo* may be the DCs (Langerhance cells or dermal DCs) in the skin of infected animal. DCs are the sentinels of the immune system that constantly sample the environment for the “danger signal”. Thus, they represent one of the candidate cells in the derma to be targeted by *Bartonella* after inoculation of the bacteria from the feces of arthropod vector. Infected DCs could serve as Trojan horses to carry and disseminate *Bartonella* from derma to lymphatic–blood system. The time course of the *i.d.* infection of *Rosa 26-loxP-egfp* Balb/c mice with *Bbi* showed that bacteremia started at 4-5 days post infection (dpi). Thus, the time point to observe infected DCs migrated from derma to lymph nodes should be rather 3 dpi.

5 - Outlook

5. Outlook

In this chapter I will highlight the open questions regarding the BepE function *in vivo* and interference with the cell fragmentation phenomenon and provide the suggestions of experimental setups that allow addressing the open points. In the end, I emphasize how the research carried out in the frame of my thesis may generate the impact by providing new insights on general microbiological and cell biological problems.

The two phenotypes of BepE C-terminal BID domains were observed: (i) *in vivo* in the absence of BepE *Btr ΔbepDE* is not able to reach the blood, assumably bacteria are cleared by innate immune system at the site of infection or on the way to blood stream. (ii) *in vitro* HUVECs infected with the *Bhe* strains lacking BepE develop a problem to detach at the rear edge during migration and undergo subsequent fragmentation. Whether these two observations are the result of the same effect of *Bartonella* on infected cells and the primary infected cells *in vivo* also develop disturbed migration needs further elucidation.

The mouse model, *Rosa 26-loxP-egfp* Balb/c *i.d.* infection with *Bbi-Tn-cre*, provides possibility to demonstrate the migration of primary infected cells to lymph nodes by detecting GFP-expressing cells in draining lymph nodes with FACS analysis or histological examination. Infection with *Bbi-Tn-cre ΔbepE* adds the possibility to detect the impaired migration of infected cells to the lymph nodes. The decreased numbers (or absence) of GFP-positive cells in lymph nodes could give a strong evidence that BepE is a factor *in vivo* that interferes with the impaired migration of infected cells. At the same time, it would help to understand whether GFP-expressing cells have migrated from the primary infection site, derma, or they are the resident cells of lymph node and infected with *Bartonella* already at the place of detection.

On the other hand, the *in vitro* infectivity of BMDCs (from *Rosa 26-loxP-egfp* Balb/c) with *Bbi-Tn-cre* enables us to investigate the migration of potential target cells, DCs, *in vitro*. The homing factors for DC migration to lymph nodes, CCL19 and/or CCL21, may be used as a chemoattractant for *Bbi-Tn-cre* and *Bbi-Tn-cre ΔbepE* infected DCs to examine their migration properties in directional movement, thus mimicking the migration of infected DCs from derma to the nearest lymph node in respond to the chemoattractant gradient.

Bbi-Tn-cre and *Bbi-Tn-cre ΔbepE* infected BMDCs need to be investigated carefully for the expression of DC maturation markers and for upregulation of the adhesion molecules (ex. CCR7) for migration and effective stimulation of T cells.

For the understanding of molecular mechanisms of cell fragmentation phenomenon of *Bhe ΔbepE* (and *ΔbepDEF*)-infected HUVECs, first the induction factor needs to be revealed. Our hypothesis that the phenotype is a secondary effect of the Beps involved in the formation of invasomes, can be investigated by infection of HUVECs with *ΔbepB-G* strain complemented with *pbepB*, *pbepC* and *pbepG* or different combinations even with *pbepF*. BepF involved in the invasome formation together with BepC [1], however we know that BepF alone does not induce the cell fragmentation. Once we know the responsible Bep(s) for the fragmentation we may introduce the BepE either by T4SS-dependent or independent manner and rescue the phenotype. This would prove that *Bartonella* has evolved BepE as a fine-tune mechanism to compensate the drastic effects on host cell actin cytoskeleton when translocating Beps with invasome formation potency.

Current evidence shows that BepE rescues cells from rear detachment problem potentially by refining the focal adhesion (FA) turnover. It is a subject of interest to have a closer look on different components of the FAs and their regulation. The use of Lenti-viral systems for visualization of focal adhesions could be a possibility to monitor FA turnover in *Bhe ΔbepE* (and *ΔbepDEF*) and *Bhe ΔbepE-pbepE* (and *ΔbepDEF-pbepE*)-infected HUVECs. Of course with the interest to translate observed data on primary infected cells of the reservoir host of *Bartonella*.

Another approach to understand the underlying molecular mechanism of fragmentation phenomenon is siRNA gene silencing of the signaling components that are involved in cell rear retraction. However, for that we first need to see a similar (if not the same) phenotype in the cell line, as HUVECs are not convenient for siRNA transfection manipulations.

The hypothesis of cell fragmentation next to invasome formation is strengthened by existing knowledge. Rac signaling is able to antagonize Rho activity directly at the GTPase level, and that the reciprocal balance between Rac and Rho activity determines cellular morphology and migratory behavior in NIH3T3 fibroblasts [2]. At the same time, it was

shown that invasome formation is mediated with Rac1/Scar1/WAVE/Arp2/3 pathway [1]. This Rac1 mediated Rho inhibition may be the event leading to impaired detachment of infected HUVECs. Lysophosphatidic acid (LPA)-mediated activation of Rho GTPase [2,3] may be one possibility to look at fragmentation recovery of *Bhe ΔbepE* (and *ΔbepDEF*)-infected HUVECs.

The impact of the study on general microbiology and cell biology

Although the aim of my research was to increase the knowledge about BepE effector protein, certain aspects and established approaches may influence the other fields as well.

The *Rosa26 loxp-GFP* Balb/c mouse line is primarily used for tissue specific expression of GFP after breeding the line with the mice expressing Cre recombinase in different tissues, mainly in neurobiology field. The use of *Rosa26 loxp-GFP* Balb/c mouse line as a reporter for *in vivo* translocation of bacterial effectors was a first trial from our group on the example of Beps. Now, that we have strong evidence from *in vivo* experiments and we already showed *in vitro* infectivity of BMDCs by *Bbi-Tn-cre*, the reporter system can be broadly used for other pathogens and translocation systems. It provides a tool to chase *in vivo* targeted cells by a pathogen by visualizing effector translocation in infected cells even in a “bystander mechanism”, the translocation without bacterial entry into the cells.

Most of the findings and the knowledge in cell migration accumulated after the use of bacterial factors targeting different components important for cell migration. These factors induce cytoskeleton rearrangements by targeting regulator factors or directly mimicking them. The best example, amongst many others, is C3 toxin from *Botulinum*, the inhibitor of Rho GTPase [3,4]. In this regard the molecular mechanisms of BepE effect have a great importance, as it refines the rear detachment problem and seems to be actively involved in the regulation focal adhesion turn over in migrating cell. Thus, further research on BepE would provide new insights into cell biology by strengthening the knowledge or even revealing new mechanisms in the regulation of cell migration, which itself has a great importance in understanding of metastasis, angiogenesis, immune response and developmental biology.

References:

1. Truttmann, M. C., T. A. Rhomberg, et al. (2011). "Combined action of the type IV secretion effector proteins BepC and BepF promotes invasome formation of *Bartonella henselae* on endothelial and epithelial cells." Cell Microbiol **13**(2): 284-299.
2. Sander, E. E., J. P. ten Klooster, et al. (1999). "Rac downregulates Rho activity: reciprocal balance between both GTPases determines cellular morphology and migratory behavior." J Cell Biol **147**(5): 1009-1022.
3. Kumar, J. and D. L. Epstein (2011). "Rho GTPase-mediated cytoskeletal organization in Schlemm's canal cells play a critical role in the regulation of aqueous humor outflow facility." J Cell Biochem **112**(2): 600-606.
4. Worthylake, R. A., S. Lemoine, et al. (2001). "RhoA is required for monocyte tail retraction during transendothelial migration." J Cell Biol **154**(1): 147-160.

6 - Acknowledgments

6. Acknowledgments

This work was carried out in the group of Prof. Christoph Dehio in the Focal Area Infection Biology at the Biozentrum of the University of Basel.

First, I would like to thank Prof. Christoph Dehio for his guidance and supervision. He provided an excellent framework for doing experimental research. His valuable suggestions, analytical criticism, and positive attitude were an immense contribution and support.

I also want to thank the other members of my thesis committee, Prof. Antonius Rolink and Prof. Dirk Bumann, for accompanying me with my work, giving me guidelines and advices.

I would like to thank Dr. Patrick Guye for introducing me as a PhD student to the BepE and *Bartonella* field, for his valuable advice, for making and developing methods which laid the foundations for my work with *Bartonella*.

For the critical and careful reading of my thesis I am very grateful to Dr. Florine Scheidegger and Dr. Nona Janikashvili.

I am very grateful to Dr. philipp Engel, Claudia Mistl and Marco Faustmann for their assistance with the animal experiments.

I also want to thank to Maxime Quebatte for always having time to discuss problems and strategies in the world of cloning.

In addition to those mentioned above, I wish to express my thanks to all present and past members of the Dehio lab for all the help, discussions, ideas, and the extra-lab activities. I thank Dr. Arto Pulliainen, Yvonne Elnor, Dr. Raquel Conde, Dr. Matthias Truttmann, Arnaud Goepfert, Dr. Houchaima Ben Tekaya, Shyan low, Kathrin Pieleles, Simone Muntwiler, Frederic Stander, Jérémie Gay-Fraret, Barbara Hauert, Sonja Huser, Alexander Harms, Dr. David Topel, Dario Behringer, Alain Casanova, Mario Emmenlauer and Dr. Pauli Ramo.

For the collaboration on the analysis of transgenic mice, I want to thank Dr. Lee Kim Swee at DBM, Basel.

Also, I would like to acknowledge the invaluable support from the people working on the technical and administrative staff of the 4th floor. Thank you all very much for all the things running in the back of the everyday business of science.

Finally, I want to thank my whole family for their support throughout my studies and their interest in my work. This Ph.D. thesis would have never been possible without them.

A special thank goes to my husband - Vladimer Botsvadze and to my little boy Giorgi, my greatest source of equilibrium during the years, for being patient and providing me environment for both, work and leisure.

At the end, in loving memory, I want to thank to my grandmother – Rusudan, for being the first guide for me, as a child, through the Biology field, the fascinating living world around me.

7 - Curriculum Vitae

Curriculum Vitae

Name Rusudan
Surname Okujava
Date of Birth 07.04.1981
Nationality Georgian

Address Office

Klingelbergstrasse 50/70
 CH – 4056, Basel
 +41 61 267 21 39
 rusudan.okujava@unibas.ch

Address private

Landskronstrasse 28
 CH – 4056, Basel
 +41 77 421 98 28

Education and working experience

- 2007 – 2011 Ph.D theses
 Focal Area of Infection Biology, Biozentrum, University of Basel CH
 Supervisor, Prof. Dr. Christoph Dehio
 Committee members, Prof. Dr. Antonius Rolink and Prof. Dr. Dirk Bumann
 “Functional characterization of *Bartonella* effector protein – BepE during *in vivo* and *in vitro* infection”
- 2004 – 2006 Technician to the Senior Laboratory Assistant Lela Kardava,
 Immunodiagnostic Center - “Immunodiagnosics XXI”, Tbilisi, Georgia.
- 2002 – 2004 MSc Immunology, department of Immunology, Faculty of Biology, Tbilisi
 State University, Georgia.
 Supervisor, Prof. Dr. Nino Porakishvili, Dr. Khatuna Gabunia.
 “Phagocytic functions of activated and nonactivated neutrophils (ex vivo)
 from treated and untreated B-CLL patients “
- 1998 – 2002 BSc Biology, Faculty of Biology, Tbilisi State University (TSU), Georgia

Publications

- Kulikova N., **Okujava R.**, Kardava L., Kartvelishvili M., Iosava G., Ghirdaladze D., Porakishvili N.: Apoptosis induction in B-chronic lymphocytic leukemia cells *in vitro* via ligation of CD19. Proc.Georgian Acad., Sci.,Biol.Ser.A, 2006 Vol 32,No.2, pp.331-339.
- Jordania Ts., Kulikova N., **Okujava R.**, Shelegia K., Baloyan D., Sereda L., Tevzadze M., Ghirdaladze M., Iosava G., Porakishvili N.: Detection of cell cycle phase distribution in B-chronic lymphocytic leukemia (B-CLL) cells after *in vitro* ligation with anti-CD5 or anti-CD19 monoclonal antibodies. Proc.Georgian Acad., Sci.,Biol.Ser.A, 2006 Vol 32, No.3, pp.597-603.
- Kulikova N., **Okujava R.**, Janikashvili N., Gabunia Kh., Mitskevichi N., Tsertsvadze T., Tsagareishvili P., Ghirdaladze M., Porakishvili N.: Toll-like receptors expression profile in patients with B-Chronic Lymphocytic Leukemia (B-CLL). Proc.Georgian Acad., Sci.,Biol.Ser.A, 2006 Vol 32, No.3, pp.523-529.